AFWL-TR-75-181

AFWL-TR-75-181

FG

(2)

AD A023927

# ELECTROMAGNETIC PULSE ANALYSIS OF SMALL POWER SYSTEMS

David D. Babb
Joe P. Martinez

S/C 112850

Dikewood Industries, Inc.
1009 Bradbury Drive, SE
Albuquerque, NM 87106

March 1976

Final Report

Approved for public release; distribution unlimited.

Prepared for
DEFENSE CIVIL PREPAREDNESS AGENCY
Support Services Division (Research)
Washington, DC 20301

AIR FORCE WEAPONS LABORATORY
Air Force Systems Command
Kirtland Air Force Base NM 87117

DDC
RECEIVED
MAY 3 1976

AFWL-TR-75-181

This final report was prepared by the Dikewood Industries, Inc., Albuquerque, New Mexico, under Contract F29601-74-C-0010, Job Order 920W0901 with the Air Force Weapons Laboratory, Kirtland Air Force Base, New Mexico. This research was sponsored by the Defense Civil Preparedness Agency, Washington, DC. Mr. Prather (ELP) was the Laboratory Project Officer-in-Charge.

When US Government drawings, specifications, or other data are used for any purpose other than a definitely related Government procurement operation, the Government thereby incurs no responsibility nor any obligation whatsoever, and the fact that the Government may have formulated, furnished, or in any way supplied the said drawings, specifications, or other data, is not to be regarded by implication or otherwise, as in any manner licensing the holder or any other person or corporation, or conveying any rights or permission to manufacture, use, or sell any patented invention that may in any way be related thereto.

This report has been reviewed by the Information Office (OI) and is releasable to the National Technical Information Service (NTIS). At NTIS, it will be available to the general public, including foreign nations.

This technical report has been reviewed and is approved for publication.

William D. Prather

WILLIAM D. PRATHER
Project Officer

FOR THE COMMANDER

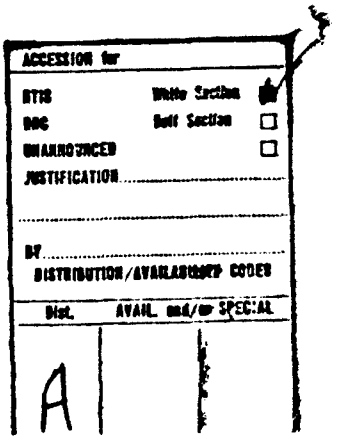
Larry W. Wood

LARRY W. WOOD
Lt Colonel, USAF
Chief, Phenomenology and Technology Branch

James L. Griggs

JAMES L. GRIGGS, JR.
Colonel, USAF
Chief, Electronics Division

DO NOT RETURN THIS COPY. RETAIN OR DESTROY.



UNCLASSIFIED

SECURITY CLASSIFICATION OF THIS PAGE (When Data Entered)

# REPORT DOCUMENTATION PAGE

READ INSTRUCTIONS BEFORE COMPLETING FORM

| | |
|---|---|
| 1. REPORT NUMBER: AFWL-TR-75-181 | 2. GOVT ACCESSION NO. |
| 3. RECIPIENT'S CATALOG NUMBER | |
| 4. TITLE (and Subtitle): ELECTROMAGNETIC PULSE ANALYSIS OF SMALL POWER SYSTEMS. | 5. TYPE OF REPORT & PERIOD COVERED: Final Report. |
| 6. PERFORMING ORG. REPORT NUMBER | |
| 7. AUTHOR(s): David D. Babb, Joe P. Martinez | 8. CONTRACT OR GRANT NUMBER(s): F29601-74-C-0010, Work Order DCPA01-74-C-0330 |
| 9. PERFORMING ORGANIZATION NAME AND ADDRESS: Dikewood Industries, Inc., 1009 Bradbury Drive, SE, Albuquerque, NM 87106 | 10. PROGRAM ELEMENT, PROJECT, TASK AREA & WORK UNIT NUMBERS: 920W0901 |
| 11. CONTROLLING OFFICE NAME AND ADDRESS: Defense Civil Preparedness Agency, Support Services Division (Research), Washington, DC 20301 | 12. REPORT DATE: March 1976; 13. NUMBER OF PAGES: 188 (191p.) |
| 14. MONITORING AGENCY NAME & ADDRESS (if different from Controlling Office): Air Force Weapons Laboratory, Kirtland Air Force Base, NM 87117 | 15. SECURITY CLASS. (of this report): UNCLASSIFIED; 15a. DECLASSIFICATION/DOWNGRADING SCHEDULE |

16. DISTRIBUTION STATEMENT (of this Report)

Approved for public release; distribution unlimited

17. DISTRIBUTION STATEMENT (of the abstract entered in Block 20, if different from Report)

18. SUPPLEMENTARY NOTES

19. KEY WORDS (Continue on reverse side if necessary and identify by block number)

Electromagnetic Fields and Waves
Electromagnetic Pulse
Interaction
Power Systems

20. ABSTRACT (Continue on reverse side if necessary and identify by block number)

A rural electrical cooperative system is analyzed for EMP vulnerability. The coupling to a particular substation within the system is determined by considering the power distribution lines as antennas which pick up the incident EMP and treats the substation as a load. The most vulnerable components within the substation are determined and the energy levels necessary for failure are calculated. From the coupling problem the energy levels at various locations within the substation are known and the coupling to the vulnerable ports are

(OVER)

over

ABSTRACT (Cont'd)

determined. A ratio of coupled to threshold values is calculated; and if the ratio is above 1, failure is assumed, and if below 1, no failure is assumed. If failure is indicated the reasons are determined so as to recommend "hardening" techniques. Although the detailed analysis is performed on one particular substation, the results may be compared to other similar systems throughout the country and perhaps knowledge of their response to an EMP may be gained from this analysis.

## SUMMARY

A rural electrical cooperative system is analyzed for EMP vulnerability. The coupling to a particular substation within the system is determined by considering the power distribution lines as antennas which pick up the incident EMP and treats the substation as a load. The most vulnerable components within the substation are determined and the energy levels necessary for failure are calculated. From the coupling problem the energy levels at various locations within the substation are known and the coupling to the vulnerable ports are determined. A ratio of coupled to threshold values is calculated; and if the ratio is above 1, failure is assumed, and if below 1, no failure is assumed. If failure is indicated the reasons are determined so as to recommend "hardening" techniques. Although the detailed analysis is performed on one particular substation, the results may be compared to other similar systems throughout the country and perhaps knowledge of their response to an EMP may be gained from this analysis.

## PREFACE

The authors wish to thank the following people for their helpfulness in providing information and their interest in this study: Mr. John Ragland, Mr. Mark Sullivan, and Mr. Clayton Bedker of the Hicks & Ragland Engineering Company, Inc. for their assistance in providing information about the Kit Carson Electrical Cooperative system; Mr. Jose Rodriguez, manager of the Kit Carson Cooperative, for his help and permission to use Kit Carson as the particular system to be studied; Mr. O. G. Atewell, Mr. J. M. Payne, and Mr. Blaine Schultz of the McGraw-Edison Company for their assistance in providing information about the McGraw-Edison recloser and recloser control units. In addition, we would like to thank Mr. James Kerr of the Defense Civil Preparedness Agency, and Mr. Bronius Cikotas and Mr. William Prather of the Air Force Weapons Laboratory for their encouragement, helpful discussions, and interest in this work.

CONTENTS


| Section | | | Page |
|---|---|---|---|
| I | INTRODUCTION | | 11 |
| | 1. | Objective and Scope | 11 |
| | 2. | Methodology | 12 |
| II | THE KIT CARSON ELECTRIC COOPERATIVE | | 16 |
| | 1. | Organization and Layout | 16 |
| | 2. | The Los Cordovas Substation | 18 |
| III | EXTERNAL COUPLING MODELS | | 25 |
| | 1. | Distribution Lines as a Beverage Antenna | 25 |
| | 2. | The Eighty-Foot Section | 29 |
| | 3. | Coupling to the McGraw-Edison Recloser | 32 |
| | 4. | A Problem Involving Autotransformers | 51 |
| | 5. | Bushing Breakdown | 56 |
| | 6. | The Coupling to a General Electric Recloser | 58 |
| | 7. | Polyethylene Breakdown | 64 |
| IV | EQUIPMENT FAILURE MODELING | | 65 |
| | 1. | Selection of Ports in the McGraw-Edison Recloser | 65 |
| | 2. | Port Circuit Simplification | 72 |
| | 3. | The General Electric Recloser | 96 |

CONTENTS (Cont'd.)


| Section | | Page |
|---|---|---|
| V | INTERNAL COUPLING MODELS | 101 |
| | 1. General | 101 |
| | 2. Magnetic Transformer Coupling | 102 |
| | 3. Electric Transformer Coupling | 104 |
| | 4. Electric Internal Cable Coupling | 105 |
| | 5. Electric Coupling to the Sense Switch, Rotary Solenoid, and Trip Coil Terminals with a Sum Mode Drive | 110 |
| | 6. Difference Mode Ports Magnetic Coupling | 111 |
| | 7. The Cable Between the Recloser and the Control | 113 |
| | 8. Equivalent Circuits for Internal and Between-Box Coupling | 123 |
| VI | RESULTS AND CONCLUSIONS | 129 |
| | 1. Bushing Breakdown Analysis | 129 |
| | 2. Polyethylene Breakdown Analysis | 133 |
| | 3. Voltages Across Capacitors at the Ports | 136 |
| | 4. Semiconductor Failure | 137 |
| | 5. Summary | 145 |
| | APPENDIX A | 149 |
| | APPENDIX B | 164 |
| | APPENDIX C | 170 |

CONTENTS (Cont'd.)


| Section | | Page |
|---|---|---|
| | APPENDIX D | 180 |
| | APPENDIX E | 184 |
| | REFERENCES | 187 |

## ILLUSTRATIONS


| Figure | | Page |
|---|---|---|
| 1 | The Number of Days per Year on Which Thunder is Heard at Various Locations in the U. S. A. | 17 |
| 2 | Kit Carson Electric Cooperative System of Substations | 19 |
| 3 | Los Cordovas Substation and its Distribution Lines | 20 |
| 4 | The Los Cordovas Substation | 22 |
| 5 | Photographs of the Los Cordovas Substation | 23 |
| 6 | Poles which Support the Terminals of the Beverage Antenna and its Junction with the Eighty-Foot Section | 27 |
| 7 | Antenna Open Circuit Voltage vs. Angle of Incidence at End of Eighty-Foot Section | 31 |
| 8 | Physical Layout of Wires in the Old Section of the Los Cordovas Substation | 33 |
| 9 | "Wiring" Layout of Old Los Cordovas Substation | 34 |
| 10 | "Receiver" Block Diagram of Old Los Cordovas Substation | 35 |
| 11 | "Stick" Model of the Old Los Cordovas Frame | 37 |
| 12 | Circuit Diagram of the Old Los Cordovas Main Frame with the Lightning Arrestor Circuit and Ground Resistance Included | 39 |
| 13 | Photograph of Old Los Cordovas Substation McGraw-Edison Recloser | 43 |
| 14 | Recloser, Stand, Cable, and Recloser Control Box Interaction | 44 |

ILLUSTRATIONS (Cont'd.)


| Figure | | Page |
|---|---|---|
| 15 | Nameplate of 69 kV/12.47 kV Power Transformer | 49 |
| 16 | External Coupling to McGraw-Edison Recloser | 50 |
| 17 | Set of Autotransformers for Line LI-500 | 52 |
| 18 | Pictorial and Schematic Representations of Autotransformer System | 54 |
| 19 | Open Circuit Voltage to Point "A" Above McGraw-Edison Recloser | 55 |
| 20 | Bushing Configuration for Breakdown Analysis | 57 |
| 21 | Photograph of New Part of Los Cordovas Substation Showing where Power Cable Submerges, Knifeswitch and Lightning Arrestor Array, and Recloser | 61 |
| 22 | Pictorial and Schematic Representation of Model for the New Part of the Los Cordovas Substation | 62 |
| 23 | Block Diagram of Electronic Recloser Control | 66 |
| 24 | Portion of McGraw-Edison Recloser Schematic Depicting Battery Charge, Phase Trip, and Ground Trip Ports of Entry | 69 |
| 25 | Portion of McGraw-Edison Recloser Schematic Depicting Sense Switch, Rotary Solenoid, and Trip Coil Ports | 71 |
| 26 | Battery Charging Port | 73 |
| 27 | Battery Charging Port Simplified Circuit | 74 |
| 28 | Final Simplified Battery Charging Port | 78 |

ILLUSTRATIONS (Cont'd.)


| Figure | | Page |
|---|---|---|
| 29 | Ground Trip Port Schematic | 79 |
| 30 | Intermediate Stage of Ground Trip Port Circuit Simplification | 82 |
| 31 | Portion of Phase Trip Circuit | 82 |
| 32 | Breakdown of Phase Trip Impedance | 84 |
| 33 | Portion of McGraw-Edison Recloser Schematic Applicable to the Sense Switch Port | 87 |
| 34 | Sense Switch Difference Mode Port, Port 4 | 89 |
| 35 | Sense Switch Sum Mode Port, Port 7 | 90 |
| 36 | Rotary Solenoid Port of Entry | 92 |
| 37 | Rotary Solenoid Port Sum Mode - Port 8 | 94 |
| 38 | Trip Coil Difference Mode Port - Port 6 | 95 |
| 39 | Trip Coil Sum Mode Port - Port 9 | 96 |
| 40 | Portion of General Electric Schematic | 98 |
| 41 | General Electric Ground Trip Port | 100 |
| 42 | Dimensions of the McGraw-Edison Recloser, Three Views | 106 |
| 43 | Configuration for Electric Field Coupling to Cable | 107 |
| 44 | Internal Coupling Circuits | 126 |
| 45 | Bushing Voltage Ignoring Failure | 131 |
| 46 | Voltage at Insulation of Cable | 134 |

ILLUSTRATIONS (Cont'd.)


| Figure | | Page |
|---|---|---|
| 47 | Magnitude of Voltage at the Port 1 Terminals | 138 |
| 48 | Vulnerability Ratio versus Frequency for the McGraw-Edison and General Electric Reclosers | 141 |
| 49 | Threshold and Coupling Currents for Port 2 of the McGraw-Edison Recloser and the General Electric Recloser Ground Trip Port | 143 |
| A-1 | Circuit Diagram of 80-Foot Section | 158 |
| C-1 | Portion of Buried Cable Data Sheet | 172 |
| C-2 | Circuit Diagram Representation of Buried Cable | 175 |
| C-3 | Sequence of T and $\pi$ Transformations on a Line Section Performed for Simplification | 176 |

## TABLES


| Table | | Page |
|---|---|---|
| 1 | Sum Mode Ports Field Potential and Capacitance Values | 110 |
| 2 | Ratio of Area Times Number of Turns to the Radius for Magnetic Coupling Calculations of the Difference Mode Ports | 113 |
| 3 | Failure Ratios for the Nine McGraw-Edison Recloser Ports | 139 |
| A-1 | Ground Conductivity and Dielectric Constant at the Los Cordovas Substation, Taos, New Mexico | 151 |
| A-2 | Magnitude of Open Circuit Voltage in Megavolts at Terminals of Beverage Antenna | 157 |
| A-3 | Magnitude of Open Circuit Voltage in Megavolts at End of 80-Foot Section | 162 |
| A-4 | Magnitude of the Characteristic Impedance at the End of the 80-Foot Section for $\psi = 10^{o}$ | 163 |
| B-1 | Parameters Pertinent to the Old Los Cordovas Substation | 169 |

# SECTION I

# INTRODUCTION

## 1. OBJECTIVE AND SCOPE

The object of this study is to perform an analysis of the probability of failure due to nuclear electromagnetic pulse (EMP) effects of a rural electrical cooperative. A high altitude burst, which could have a large ground area coverage, is the assumed source of the pulse. If the results of the study indicate failure, the consequences may have a large impact on electrical power availability in case of attack. Pre- and post-attack countermeasures will then need to be implemented to insure a high rate of survivability.

The rural electrical cooperative chosen for this study is the Kit Carson Electrical Cooperative of Taos, New Mexico. This system is assumed to be fairly typical of such power distribution systems throughout the country. It buys its power from a supplier, having no generation capability, and distributes it to its customers by way of substations. The substation equipment is the most likely part of the system to respond to an EMP, and if failure is likely to occur, it is there where the probability is highest.

Studies on EMP effects on other facets of power systems have been performed and will be referred to in the text. This study analyzes the

special case of one particular substation with its geometric configurations, wire lengths, equipment type, and so forth. These factors will vary for other substations and other systems, but perhaps the results here may be generalized as being typical or the methodology can be applied to other systems and better figures for survivability may be obtained.

## 2. METHODOLOGY

The analytical approach followed is to break up the problem into several parts and then assemble the separate results to obtain the one word answer - "yes" it will or "no" it will not survive. The separate parts are as follows:

### a. The External Coupling Analysis

External coupling begins with the definition of the pulse and how the pulse couples to the system under analysis. The pulse assumed is described in an expression of the form

$$E(t) = E_o(e^{-\alpha t} - e^{-\beta t})$$

or its transform

$$E(\omega) = E_o\left(\frac{1}{\alpha + j\omega} - \frac{1}{\beta + j\omega}\right)$$

where E is the field in volts per meter, $\omega$ is the radian frequency under consideration, t is elapsed time, and $\alpha$, $\beta$, and $E_o$ are appropriately chosen parameters.

Once the pulse is described, the pickup or antenna system by which it couples needs to be known. The antennas of concern at a substation are the overhead customer distribution lines. With an appropriate model of the antenna and the pulse, one has values of impedance, current, and voltage at the entrance to the substation.

The external coupling model continues with the description of the substation system by means of circuit parameters. Wire lengths are represented as lumped element artificial transmission lines, or, if short enough, by their self-inductances and capacitances to ground. Equipment such as voltage regulators and transformers are represented by the best models available either from previous studies or new development for this study. Metallic support structures such as frames and stands also have inductances and capacitances which contribute to the coupling model and need to be calculated.

b. The Internal Coupling Analysis

A particular piece of equipment is assumed to be the most vulnerable because it may have solid state elements in its circuits. At Kit Carson the only solid state devices are contained in equipment known as reclosers, which are electronically controlled circuit breakers. Once we have solved the external coupling problem, voltages and currents may be calculated anywhere in the system, and we particularly need them at the recloser. The coupling to the control box containing solid state devices from circuit voltages and currents at the recloser is described as the internal coupling problem.

c. Port Selection and Threshold Analysis

This analysis involves identifying the most vulnerable components in a circuit by virtue of their being in circuits with paths coming directly from internal energy coupling mechanisms. When this is accomplished, the circuit is reduced by eliminating high impedance paths. The vulnerable component is modeled for breakdown so as to calculate the necessary threshold current. The port is then considered a "black box" with a certain impedance and requiring a certain minimum current for its failure.

d. Combining Results

With the external coupling problem solved we have, with the equivalent circuit, values of voltage and current at the vulnerable equipment. The internal coupling problem gives a voltage and current at the port. The port requires certain values for failure, and if the coupling indicates the port is receiving less than the threshold, then we can assume that the port does not fail. If the energy coupled to the port is greater, then the assumption is that the port does fail.

e. Conclusions

If a port does fail, the reason why should be apparent from the coupling and port analysis. Recommendations are made on the basis of the analysis to "harden" the port by some means. Perhaps failure is due to improper design, and the design stage of the equipment or system layout should be criticized.

The impact of failure on the system and how to return to operation, normal or limited, is considered.

## SECTION II

## THE KIT CARSON ELECTRIC COOPERATIVE

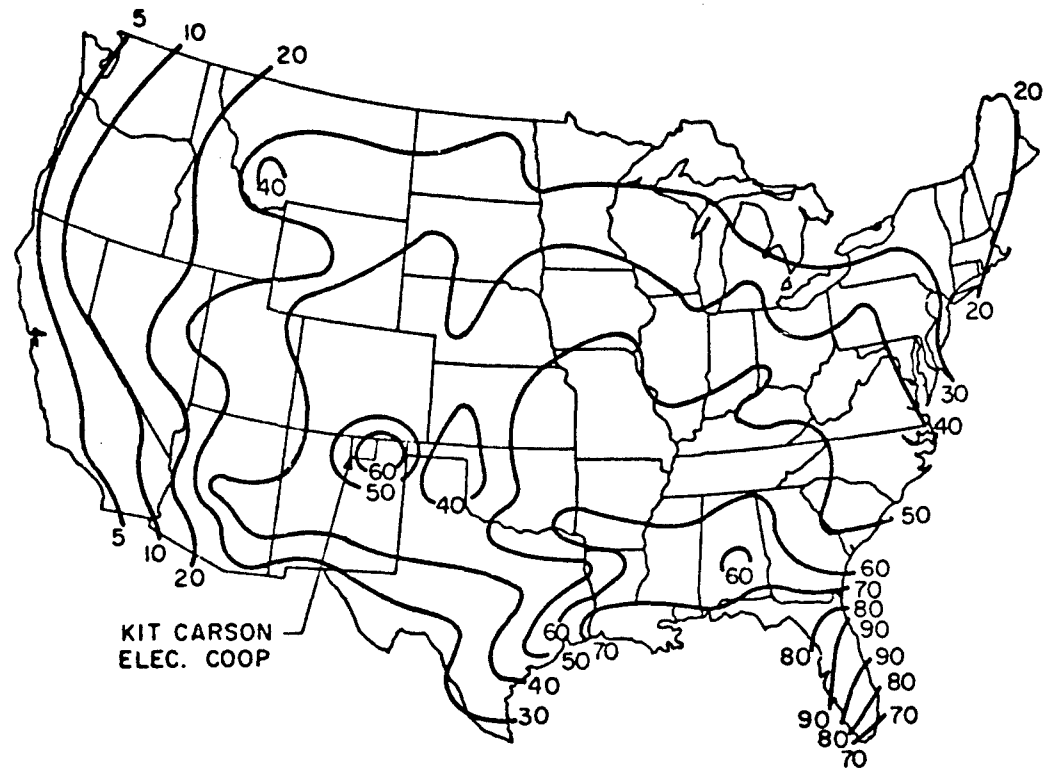
### 1. ORGANIZATION AND LAYOUT

The Kit Carson Electric Cooperative is one of seventeen rural electric cooperatives in New Mexico. In the United States there are 996 similar systems. The majority of these rural systems purchase their electricity from another source and distribute it to customers through systems of substations. In general, they do not have generation capacity of their own. In New Mexico only one of the seventeen electric cooperatives can be considered to be self-sustaining.

The supplier for Kit Carson is Plains Electric Generation and Transmission Cooperative Inc. The supply is delivered by 115 kV lines to a Plains Electric substation which transforms it to 69 kV before distribution to the Kit Carson substations.

Kit Carson has a system of five substations which are fed by two Plains Electric substations. Each of the substations of Kit Carson has a power transformer which transforms the 69 kV to a lower voltage, typically 12.47 kV. In each instance this is three-phase power.

The headquarters for Kit Carson Electric are in Taos. Figure 1 is a map of the United States with contour lines giving number of days per year on which thunder is heard. The location of the Kit Carson




Mean Number of Days
Based on Summaries for
266 Stations Through 1951

Figure 1. The Number of Days per Year on Which Thunder is Heard at Various Locations in the U.S.A. Adapted from "Mean Number of Thunderstorm Days in the United States," Technical Paper No. 19, Climatological Services Division, Weather Bureau, September 1952.

Cooperative is indicated. It is interesting to note that this area of Northern New Mexico lies within a large number contour of thunderstorm days. This implies heavy use of lightning arrestors. These, as will be seen below, are important in the analysis.

All of the administrative and maintenance personnel with the Kit Carson Electric Cooperative are located in Taos, about 150 miles north of Albuquerque. Kit Carson does not have a professional engineer on its staff, and for this purpose, like most rural cooperatives, they employ a professional engineering firm. In the case of Kit Carson the firm is Hicks and Ragland Engineering Co., Inc., of Lubbock, Texas.

Figure 2 is a map of the Kit Carson system showing the various substations of both Plains Electric and Kit Carson. The primary substation is the one at Los Cordovas. This substation feeds the distribution lines to the Taos vicinity, which has the highest population density in the area within the system. It is this substation which receives the greatest emphasis in the analysis.

## 2. THE LOS CORDOVAS SUBSTATION

The Los Cordovas Substation is located about three miles southwest of the center of Taos. This is the substation which serves the greatest number of customers in the Kit Carson system and the one in this study on which the analysis is focused. Figure 3 shows the station with its configuration of source and distribution lines out to about one

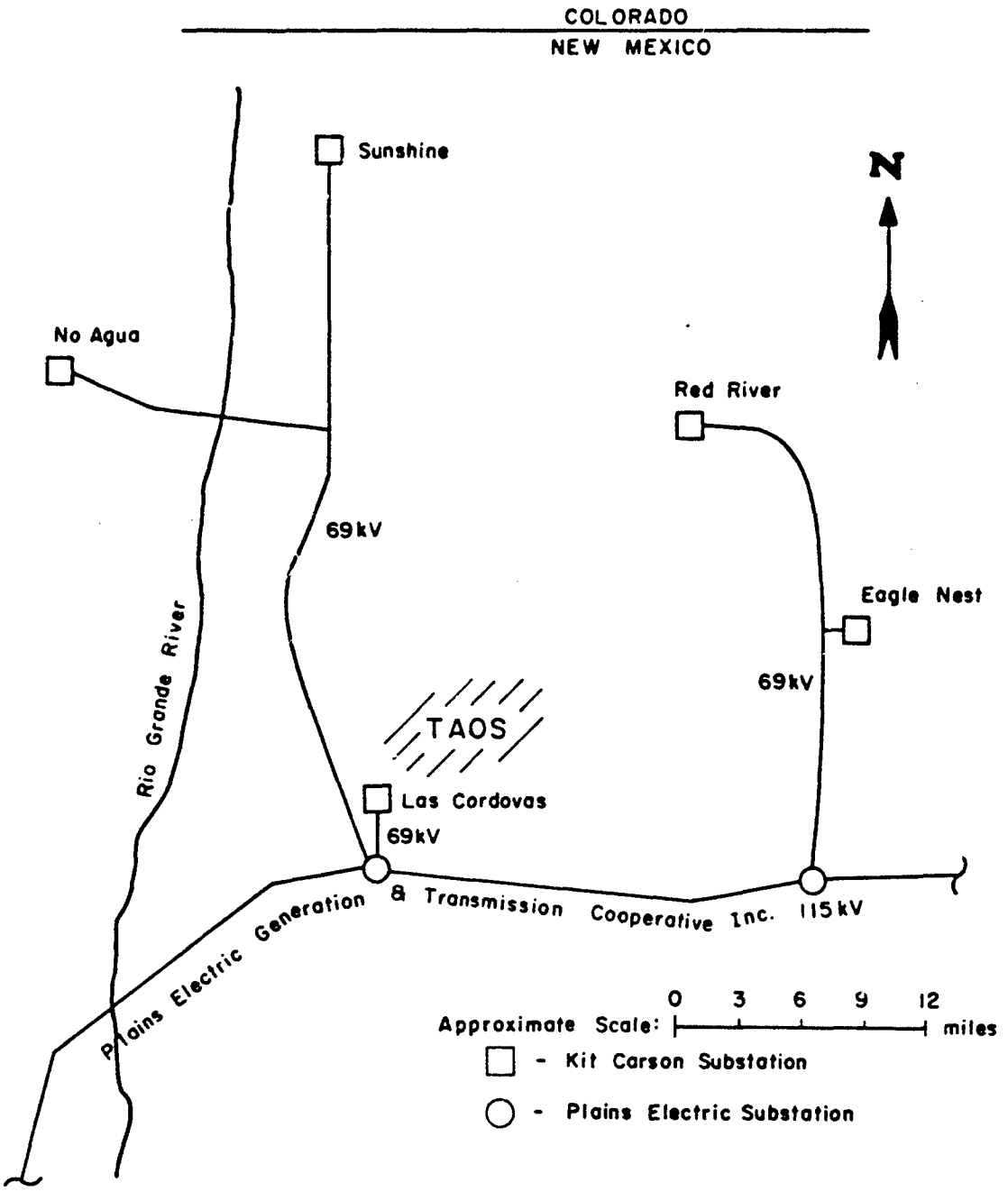



Figure 2. Kit Carson Electric Cooperative System of Substations

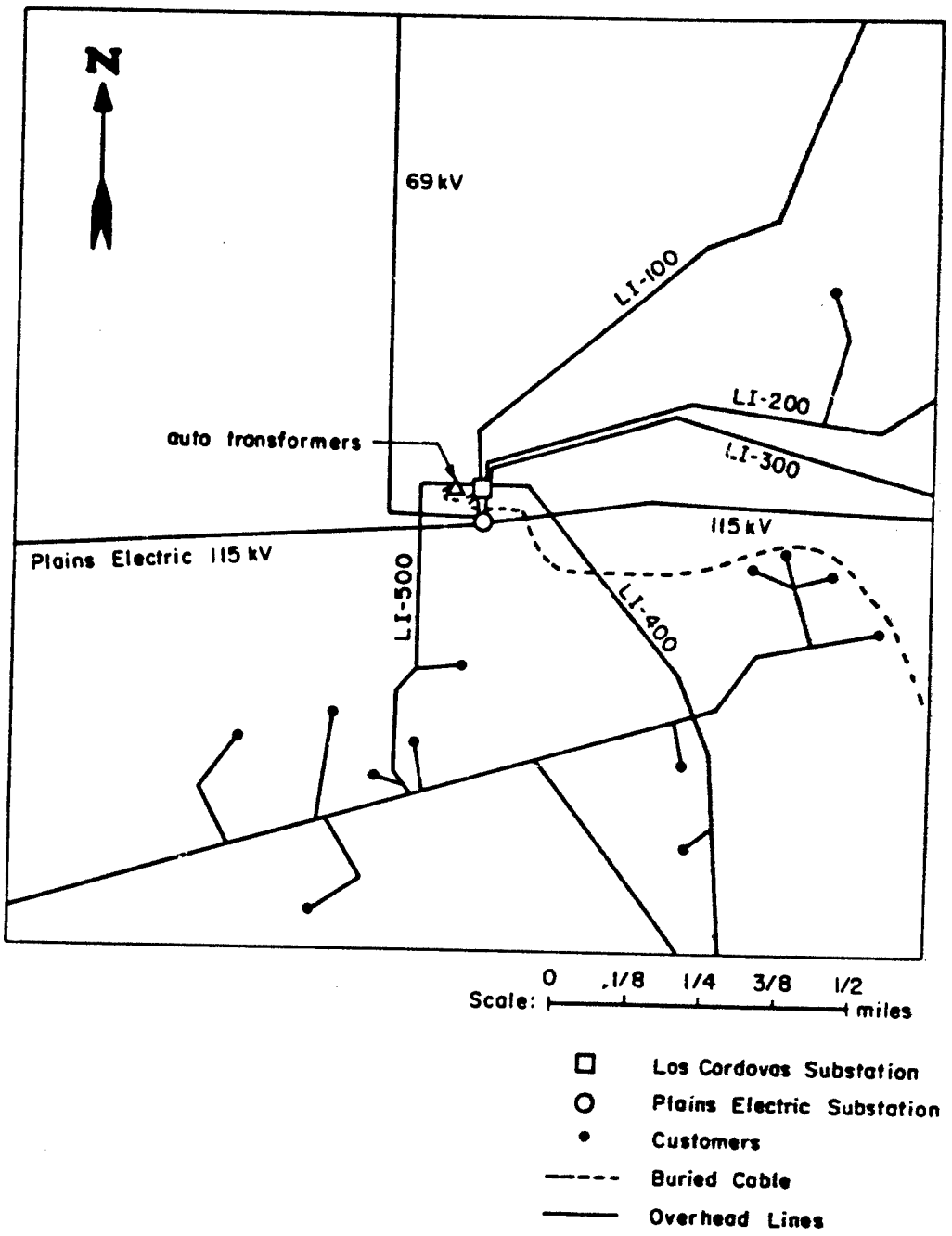



Figure 3. Los Cordovas Substation and its Distribution Lines

mile from the substation. At present, it has six distribution lines, one of which is buried cable, and is fed by two 69 kV lines from the Plains Electric substation.

When this study started, the substation had only one power transformer which fed five overhead distribution lines. But, during the course of the study a new addition to the substation was activated. This new addition has a transformer, and it feeds two distribution lines. One of the distribution lines is the buried cable, but the other is one of the overhead lines previously fed by the old part of the substation. The distribution lines, except for the buried cable, are labeled in figure 3 as lines LI-100 through LI-500. Previously, LI-500 originated in the old part of the substation as a 12.47 kV line. About 145 feet to the west of the substation was a set of autotransformers which stepped up the voltage to 14.4 kV. LI-500 then went on to serve its customers. In the new configuration, a buried cable goes from the new part of the substation, bypasses the autotransformers, and connects to LI-500.

Figure 4 shows the general layout of the components which comprise the Los Cordovas substation. The actual lines which carry the power are eliminated from this drawing in order to avoid confusion. Figure 5a is a photograph of the old part of the substation and is taken in a northeasterly direction. Figure 5b, taken in a northwesterly direction, is of the new part of the substation recently activated. At the

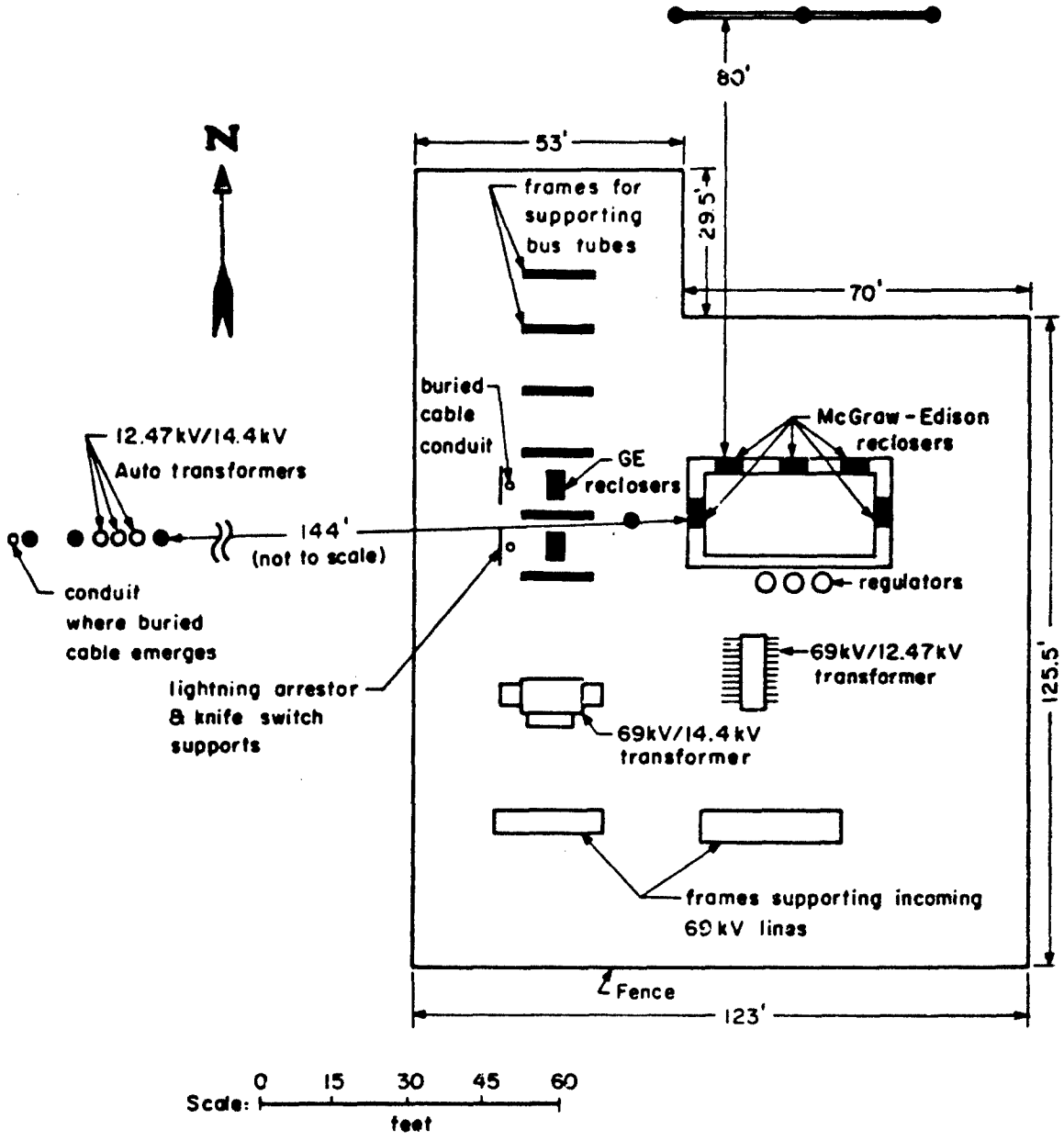
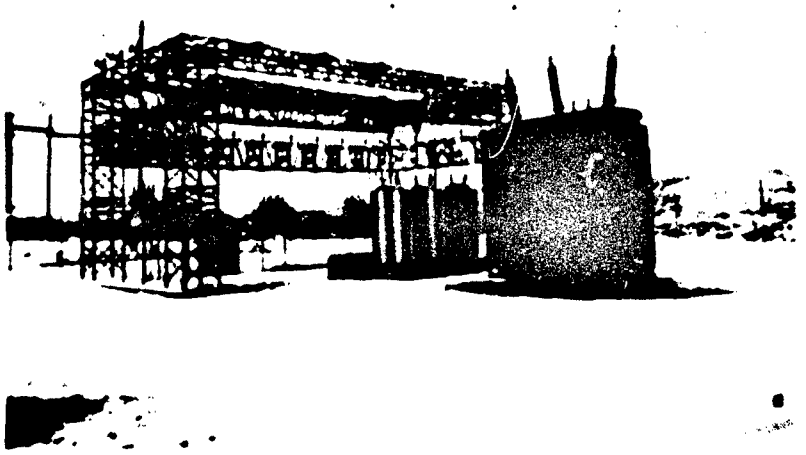
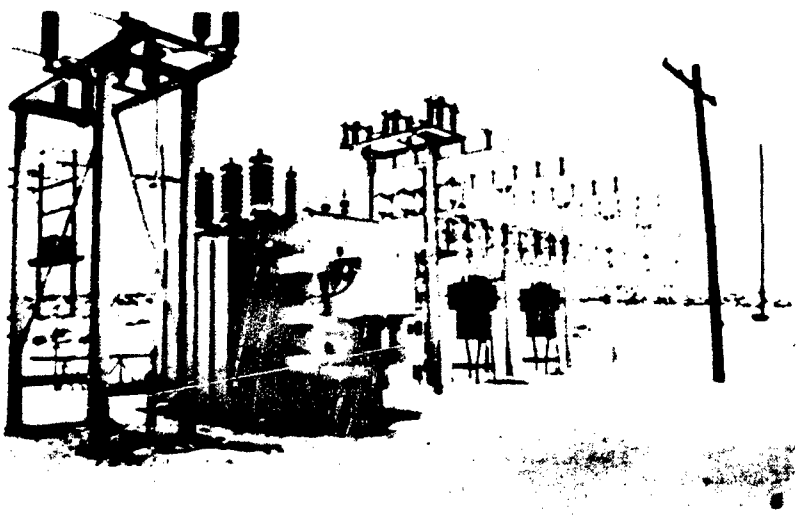



Figure 4. The Los Cordovas Substation



a. The old section of the Los Cordovas Substation



b. The new section of the Los Cordovas Substation

Figure 5. Photographs of the Los Cordovas Substation

present the new facility services two customer lines, but there is the capacity for expansion to five lines.

There are two kinds of electronically controlled reclosers in use at Los Cordovas. An electronically controlled recloser is much like a circuit breaker in that when large currents are sensed on the line, a switch is opened to break the circuit. After a time lapse the switch is closed, but if a large current is still present it reopens, indicating a possible fault in the line. This process repeats itself up to three times, and if the fault is still on line, the recloser locks out, and it will then have to be manually reset. The old facility at Los Cordovas uses reclosers manufactured by the McGraw-Edison Company while the new facility reclosers are by General Electric. More detailed descriptions of the reclosers are given in the analysis sections.

In this study the two parts of the substation are analyzed separately. More information was initially available on the McGraw-Edison recloser so the old section was studied first.

## SECTION III

## EXTERNAL COUPLING MODELS

### 1. DISTRIBUTION LINES AS A BEVERAGE ANTENNA

A form of nonresonant antenna which may be used in the reception of signals is known as a wave antenna or Beverage antenna (ref. 1). This type of antenna may be from one-half to several wavelengths long pointed in the approximate direction of the signal. When the signal is travelling in the approximate direction of the wire toward the receiver, the current induced in the wire travels with similar velocity as the wave and they keep in approximate step with each other.

As an example of EMP effects on the Kit Carson System it has been taken as an intermediate objective of this study to analyze the effects of EMP on the possibly vulnerable components in the Los Cordovas substation. The most important antennas which may pick up and carry the EMP are the customer distribution lines. As can be seen in figure 3, distribution lines radiate from the substation and travel appreciable distances before any perturbations (customers) occur. So, one may treat these lines as Beverage antennas, with the termination of each occuring at poles or frames which support both the lines from the substation and the antenna. It is assumed that the direction and polarization of the EMP

1. Beverage, Harold H., Chester W. Rice, and Edward W. Kellogg, "The Wave Antenna - A New Type of Highly Directive Antenna," Trans. A.I.E.E., Vol. 42, p. 215, 1923.

wave is such as to maximize the coupling to the line under study. This results in a vertically polarized wave propagating approximately along the line for a worst case condition.

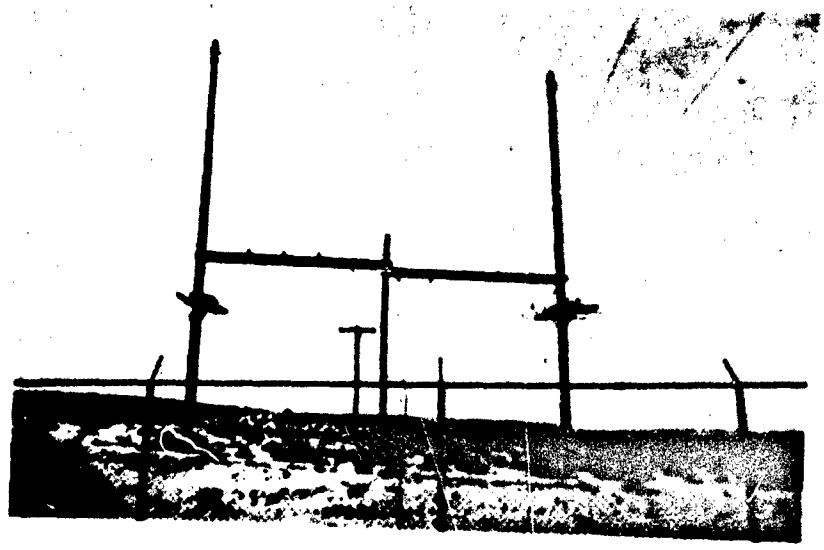
As seen in figure 4, there is a certain symmetry in the placing of the McGraw-Edison reclosers in the old substation. When this study started, all five were in use, although, as explained earlier, one of these was placed out of service. For the purpose of the analysis on the old substation, all five are considered to be in use. The symmetry in the old substation is around the center recloser. This is the recloser which services LI-200, so the Beverage antenna in this study will be this distribution line.

Also seen in figure 4 is a set of three poles directly north of the old main frame. These poles are shown in two views in the photos of figure 6 and are the termination for the lines (antenna) coming in from the east. LI-200 comes in at an angle of about eight degrees relative to the perpendicular of the eighty-foot section of line from the main frame to these poles.

In the calculation of an open circuit voltage and an impedance at the terminals of the Beverage antenna formulas out of Vance and Dairiki (ref. 2) and from Sunde (ref. 3) are employed. Appendix A of this report

2. Vance, E. F., and S. Dairiki, Analysis of Coupling to the Commercial Power System, AFWL TR-72-21, Air Force Weapons Laboratory, Kirtland AFB, NM, August 1972.

3. Sunde, Erling D., Earth Conduction Effects in Transmission Systems, Dover Publication, New York, 1968.



a. View Looking North



b. View Looking Northeast

Figure 6. Poles which Support the Terminals of the Beverage Antenna and its Junction with the Eighty-Foot Section

gives derivations of formulas and techniques employed in the calculation of these values. Table A-2 in appendix A gives the magnitudes of the open circuit voltages which are obtained using these methods. Table A-2 shows these voltages as functions of angle of incidence (above horizon) and frequency. The EMP propagation vector and the EMP electric field vector are assumed to be in the plane which contains the antenna and is perpendicular to the earth. Ten frequencies between 10 kHz and 10 MHz are used in the analysis.

Analysis is performed for five angles of incidence in order to select the worst case condition. Similar calculations were performed in reference 2 and other reports (refs. 4, 5, and 6), but the calculations in this report include earth and line parameters particular to the Los Cordovas substation and the Taos area.

The Beverage antenna concept implies that all three wires which carry the three phase currents are excited in the same way. This is called the sum mode of excitation. But the three wires in the antenna

4. Marable, J. H., J. K. Baird, and D. B. Nelson, Effects of Electromagnetic Pulse (EMP) on a Power System, ORNL-4836, Oak Ridge, Tennessee, December 1972.

5. Baird, J. K. and N. J. Frigo, Effects of Electromagnetic Pulse (EMP) on the Supervisory Control Equipment of a Power System, ORNL-4899, Oak Ridge, Tennessee, October 1973.

6. Babb, D. D., R. M. Brown, and H. Frank, Analysis of Communications Systems, AFWL TR-74-149, Air Force Weapons Laboratory, Kirtland AFB, NM, November 1974.

could be excited in an unbalanced fashion, or a difference mode exictation. The sum mode voltage is actually the average of the open circuit voltages from each wire in the antenna to ground, while the difference mode voltage is the difference in voltage between the outer two, the middle one being neutral. Calculations were performed to produce figures for the difference mode open circuit voltages in order to determine the importance of this mode. The results indicate that sum mode voltages were from about 2.3 to 120 times larger than the difference mode values. So, in considering loads, coupling, and so forth, primary emphasis will be placed in the sum mode, or Beverage antenna mode of excitation.

Although only the magnitudes of complex quantities are presented in table A-2 and in other results, calculations are performed with complex arithmetic, and the phase values are included in the computer output. The Control Data Corporation 6600 computer at Kirtland Air Force Base was employed in the numerical calculations using the FORTRAN language.

## 2. THE EIGHTY-FOOT SECTION

A similar table to table A-2 may be presented to give the characteristic impedance values for the antenna. However, at this point, we will add the effects of the eighty-foot section between the end of the Beverage antenna and the insulators at the main frame. The southern end of the eighty-foot section is really the entry point into the old Los Cordovas substation, and open circuit voltages and characteristic impedances at this point are of interest.

The eighty-foot section is treated in two ways. First it is considered to be driven only by the Beverage antenna. This is the case where perfect shielding of the substation is considered to exist from illumination by direct means. Secondly, the section, in its own right, was considered to be an antenna, assuming the no-shielding condition. There does exist a grid of wires over the substation which could act as a shield, but the spacing between the wires of the grid is such that it may be considered ineffective. Techniques employed in the calculation of values pertinent to the eighty-foot section are also given in appendix A. In comparing the shielded and non-shielded calculations, it was noted that the unshielded answers were less than five percent higher than in the shielded case. Since the wire grid over the substation is considered ineffective as an EMP shield, in the analysis the eighty-foot section is considered to be an antenna.

Table A-3 in appendix A gives the open circuit voltages at the insulator at the end of the eighty-foot section, again as functions of angle of incidence and frequency. The effects of the eighty-foot section as a transmission line are readily seen, as the numbers are smaller than those in table A-2. Figure 7 is a plot, for some selected frequencies, of these voltages as functions of the angle of incidence. It is apparent from both tables and the graph that the angle of incidence for a worst case condition is ten degrees. In the coupling calculations for the interior of the substation, the driving voltages are those of the ten degree angle of incidence.

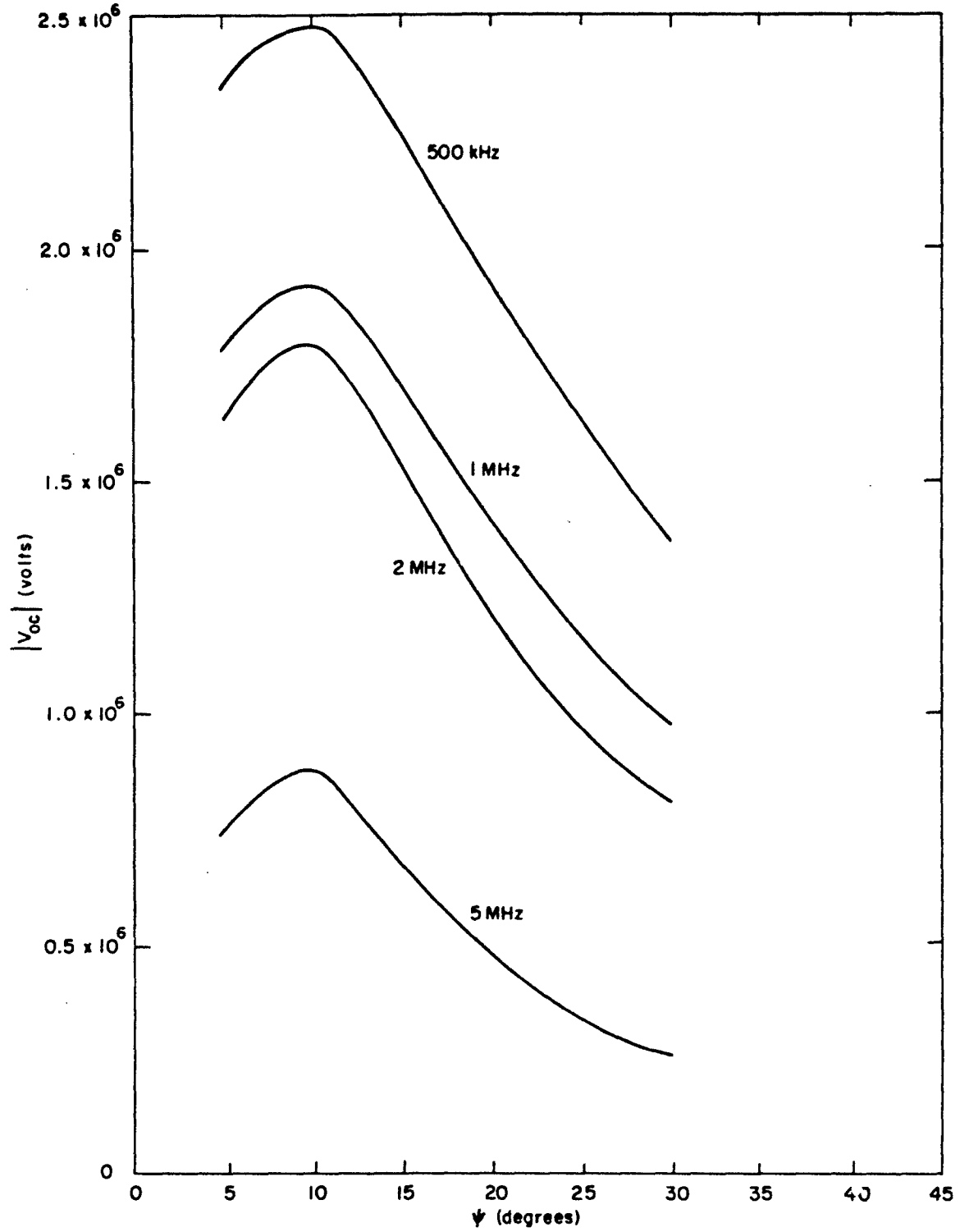



Figure 7. Antenna Open Circuit Voltage vs. Angle of Incidence at End of Eighty-Foot Section

The other parameter needed at the end of the eighty-foot section is the characteristic impedance. Table A-4 in appendix A gives the calculated values for the frequencies of interest, for a ten degree angle of incidence.

## 3. COUPLING TO THE McGRAW-EDISON RECLOSER

In performing a vulnerability study the first task is to identify components of a system which are the most vulnerable. The most obvious are any solid state devices, i.e., transistors, diodes, and the like. In the old part of the Los Cordovas substation, the only solid state devices are located in the control units of the reclosers. Other tasks then involve identifying the ports through which the EMP energy can enter and fail the device and identifying coupling paths and loads which affect the amount of energy which may reach the device.

Figure 8 identifies the physical layout of the old part of the Los Cordovas substation. This is translated into the "wire" diagram of figure 9 and the block diagram of figure 10.

Up to now the only numerical values we have presented are the open circuit voltages and antenna impedances for several frequencies at point "A" in figure 10. So assuming one wants values at the recloser control box, one must model the boxes of figure 10 in terms of electrical parameters. In doing so one must keep in mind the frequency range which is being considered. The highest frequency is 10 MHz, so lengths of wires

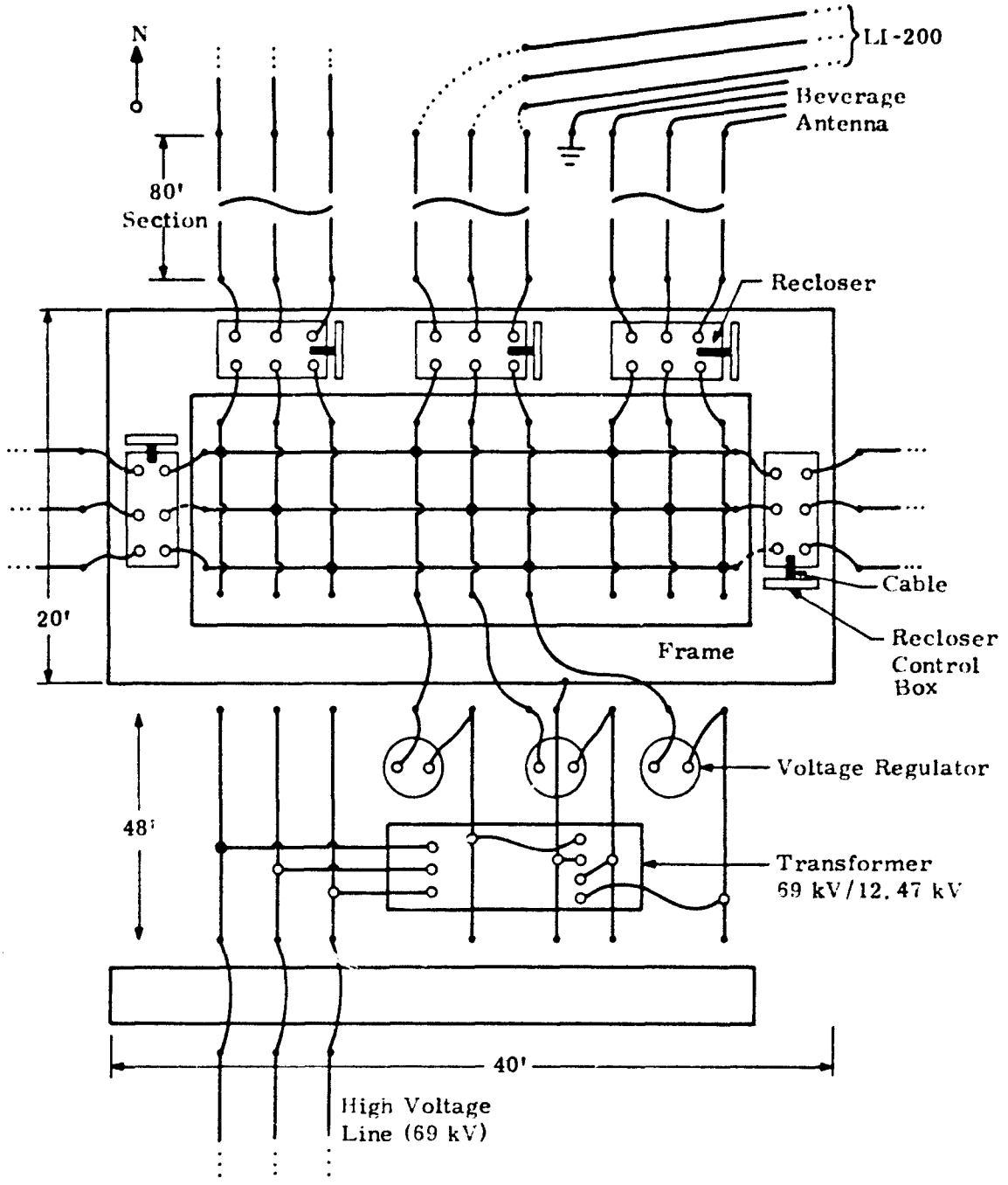



Figure 8. Physical Layout of Wires in the Old Section of the Los Cordovas Substation. Diagram is not to scale, but some dimensions are given.

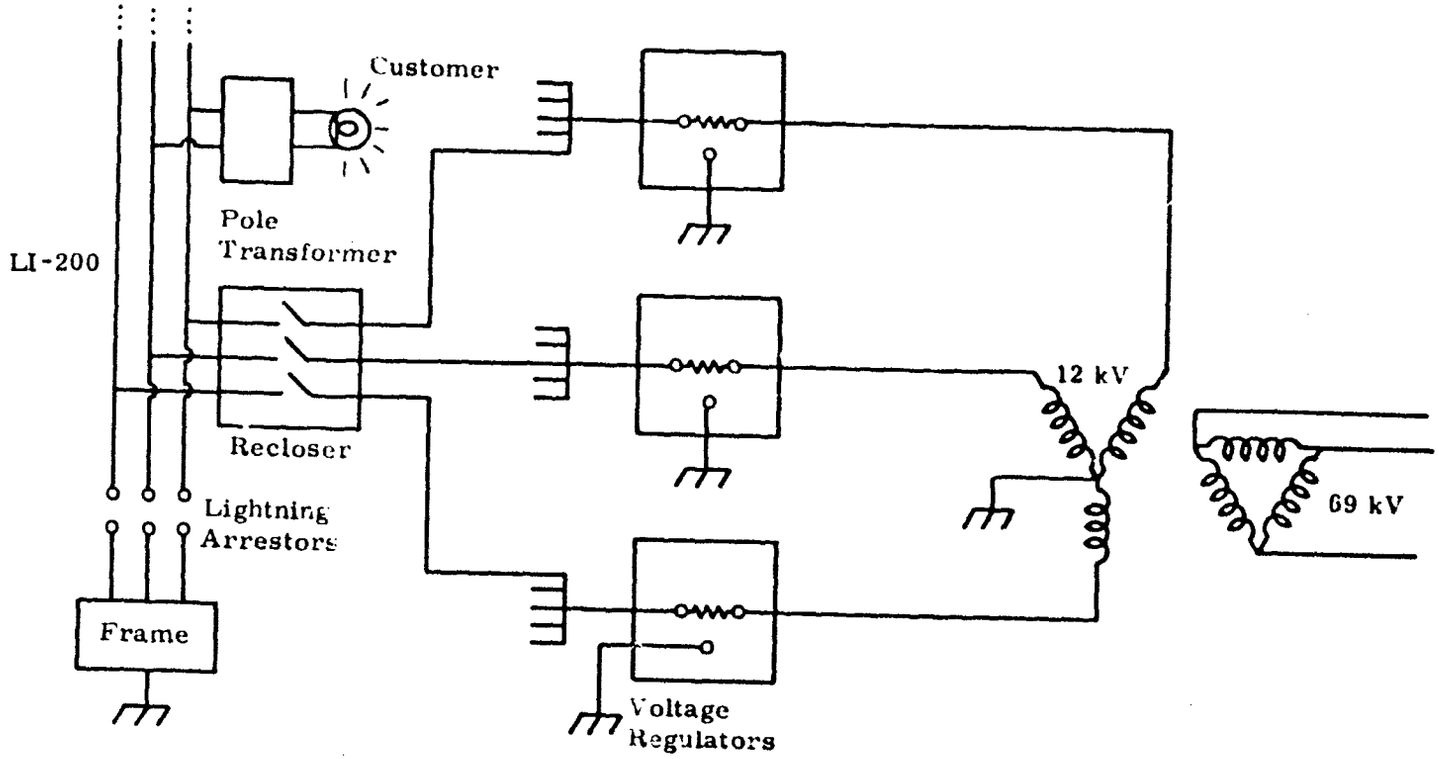



Figure 9. "Wiring" Layout of Old Los Cordovas Substation

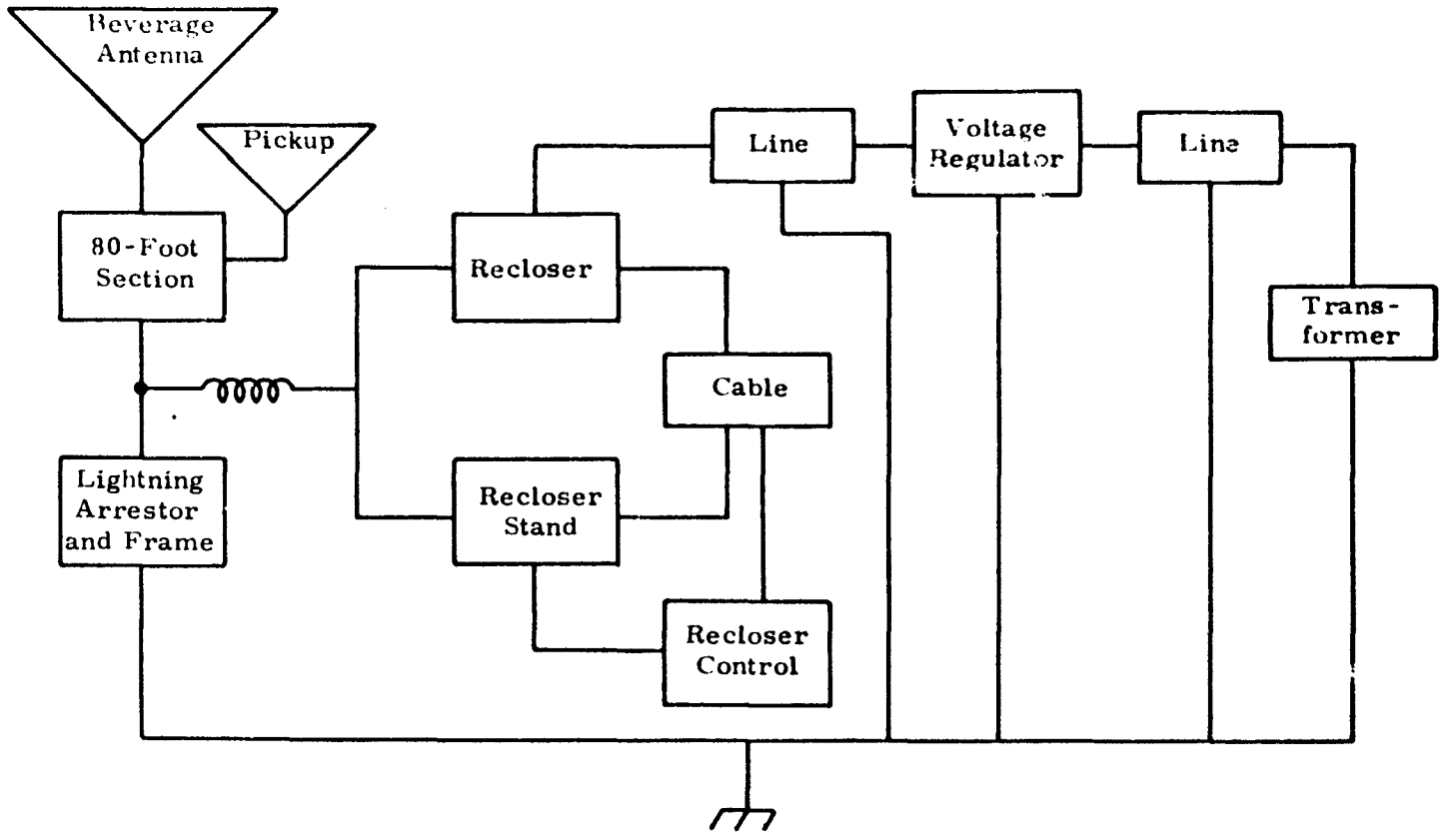



Figure 10. "Receiver" Block Diagram of Old Los Cordovas Substation

and structures must be kept below some maximum in order to avoid unwanted effects, such as cutoffs and resonances, that are not really there. One criterion for determining this length is to keep lumped wire lengths below one radian wavelength. For 10 MHz the wavelength is 30 meters, so one radian would be $30/2\pi$ meters or 4.775 meters. This is about 188 inches. Another criterion which is considered to be good engineering practice is to make the lengths shorter than 1/8 wavelength. For 10 MHz this is about 148 inches. For this study a value in between these two is chosen, namely 160 inches. So relatively long lengths of wire are broken up into segments of about 160 inches and considered to be sections of lumped element artificial transmission lines.

Point "A" in figure 10 is the end of the Beverage antenna plus eighty-foot section and therefore the entry point into the substation proper. This point branches in two directions, one to the McGraw-Edison recloser and the other to a lightning arrestor. The lightning arrestor will connect point "A" to the main frame if it fires, otherwise the arrestor and frame will remain out of the system.

If the arrestor does fire, one is faced with the problem of how to model the arrestor and frame. Pages 54 through 57 of reference 2 and section 4.2 in reference 4 both have discussions concerning lightning arrestors. Page 55 in reference 2 states that lightning arrestors are selected to fire at voltages three to four times as large as the rms value

of the circuit voltage. The old part of Los Cordovas is a 12.47 kV system, but the arrestors are rated for 18 kV. In our analysis we took three times the 18 kV, or 54 kV, as the breakdown and sustained discharge voltage, $E_d$, for all frequencies. So if the voltage at a lightning arrestor meets or exceeds 54 kV, it is represented as a 54 kV source with the phase set such as to minimize the current going through the arrestor.

The lightning arrestor is tied to the frame for its discharge path. Figure 11 is a three-dimensional "stick" drawing of the frame, with

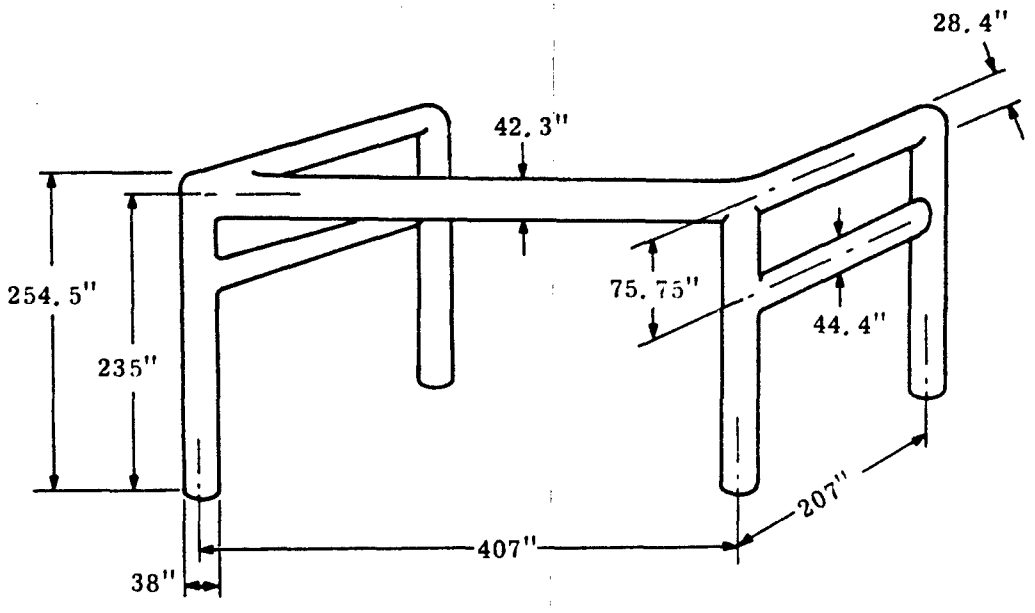



Figure 11. "Stick" Model of the Old Los Cordovas Frame

dimensions. In treating the frame as wires of the dimensions given, the formulas of section 2 in Terman (ref. 7) may be used in estimating the inductance and capacitance to ground values. In doing the calculations, lengths were kept at or below the 160 inches mentioned earlier. The resultant circuit diagram of the frame represented as an artificial transmission line is shown in figure 12.

The values indicated in figure 12 include the wire lengths from point "A" to and through the lightning arrestor and to the point where the wire actually connects to the frame. Appendix B in this report gives techniques and details in the computation of these values, but at this point it is important to note that the antenna and eighty-foot section actually consist of three wires since it is a three-phase power system. So point "A" really consists of three points, and there are three lightning arrestors and so forth. Therefore the inductor value of the wire from point "A" to the point where the wire connects to the frame is divided by three and the capacitance is multiplied by three. In other words the wires which carry the three phases are thought of as being in parallel.

Similarly, although there is only one main frame, there are a total of five customer distribution lines which come into the substation and tie on to lightning arrestors. The currents due to the discharge are not the

7. Terman, F. E., Radio Engineer's Handbook, McGraw-Hill Book Company, New York, 1943.

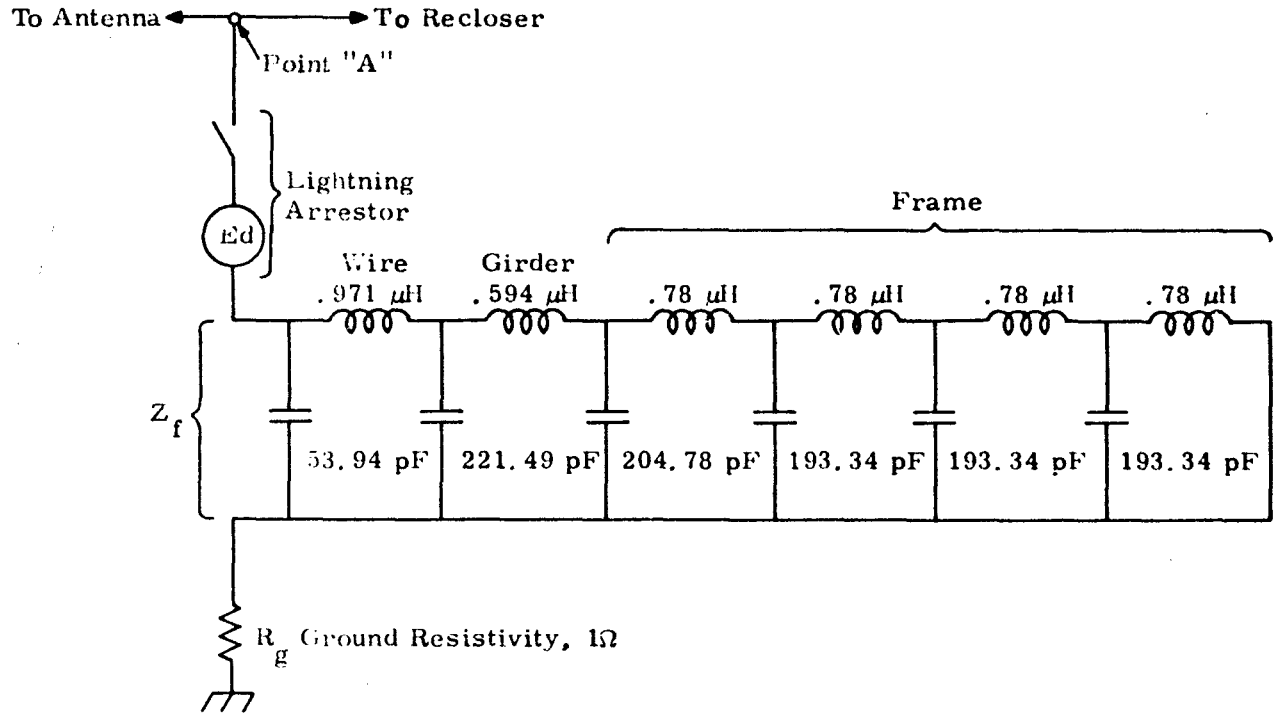



Figure 12. Circuit Diagram of the Old Los Cordovas Main Frame with the Lightning Arrestor Circuit and Ground Resistance Included. The Frame is Represented as a Lumped Element Artificial Transmission Line.

same for all five lines however, since the direction of incidence is picked for a worst case condition on line LI-200. As a rough estimate of the ratio of current which the other four lines have compared to LI-200, figures from section II-C in reference 2 can be used. The results of our rough estimates say that LI-100 will have about 50%, LI-300 will have 100%, and both lines LI-400 and LI-500 about 20% of the value for LI-200. Adding the percentages we have come up with a factor of 2.9 times the value of the current due to LI-200 alone. This factor is equivalent to having the impedance of the common current path multiplied by 2.9. In the calculations below then, when all five lines have something in common the factor of 2.9 will be applied to the impedance along that path, i.e., inductances will be multiplied and capacitances divided by 2.9. Referring to figure 12 the circuit parameter values reflect the factor of three due to the three wires per line and the factor of 2.9 due to the five customer lines.

The frame of course goes to ground, so at this point mention of the ground resistance at the substation is in order. There is a ground mat consisting of a wire grid buried below the substation. Twelve-foot ground rods are tied to the mat at various locations throughout the substation. The mat itself is buried a few feet below the ground surface. Values of ground resistivity were measured during one of the trips to Los Cordovas with a Hicks and Ragland engineer, yielding low frequency

figures for the ground resistance. The measurements were made using a three-electrode meter, which applies a current between two electrodes and measures the voltage between one of these electrodes (the common electrode) and the third electrode. The frequency of the current source is about 100 Hz. The meter measures the ratio of the measured voltage to the impressed current by use of a hand adjusted null bridge. In obtaining values at Los Cordovas the electrodes were placed about ten feet from each other with the common electrode connected to the ground mat, and the other two stuck about six inches into the ground. Ground resistance values obtained varied from 2 to 5 ohms within the station. In the model, the ground resistance is taken to be 1 ohm. This lower value was chosen since all the resistance readings, tied to the ground mat, may be considered to be due to resistance in parallel. Also with the electrodes being only six inches into the ground the readings can be expected to be higher than if they were deeper. This value is estimated to be good for all frequencies under consideration. Modeling the ground system with all its complexities as a function of frequency and location is beyond the scope of this study.

The next step in building the model for figure 10 is to go from point "A" to the boxes associated with the recloser itself. First there is a bit of inductance leading away from point "A". This represents the wire from the tie point near the insulator, through a knifeswitch, and to

the top of the high voltage insulator which surrounds the wire at the point of entry into the recloser. The wire-surrounding insulator is called a bushing. There is also a wire connecting the box labeled "recloser stand." There is coupling between the line and the stand due to bushing capacitance. Greenwood in table 15.3 of reference 8 gives the capacitance value of a 15 kV class, 1200-ampere rating bushing as 190 to 220 pF. This study uses 200 pF as the estimate for bushing capacitances. The path between the two bushings through the recloser itself is represented as an inductance.

Figure 13 is a photograph of the recloser, its stand, the control box, and the cable connecting the recloser with its control. From this figure we can see that current flowing in the stand couples through the field it establishes to the control cable and into the recloser control box. There is coupling inside the recloser to the control cable, which of course leads to the control box. It is in the recloser control box where the solid state devices which may fail are located. The actual methods used in computing parameter values and in modeling this set of boxes is discussed in later sections and in appendix B, but figure 14 is a diagram, with parameter values, of the results.

8. Greenwood, Allan, Electrical Transients in Power Systems, John Wiley & Sons, Inc., New York, 1971, Chapter 15.

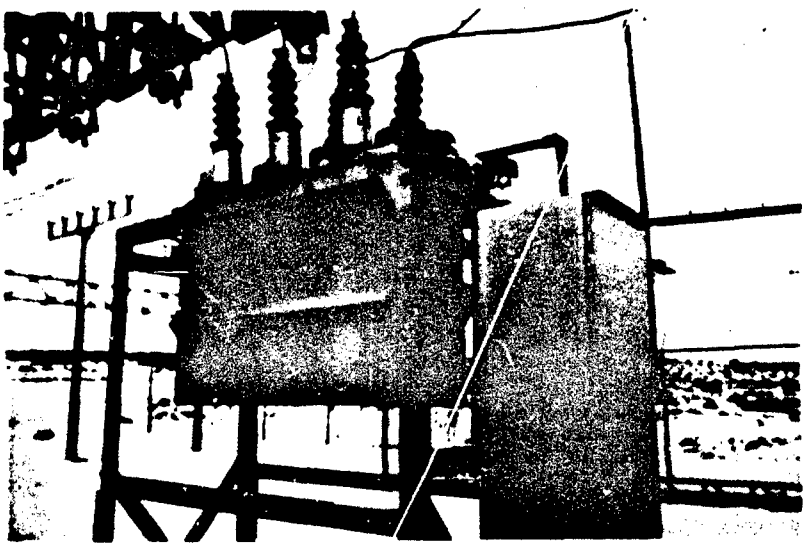


Figure 13. Photograph of Old Los Cordovas Substation McGraw-Edison Recloser

In the dashed box labeled "Recloser Control" in figure 14 are two boxes. These represent the impedances, $Z_{p1}$ and $Z_{p2}$, of two ports within the control box. These ports are places where EMP energy can couple to potentially vulnerable components directly through the cable from the recloser. We have identified a total of nine ports within the recloser control box of which only two couple directly to the lines coming into the recloser from the Beverage antenna. A third port couples directly to the antenna when it is excited in the unbalanced or difference mode mentioned earlier, but in the sum or Beverage antenna mode this port does not affect the impedance for the $Z_s$ calculations of figure 14.

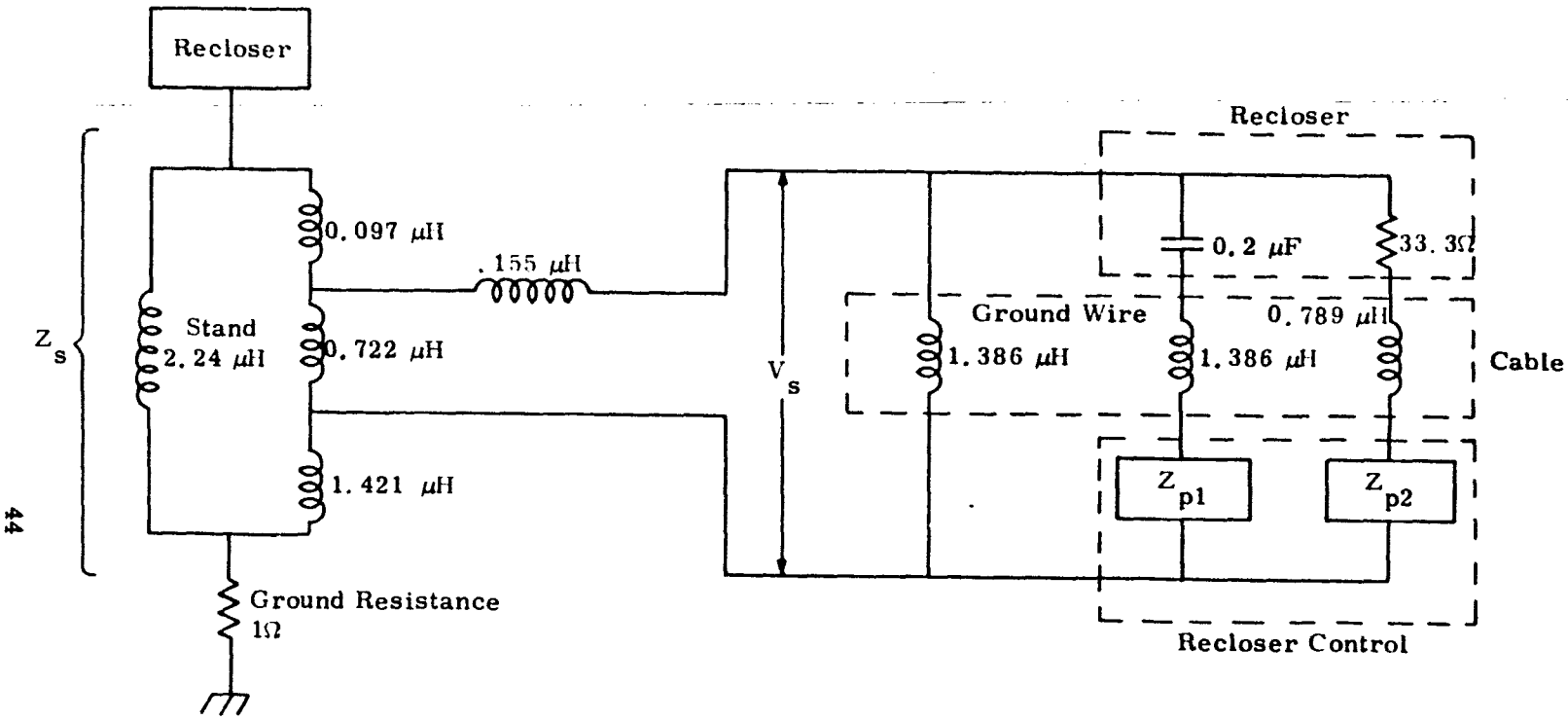



Figure 14. Recloser, Stand, Cable, and Recloser Control Box Interaction

The individual ports and their coupling mechanisms will be discussed in more detail later. The elements adjacent to the recloser are loads in the system. These loads are represented in figure 10 by the boxes to the right of the recloser. The first box is labeled "Line" and this is the set of wires leading from the side of the recloser opposite the antenna through the overhead grid of wires within the main frame, and to the bushings at the voltage regulator. The grid of wires at the frame distributes the 12.47 kV output from the transformer to five outgoing customer lines. The diagram in figure 8 shows this grid and how it is hooked up to accomplish its division into five. To put it simply, one wire, representing one of the three phases, coming from one regulator is connected to all five reclosers through the grid. In our model the line from the recloser to the point where it connects to the wire having all reclosers in common will have its parameter values when represented as a lumped element artificial transmission line operated on by the factor of three due to the three wires per line. But from this point out to the regulators and transformer, the factor of 2.9 due to the effects of all five antennas contributing to the system is considered. The line between the recloser and the regulator will be represented as a lumped element artificial transmission line with the appropriate factors of 3 and 2.9 used where applicable.

The voltage regulator is a General Electric single phase reactor type. The regulation takes place when an inductive reactance in series

with a load changes inductance according to what a sensing and feedback control circuit dictates. Shunting this reactor is a "Thyrite" resistor for protection. Thyrite is General Electric's name for a silicon carbide non-linear resistor with a negative coefficient of resistivity. Under normal operating conditions the resistance is high, such that not much power is dissipated from it, but with surges of voltage its resistance drops and much of the current is diverted through it. No values are available for the normal inductance of the reactor or the normal resistance of the Thyrite, but in modeling them one may choose values based on keeping the 60 Hz power losses, due to these components, at some kind of economical minimum, and nameplate information.

The kVA (kilovolt-ampere, apparent power) rating of the regulator according to the nameplate is 333 kVA. If this is divided by the maximum current allowed in the system, 437A (again based on nameplate information), one then gets a voltage drop across the regulator of 762 volts. The impedance then is 762/437 or 1.74 ohms. This impedance is due to a Thyrite resistor in parallel with an inductor. If one assumes that the most loss which can be tolerated due to $I^2R$ in the Thyrite is 5000 watts and if there is no resistance loss in the inductor, then the Thyrite branch will carry 6.56 A with 762 V across it. The 5000 watts represent a 1.5% loss at the kVA rating of the regulator. This means the Thyrite will have a resistance of 116 ohms. The inductor branch has the rest of the current,

or 430 amps. The impedance across the inductor will be 762/430 or 1.77 ohms. At 60 Hz this impedance implies an inductance of 4.69 mH. The impedance due to the inductor would be very high at the frequencies of concern and may be ignored. This leaves the Thyrite to model.

Under normal conditions at 60 Hz the Thyrite has an impedance of approximately 116 ohms with a current of 6.56 A flowing through it. However, our calculations show that the current flowing through the resistor during an EMP is as high as three orders of magnitude greater. The voltage drop across the Thyrite will increase by much less than one order of magnitude. Section 12.2 in reference 8 discusses properties of the silicon carbide nonlinear resistors and in applying the formulas and curves given there one finds that the Thyrite has a resistance as low as 0.4 ohm during peak current conditions. The resistance is higher for lower currents, so in modeling the Thyrite one may represent it as a fixed resistor and assign it values of 0.4 ohm in one calculation and 4 ohms in another for comparison. The difference in the results are negligible, so in the final model the 0.4 ohm is used. This resistance is divided by three for the three parallel circuits and multiplied by 2.9 for the five sources of current, thereby appearing as 0.387 ohm in the model.

The voltage regulator also has bushings with capacitances to the case. Capacitance values are estimated as above, as with the recloser

bushings. Furthermore the inductance of the current path from the input bushing through the regulator with its Thyrite and to the output bushing is calculated and included in the model. Again as above, the factors of 2.9 and 3 are taken into account.

The line between the voltage regulator and the power transformer is modeled as a lumped element artificial transmission line. This takes us to the transformer. The power transformer is a three-phase delta-wye General Electric 69 kV/12.47 kV transformer with a delta winding primary and a center grounded wye secondary. Shown in figure 15 is the nameplate which aids us in determining the characteristics of the transformer.

One can see from the nameplate that the BIL (Basic Insulation Level) for the low voltage winding is 110 kV, and the transformer size is 7500 kVA. Greenwood in chapter 15 of reference 8 describes methods by which one may obtain parameters such as capacitance to the case of the windings. Using his tables and graphs and the nameplate information, we have obtained a winding to case capacitance of 6200 pF. On page 423 of reference 8 Greenwood states that the winding capacitance obtained from the graphs must be multiplied by 0.33 to 0.406 for a wye winding, so the 6200 pF figure we obtained is multiplied by the average of these two numbers, or 0.368, to get an effective capacitance of 2282 pF. The total capacitance per phase is then 2482 pF, including a 200 pF bushing-to-case capacitance. The factors of 2.9 and 3 are then taken into account

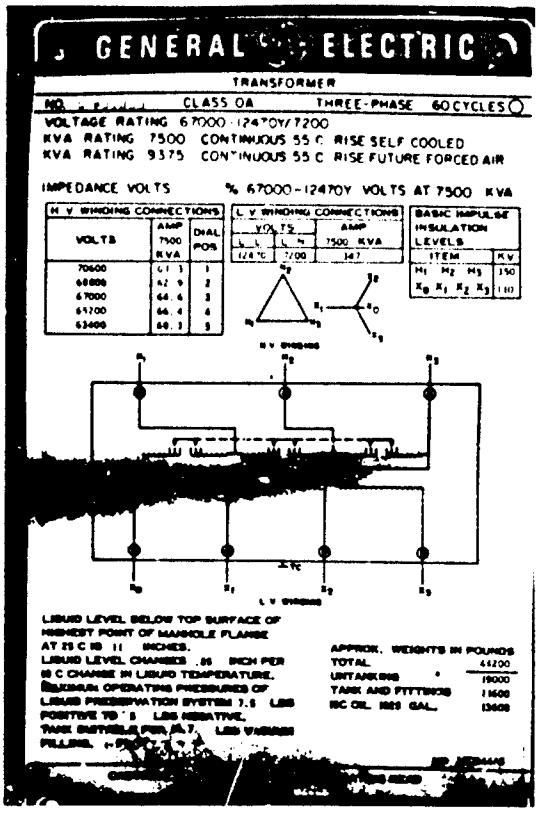



Figure 15. Nameplate of 69 kV/12.47 kV Power Transformer

as above. For the frequencies of consideration, the inductance of the windings are too high to have any effect on the model, and so the transformer is modeled as a capacitor.

This completes the modeling for the external coupling to the McGraw-Edison recloser and a circuit diagram of the results is given in figure 16. The factors of 2.9 and 3 are included in the numerical values given. Appendix B gives a more detailed description of the methods used in obtaining these values.

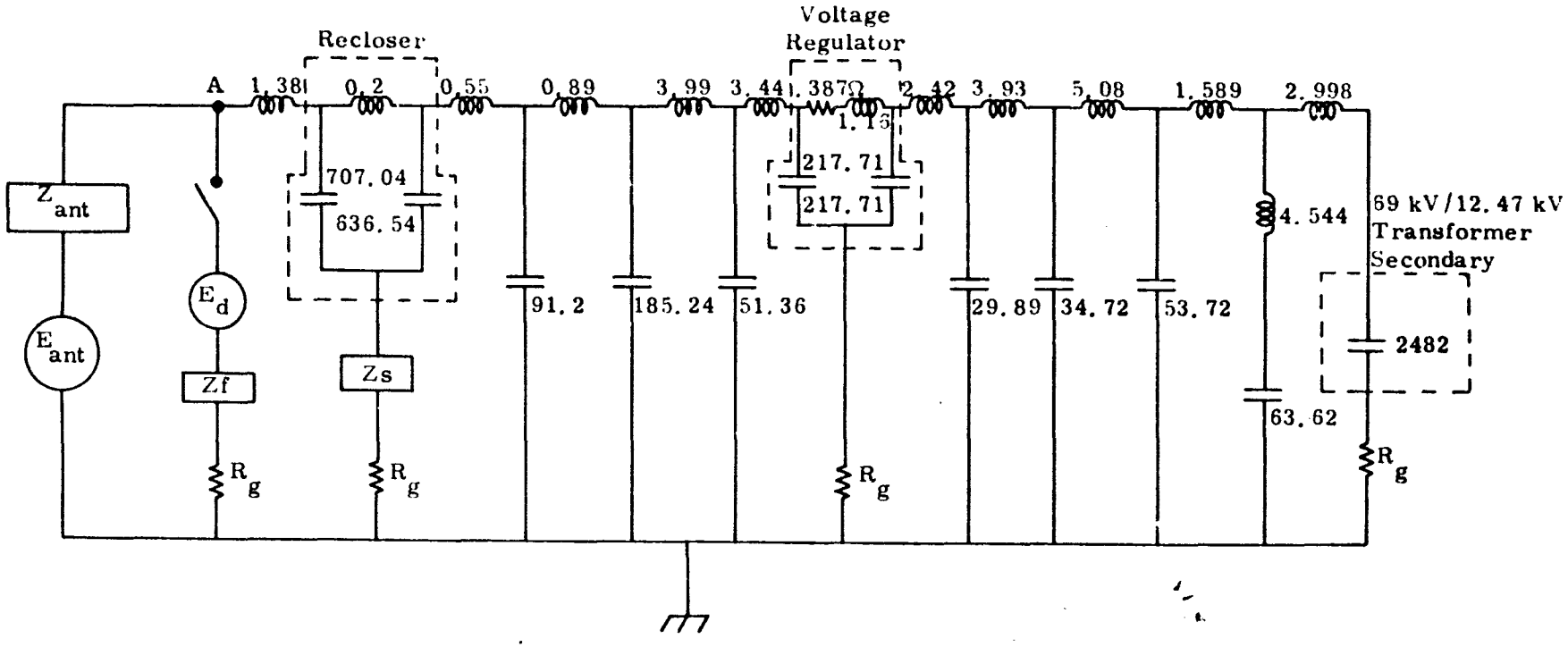



Figure 16. External Coupling to McGraw-Edison Recloser (Inductance values in microhenries. Capacitance values in picofarads. Factor of 3 and 2.9 included where applicable)

## 4. A PROBLEM INVOLVING AUTOTRANSFORMERS

There is one line, LI-500, which, when it was connected to the old section of the Los Cordovas substation, differed from the other four lines by having a set of three step-up autotransformers in its path. These transformers had the function of stepping up the voltage from 12.47 kV to 14.4 kV. Although the autotransformers are not considered in deriving a model for the external coupling to the McGraw-Edison reclosers in the preceding section, this section presents values at the corresponding point "A" for comparison. In these calculations the EMP incidence is such that LI-500, rather than LI-200, is getting maximum coupling.

Figure 17 is a photo of this set of autotransformers. Note in the photo the pole directly to the left of the transformer support structure. Next to this pole is the conduit where the buried cable from the new part of the substation emerges. At the time the photo was taken the cable from the new substation was not connected to LI-500 but the autotransformers were. The poles which support the autotransformer platform also support lightning arrestors both where the line comes in and where it leaves the transformer area. The three objects on the cross member directly above the transformers are knifeswitches for taking a transformer out of the circuit if necessary. The distance between the exit point on the right-hand pole to the equivalent point "A" over the McGraw-Edison recloser is about 144 feet.

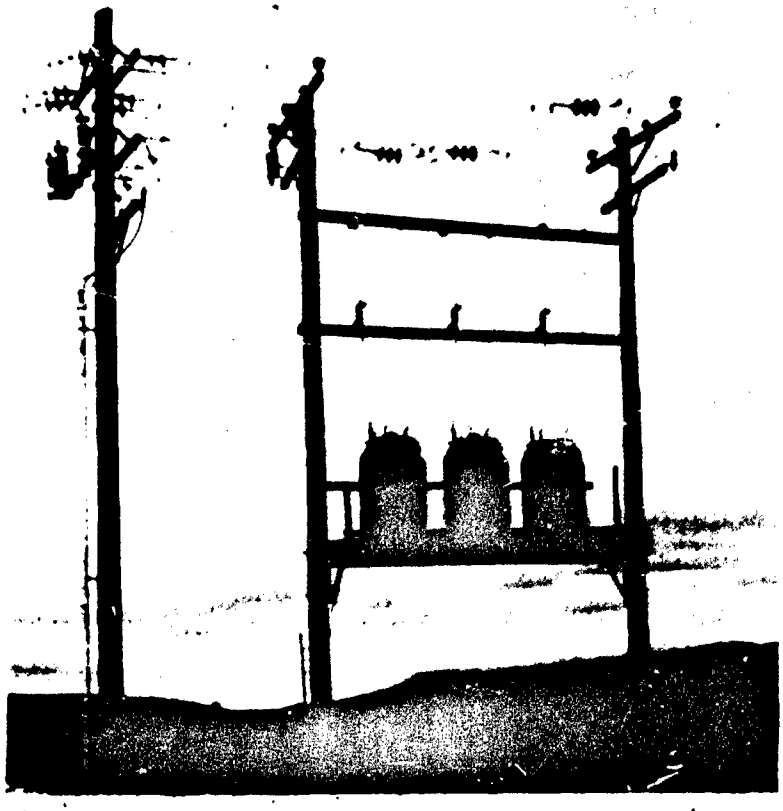


Figure 17. Set of Autotransformers for Line LI-500

In modeling the autotransformer system we consider the lightning arrestors the same way as the ones at the main frame. The autotransformers themselves are modeled as capacitances due to the bushings, with the inductive impedance due to the windings too high to be considered for our range of frequencies. The grounding system for the poles and platform which support the transformers consists of a wire which connects

the lightning arrestors to a grounding wire along the edge of the support platform and down to a ground rod buried alongside each pole. The 144-foot section between the autotransformer system and the old Los Cordovas station is represented as a lumped element artificial transmission line.

Figure 18 is a line drawing of the autotransformer configuration and its equivalent circuit diagram. In this representation only one of the three sets has its parameter values computed and then impedance results are divided by three to include the three phases in parallel. When computing values for this part of the study, we are interested in seeing results of the open circuit voltage at the end of the 144-foot section at point "A" at the old Los Cordovas substation for comparison with values at LI-200. This is to insure again that a worst case condition has been chosen. The autotransformer configuration is the only significant difference for all five lines. The open circuit voltage from the antenna and eighty-foot section peaks around 200 kHz, so to keep the calculations simple the autotransformer configuration model is less stringent from a high frequency validity standpoint than our previous calculations. Where previously the model was valid to at least 10 MHz, the present set of calculations involving the autotransformer and 144-foot section is only valid to about 2.5 MHz.

Figure 19 is a graph of the open circuit voltage at the equivalent location above the McGraw-Edison recloser for both types of customer

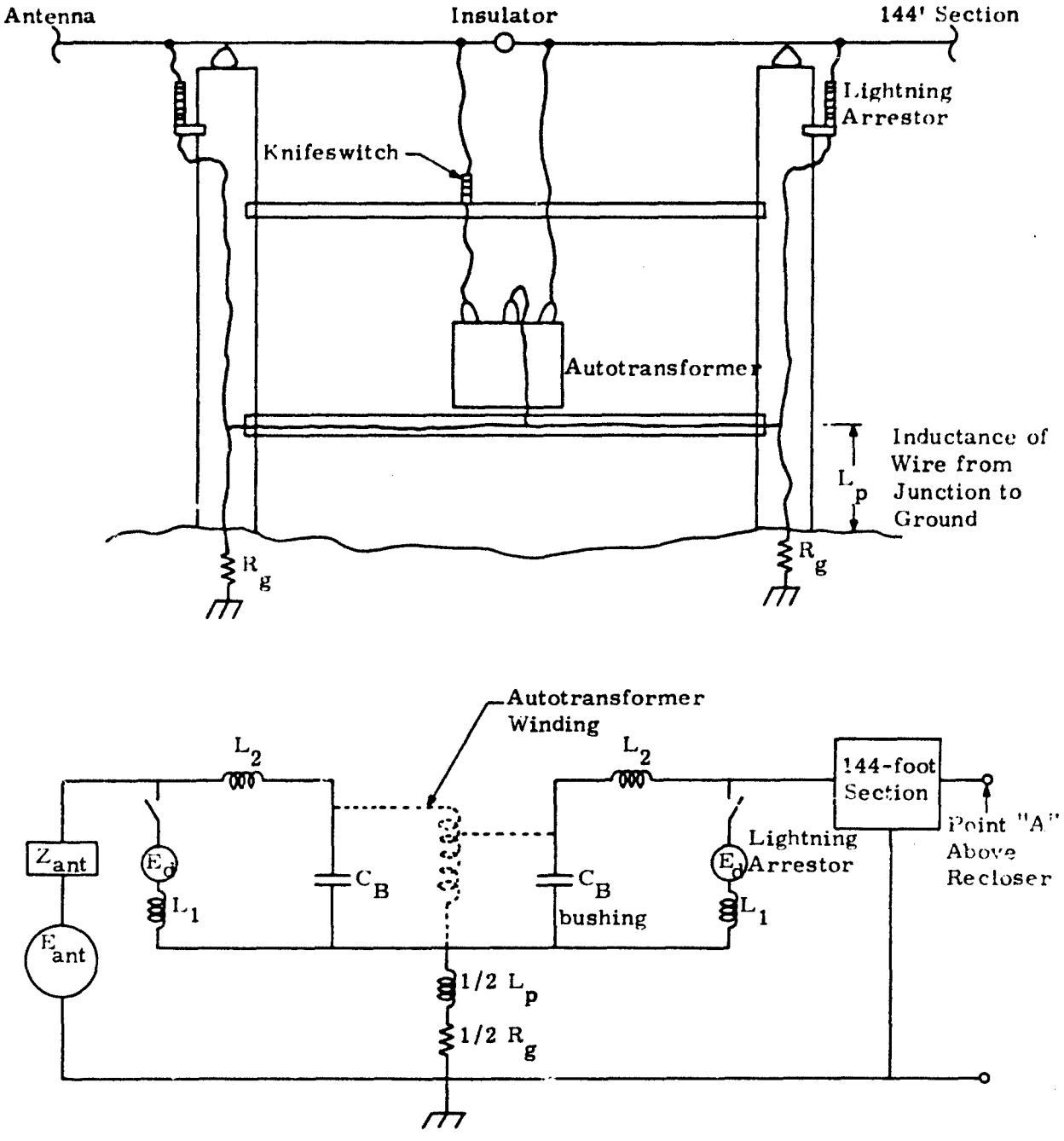



Figure 18. Pictorial and Schematic Representations of Autotransformer System

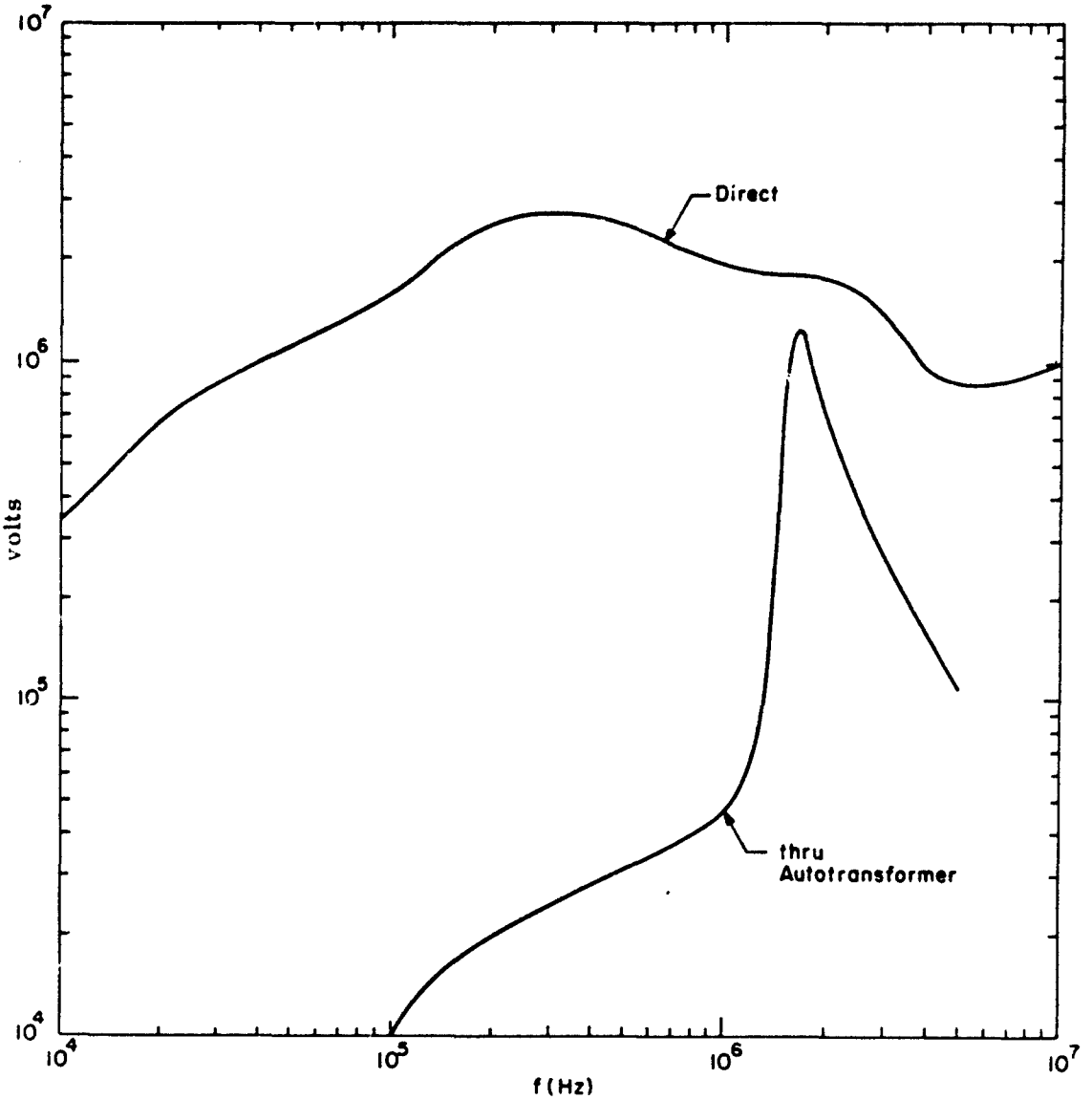



Figure 19. Open Circuit Voltage to Point "A" Above McGraw-Edison Recloser

line configurations - one with and one without the autotransformers. One can see that the configuration without the autotransformers in the circuit does indeed yield the higher voltages. There is a peak in the autotransformer circuit around 1.7 MHz. This is due to a 1/4 wavelength resonance of the 144-foot section. The effects of bushing breakdown due to high voltages are included in the graph of figure 19. This phenomenon is discussed in the following section.

## 5. BUSHING BREAKDOWN

When solving the circuits of figures 16 and 18 for values of voltages and impedances along various points in the circuit, we are concerned with the possibility of breakdown of other components besides the solid state devices in the control boxes. This leads to a consideration of what voltage is needed to break down the ceramic bushings which appear at all points of entry into the large system components like the autotransformers, reclosers, regulators, and the power transformer. The computed voltages at the autotransformers and at the McGraw-Edison reclosers are high enough to warrant this concern.

The dielectric strength of ceramics (ref. 9) varies from a low of about 40 volts/mil for alumina to about 400 volts/mil for Zircon porcelain. For our estimates we assume that the high power bushing manufacturers

9. Hodgman, M. S., R. C. Weast, and S. M. Selby, editors, Handbook of Chemistry and Physics, 39th edition, Chemical Rubber Publishing Company, Cleveland, Ohio, p. 2345, 1958.

use high quality porcelain, and we take the highest dielectric strength listed, which is 400 volts/mil or $4 \times 10^5$ volts/inch. The potential difference between the outer surface of the bushing and the outer surface of the inner conductor are calculated in order to determine the voltage at the conductor necessary to break down the ceramic. Figure 20 is a diagram of the bushing configuration.

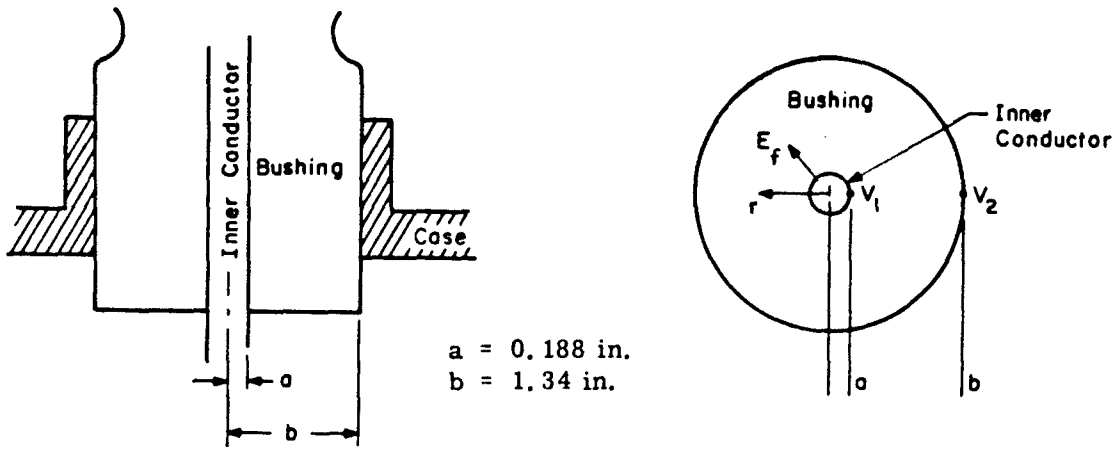



Figure 20. Bushing Configuration for Breakdown Analysis

In solving for the breakdown voltage we use the symbols introduced in figure 20. First, we know that the electric field strength, $E_f$, is inversely proportional to the distance from the center of the conductor.

$$E_f = V/r \qquad (1)$$

where V is the voltage at r. The voltage difference between points a and b may be obtained by integrating

$$V_2 - V_1 = \int_a^b E_f dr = \int_a^b \frac{V}{r} dr = V \ln \frac{b}{a} \tag{2}$$

$$= E_f r \ln \frac{b}{a} \tag{3}$$

The r of interest is at point a, since that is the place where the field strength in the ceramic is the largest. The $E_f$ is the dielectric strength of the material, so, solving for the voltage,

$$V_2 - V_1 = V_{BD} = 4 \times 10^5 \frac{\text{volts}}{\text{inch}} \times .188 \text{ inch} \times \ln\left(\frac{1.34}{0.188}\right)$$

$$= 147.7 \text{ kilovolts} \tag{4}$$

Thus, if the voltage across a bushing exceeds 147.7 kV, it is considered a breakdown, and a discharge potential is assumed at that point with a magnitude of 147.7 kV, with a phase such as to minimize the current through that path. This is much the same treatment we assume for the lightning arrestor. So in case of breakdown the bushing which is otherwise represented as a 200 pF capacitor becomes a 147.7 kV source.

## 6. THE COUPLING TO A GENERAL ELECTRIC RECLOSER

The new part of the Los Cordovas substation employs General Electric reclosers between the power transformer output and the customer

distribution lines. The coupling to these reclosers differs significantly from the McGraw-Edison recloser coupling in that the distribution lines leave the substation by way of buried cable. One of the lines is buried all the way to the customers while the other one emerges at the old LI-500 autotransformer site. In this analysis we consider LI-500 to be the antenna terminating at the pole on the left in figure 17. From the antenna to the recloser there are 150 feet of buried cable. Within the substation the only large piece of equipment to be considered in the coupling model is the power transformer. This power transformer differs from the other one in the old part of the substation in that it is a self-regulating transformer. It is manufactured by the RTE-ASEA Corporation of Waukesha, Wisconsin. The scope of this study does not permit a thorough analysis of the transformer, so it is modeled much like the one at the old part of the substation, that is, as a simple capacitor. The rest of the coupling model involves current paths from the transformer to the recloser, recloser to ground through the bushing capacitance, and from the end of the underground cable to the recloser. There is also a lightning arrestor between the underground cable and the recloser.

Wherever a current path is shared by two current flows (there are two customer distribution lines), we multiply the impedances along the path by two. This is analogous to the 2.9 factor in the model of the old part of the substation. This is a crude approximation since the second

customer distribution line is buried throughout its route, but in obtaining numerical values it is a reasonable approximation. The factor of three is still valid since the line we are studying is three-phase; therefore, it has three wires per line.

The treatment of the 150 feet of buried line from LI-500 to the inside of the substation is discussed in appendix C, as are the actual techniques for obtaining parameter values for the external coupling circuit. Figure 21 is a photo of that part of the new substation where the buried line submerges by way of a conduit. Also shown in the photo are arrays of knifeswitches by which the reclosers can be manually switched out of the circuit. The T-shaped box immediately behind the knifeswitches and lightning arrestor supports is the recloser. In the photo one can see six pipe-shaped bus lines supported by insulators above the reclosers. Three of these carry the power from the transformer, and the other three are called "transfer buses." The configuration in the new part of the substation is such that current flowing to the customers must go through a recloser. Unlike the old substation configuration the transformer cannot be connected directly to the customer line. If a recloser is down for repair or routine maintenance, it is taken out of the circuit by three sets of two knifeswitches. The customer line is then switched to the transfer buses. At the same time knifeswitches at another recloser are also switched to the transfer bus, such that the working recloser will handle the load from the other customer line.

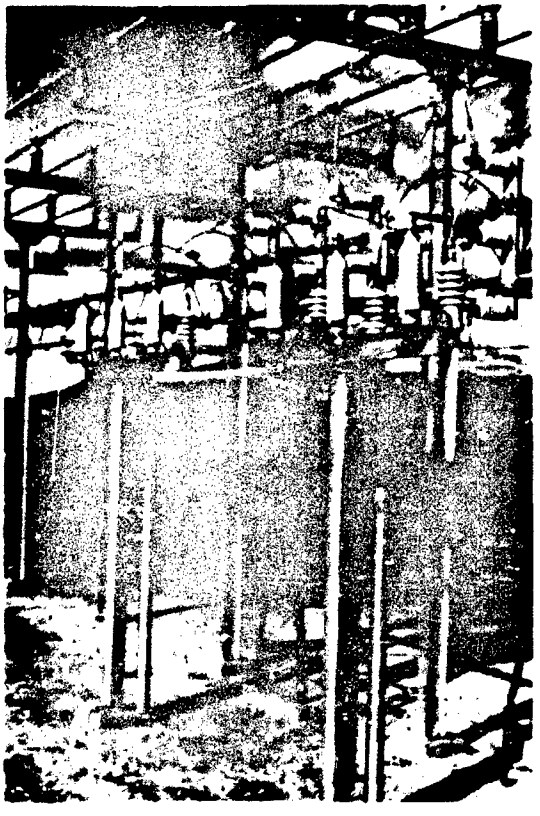


Figure 21. Photograph of New Part of Los Cordovas Substation Showing where Power Cable Submerges, Knifeswitch and Lightning Arrestor Array, and Recloser

Figure 22 consists of a line drawing and an electric circuit model of the new Los Cordovas configuration. Although a more thorough discussion as to how the various parameters were obtained and treated is found in appendix C, we point out at this time that the buried cable consists of a center conductor surrounded by polyethylene around which is a sheath of spirally wrapped wires. The sheath is not a braid as found

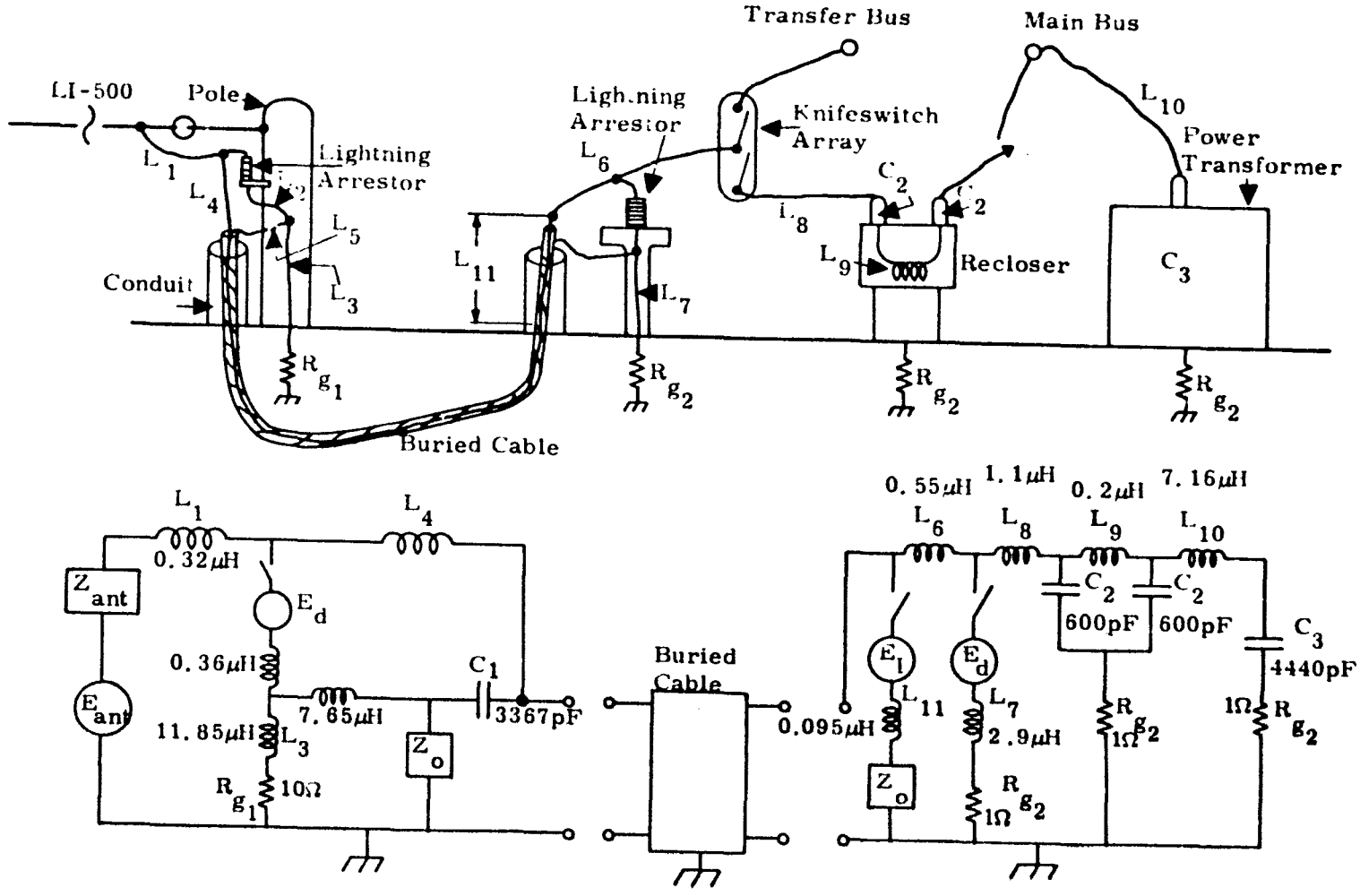



Figure 22. Pictorial and Schematic Representation of Model for the New Part of the Los Cordovas Substation

on coaxial cables and this somewhat complicates the model. The symbol $Z_o$ in the diagram is the impedance to infinite ground of the sheath taking into account the earth's parameters. $C_1$ is the capacitance between the center conductor and the sheath, through the polyethylene, for the length of cable within the conduit at the autotransformer site. The polyethylene, like the ceramic in the bushings, also is subject to high voltage breakdown. This will be discussed below, but when breakdown does happen $C_1$ is replaced in the circuit by a voltage source equal to the breakdown voltage, again much like the lightning arrestor firing and bushing breakdown. Breakdown of the polyethylene may also occur at the other end of the cable. As shown in the diagram, immediately to the right of the cable is a branch with a switch, an inductor with impedance $Z_o$, and a voltage source labeled $E_1$. This model, with the switch closed at greater than or equal to breakdown voltage, represents polyethylene breakdown at the substation end of the cable. The polyethylene may break down throughout the length of the cable, but in keeping within our scope of study, we consider only breakdown of the cable ends.

The upper frequency limit of this model is about 5 MHz, whereas the old substation is modeled to higher frequencies. This is done for two reasons; first, to keep the calculations as simple as possible and still obtain reasonable results, and secondly, because numerical work with the McGraw-Edison recloser shows that the most important range of

frequencies is well below the 10 MHz which is set as an upper limit. This simplifies the model in that lengths of wire other than the underground cable may now be longer and need not be represented as sections of lumped element artificial transmission lines. Thus their simple inductances will be a good approximation for this model.

## 7. POLYETHYLENE BREAKDOWN

As in the case of ceramic bushings, dielectrics can break down under high voltage stress. The dielectric material used for the underground cables at Los Cordovas is polyethylene. The breakdown voltage of a particular cable may be calculated using the same logic as in section II-5 of this report. First, according to reference 9, the dielectric strength of polyethylene is 465 volts/mil. The diameter of the center conductor is 0.325 inch and the distance across the cable is one inch. So for equation (3) in section II-5, r is 0.1625, b is 0.5, a is 0.1625, and $E_f$ is $4.65 \times 10^3$. The solution of equation (3) using these values, and thereby obtaining a breakdown voltage, is 84.9 kV.

The problem of dielectric breakdown as a possible failure mechanism for the Los Cordovas substation and for Kit Carson is discussed below in section IV. Up to this point we have only been discussing the coupling models, but the failure mechanisms are objectives of this study, and they are discussed in more detail below.

## SECTION IV

## EQUIPMENT FAILURE MODELING

### 1. SELECTION OF PORTS IN THE McGRAW-EDISON RECLOSER

Before discussing the analysis of the internal coupling problem in section V, we consider the analysis of the ports where potentially vulnerable components are subjected to EMP in the recloser box (for the McGraw-Edison configuration). The ports are identified by points at the surface of the control box where particular wires from the cable enter the box.

At this point an explanation as to how the McGraw-Edison recloser works is useful. The nature of the interface between the recloser and the control cabinet through the cable becomes apparent from the description. Figure 23 is a block diagram of the recloser control and its operation can be visualized by referring to it.

Bushing current transformers with a 1000:1 turns ratio at the recloser feed a current to the "rectification network." The d. c. signal from the rectifier is sent to the minimum trip and timing sections. If the minimum trip value is exceeded, timing starts, and after the correct delay a signal is sent to the output stage. The output stage connects the 24-volt battery to the solenoid trip latch and the recloser trips. At the same time a counter is advanced, and a signal is fed to the sequence relay. The sequence relay then energizes the first reclosing interval

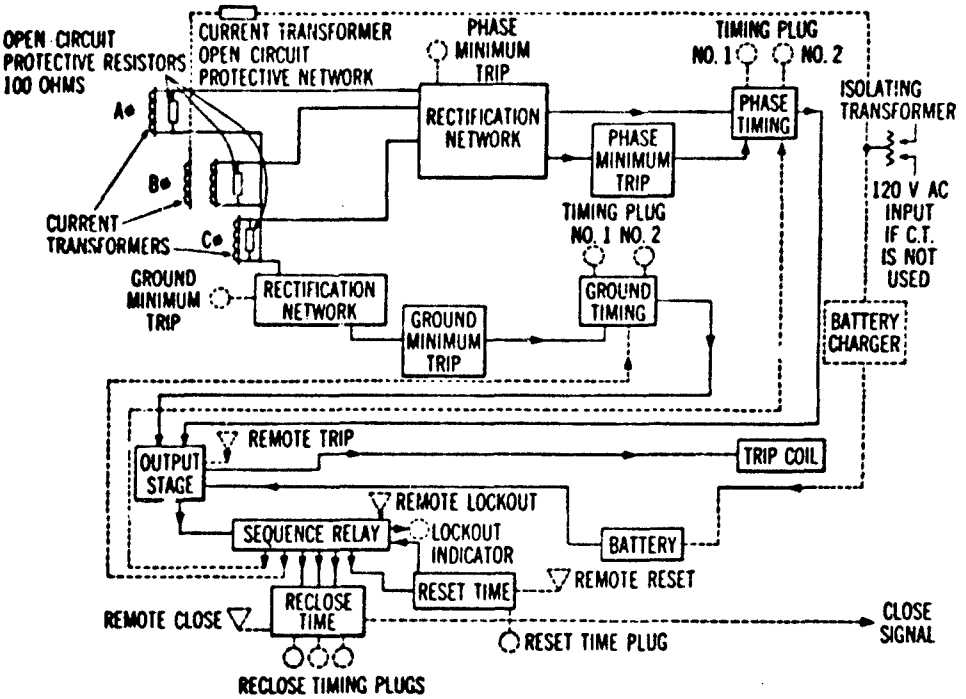



Figure 23. Block Diagram of Electronic Recloser Control

time-delay plug, and after the pre-selected interval has elapsed, the closing relay is energized so the recloser can close its main contacts. The sequence relay also energizes a resetting time-delay plug. If lock-out has not occurred before, this relay operates the control resets so that a complete sequence of events may occur if another fault takes place at another time. If the fault still exists when the recloser closes, control is set up to perform another operation. Reclosing time is governed by the second reclosing time-delay plug. A third opening and reclosing will take place in the same manner, but if the fault is still there at the

fourth opening, the sequence relay will have progressed to a point where no reclosing connections exist. This final condition is known as lockout. If lockout occurs, there is a possibility of damage existing on the lines, and repairs must be made before the recloser is reset. The resetting must be done manually at this point.

The above description applies to faults of two types, phase and ground. The phase fault detector in effect measures the sum of the magnitudes of the current for all three phases. If any one phase or combination of phases carries a current larger than that allowed, the opening and reclosing sequences are initiated. The ground fault detector measures the vector sum of the currents flowing in all three phases. Under normal operating conditions this vector sum, which is the same as a ground return current, is close to zero since the phases are 120 degrees apart, and the loads are nearly balanced. If the ground current exceeds a value greater than normal, the recloser goes into operation.

The 24-volt battery mentioned above is charged by a separate bushing current transformer located on the center-phase load-side bushing. The transformer has a zener regulated circuit which supplies constant current to the battery.

In defining ports at the recloser control we consider the point where the cable connecting the recloser box with the control box terminates at the control end. The bushing transformers all send their signals to the

control box where rectifier circuits are located. There are four current transformers at the recloser, one associated with each phase and one associated with the battery charging circuitry. The ground fault circuitry measures the current from all three phases and uses those transformers as inputs.

In defining ports of entry associated with the current transformers at the bushings of the recloser, we label the entry from the battery charging current transformer the "battery charging port" and designate this as port 1. The ground fault detector circuitry is designated as the "ground trip port" and port 2. The phase fault circuitry, which consists of three current transformers as inputs, is called the "phase trip port" and designated as port 3. Figure 24 is a portion of the schematic diagram from McGraw-Edison of the circuitry associated with these three ports of entry. The simplification of the circuits will be discussed below, as well as the way in which the lines are driven, i.e., sum or difference mode, affect the ports.

The cable, in addition to carrying signals from the bushing current transformers, also carries signals to and from relays and switches in the two boxes to accomplish the mission of opening and reclosing. In the recloser there is a switch whose contacts open when the recloser main contacts open, causing de-energization of the sequence relay coil, the counter, and the trip coil. This allows the sequence relay to advance its contacts.

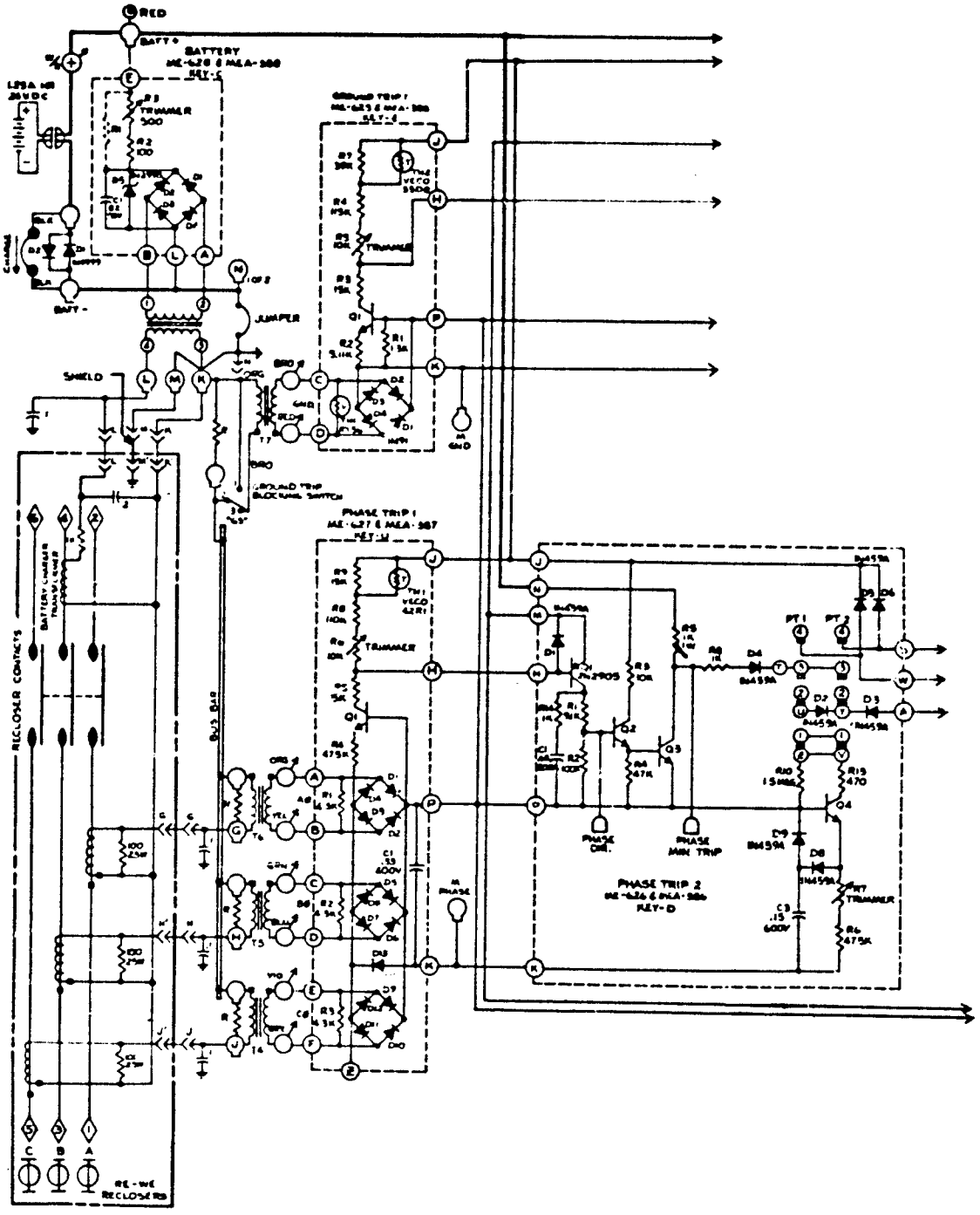



Figure 24. Portion of McGraw-Edison Recloser Schematic Depicting Battery Charge, Phase Trip, and Ground Trip Ports of Entry

Since this switch senses when the main contacts are open or closed, we call it a sense switch. The pair of wires from the sense switch leading through the cable from the recloser to the control box can be driven by EMP energy in the recloser in a sum mode or difference mode. In this study both modes are considered, and the sense switch port when driven in a difference mode is designated as port 4.

The closing solenoid is of the rotary type. This component when energized causes the recloser to reclose after a trip operation. The solenoid when driven in a difference mode is called the "rotary solenoid difference port" and is designated as port 5.

The last component in the recloser with wires leading through the cable to the control unit is the trip coil. This coil, when energized by a signal from control, releases a spring that causes the main contacts to open, breaking the circuit. This "trip coil difference port" is labeled port 6.

When the wire pairs from each of these three components are driven at the same potential they are driven in the sum mode. The sense switch driven in this manner is labeled port 7, the rotary solenoid sum port is labeled port 8, and the trip coil sum port is labeled port 9. Figure 25 gives the portion of the schematic with these three components.

The nine ports represent the entry points for EMP energy through the cable from the recloser. Vulnerable components in the path leading from the ports are examined for possible damage from the EMP energy.

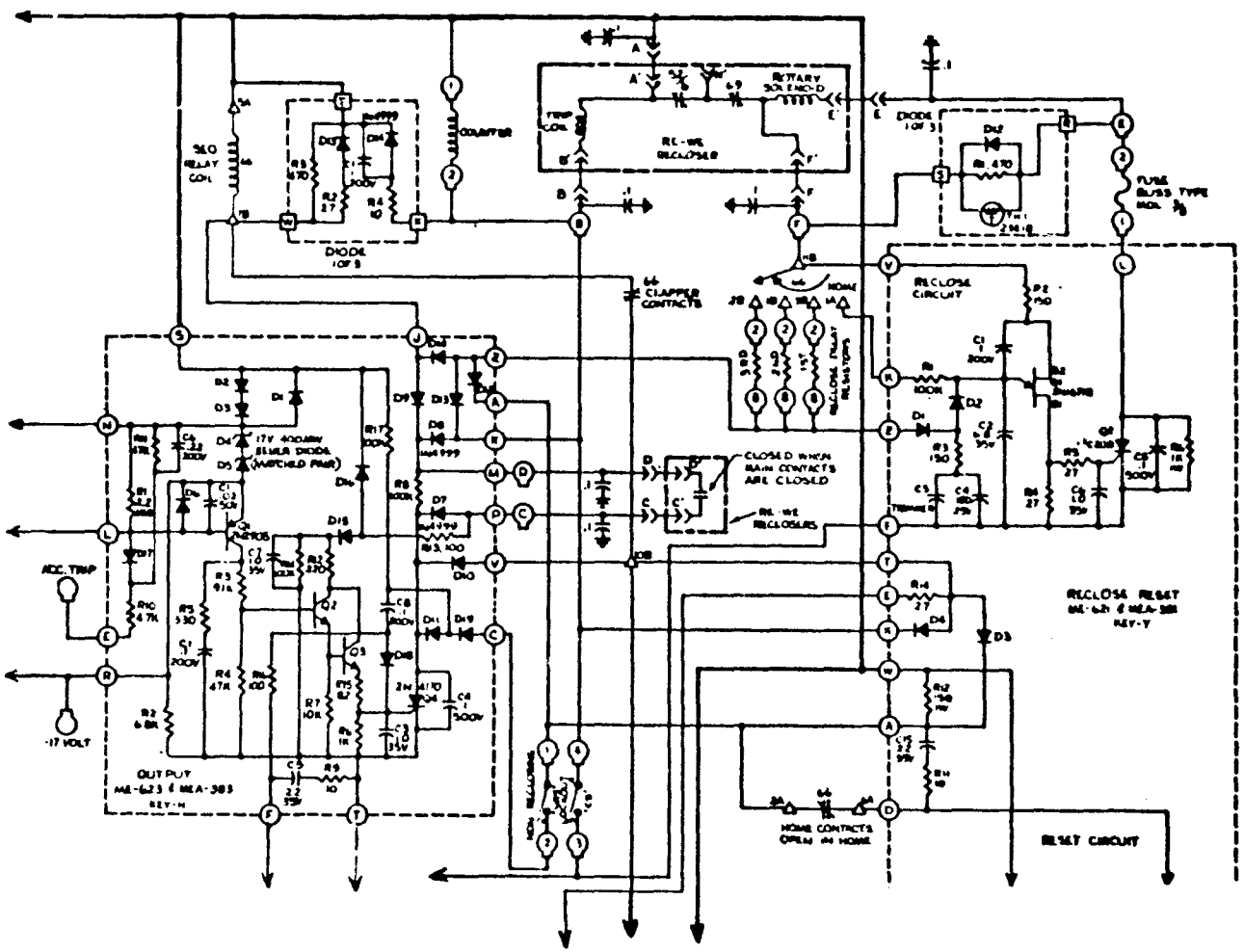



Figure 25. Portion of McGraw-Edison Recloser Schematic Depicting Sense Switch, Rotary Solenoid, and Trip Coil Ports

## 2. PORT CIRCUIT SIMPLIFICATION

In general the circuit simplification procedure follows a technique such as used in reference 6. This involves tracing low impedance paths from the port and deleting the high impedance paths. Eventually the remaining circuit will have a minimum of components including the most vulnerable in the low impedance paths. The Wunsch model (refs. 10, 11, and 12) is then used to determine threshold characteristics of the vulnerable component. In the circuit simplification procedure we proceed down the list of ports beginning with port 1, the battery charging port.

### a. The Battery Charging Port

In tracing the battery charging port circuit, we refer to the schematic of figure 24. Inside the recloser there is a bushing transformer at the center phase line. In series with the transformer is a

---

10. Wunsch, D. C., and R. R. Bell, "Determination of Threshold Failure Levels of Semiconductor Diodes and Transistors Due to Pulse Voltages," IEEE Trans. Nucl. Sci., Vol. NS-15, pp. 244-259, December 1968.

11. Boeing Company, The, and Braddock, Dunn and McDonald, Inc., EMP Electronic Analysis Handbook, Boeing Document D224-10022-1, under AFWL Contract F29601-74-C-0028, Appendix B, Air Force Weapons Laboratory, Kirtland AFB, NM, May 1973.

12. Wunsch, D. C., R. L. Cline, and G. R. Case, Theoretical Estimates of Failure Levels of Selected Semiconductor Diodes and Transistors, Braddock, Dunn and McDonald, Inc., Rep BDM/A-42-69-R, reissued August 14, 1970, under Contracts F29601-69-C-0132 and F29601-70-C-0019, AD 878-091, Air Force Weapons Laboratory, Kirtland AFB, NM.

1000-ohm resistor and then a 0.2 $\mu$F capacitor to ground. The cable then leaves the recloser and enters the control at the terminals of this port.

Figure 26 is the part of the McGraw-Edison schematic applicable to the battery charging port. In this figure circuit parameters to the right of the arrow leading away from this portion of the schematic are considered to be of high impedance and do not affect the calculations. There are two components tied to the terminals of the port, a 0.1 $\mu$F capacitor and a 1:1 transformer. One of the port terminals is connected to ground. The three input lines to the recloser as an antenna may be driven in the sum and difference modes, as noted above in section III-1. Since the current transformer is associated with the physically central wire, the only way it will be driven is if the distribution lines (antenna) are driven in the sum mode. This places the battery charging port as a sum mode port.

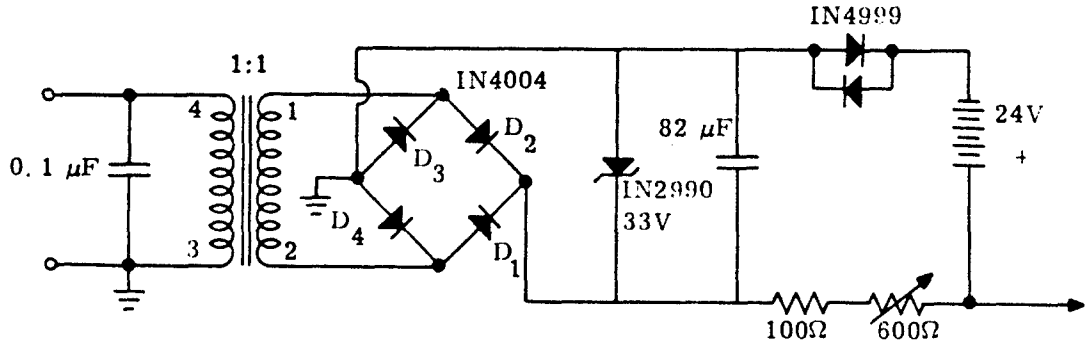



Figure 26. Battery Charging Port

In proceeding to simplify the circuit we assume that some threshold voltage and current are present and that one of the components in the circuit is particularly vulnerable and is at the threshold of failure. The most likely component to fail is a diode in the rectifier bridge, so we assume that one of these will be the one to break down.

We can begin to simplify the circuit by observing that the 82 $\mu$F capacitor has a very low impedance for all frequencies of interest compared to the resistors, battery, and diodes in series, paralleling it. The capacitor is then a short, and we can eliminate all components to the right of it. Let us assume that the polarity is such that D1 and D3 are conducting, so that D2 and D4 are backed up, and one of these breaks down because its reverse voltage rating is exceeded. Let us say that D2 breaks down first; this places D4 at a very high impedance, and we eliminate it from our simplified circuit. The transformer has a 1:1 ratio and, since it is assumed to be an ideal transformer, it also can be eliminated. The intermediate simplified circuit then looks like that in figure 27.

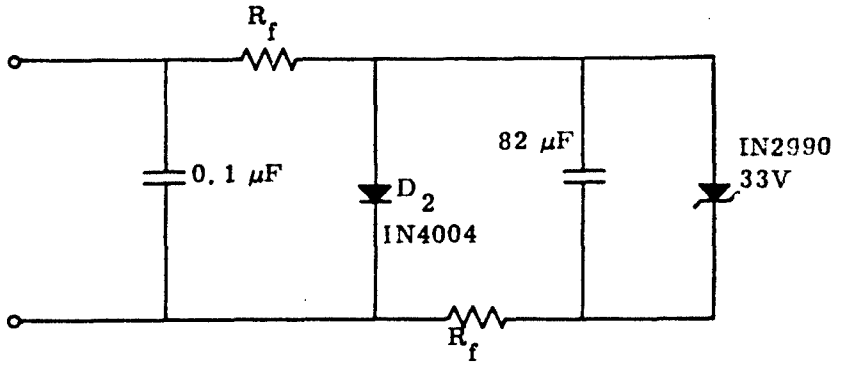



Figure 27. Battery Charging Port Simplified Circuit

$R_f$ in figure 27 is the bulk forward resistance of the two conducting 1N4004 diodes. The zener diode is conducting at voltages required to break down D2. This diode attempts to hold down the voltage at that point to its zener value of 33 volts. The next stage of simplification is to replace the zener diode by a 33-volt source. At this point we investigate the properties of the D1 (1N4004) diode so that we can solve the circuit for its critical threshold parameters.

Reference 12 suggests that a manufacturer's data sheet is the first place to look for useful data on a particular semiconductor component. The 1N4004 data sheet states that the reverse breakdown voltage rating is 400 volts. It also states that the forward voltage drop is 1.1 volts at 1 amp. This implies that when the diode is conducting in a forward direction, its bulk forward resistance is 1.1 volts/1 amp or 1.1 ohms. So the value of $R_f$ in figure 27 is 1.1 ohms.

The voltage required to break down the diode is 400 volts, and we must determine the power required to cause it to fail. The Wunsch model represents this power by the formula

$$P = Kt^{-\frac{1}{2}} \tag{5}$$

where t is in seconds, P is in watts, and K is in watt-(seconds)$^{\frac{1}{2}}$. K is also called a "damage constant" and can be determined by "thermal resistance" or "junction capacitance" models whose procedures are given in reference 12. The time, t, in the Wunsch model is the pulse width

required for damage. Our analysis is in the frequency domain, and we have related the time to the frequency with the relationship

$$t = 1/(5f) \tag{6}$$

This is the same relationship used in reference 6 and discussed further in reference 11.

If the damage constant, K, can be determined from available information, we can find the current necessary to burn out the diode from the relationship

$$I = P/V_{bd} = Kt^{-\frac{1}{2}}/V_{bd} \tag{7}$$

where $V_{bd}$ is the diode's breakdown voltage. Once the diode breakdown voltage and the diode breakdown current are known, we can solve for the circuit parameters and calculate the necessary failure threshold values at the terminals of the port.

In finding a value of K for the 1N4004 we have to determine either a junction capacitance or a thermal resistance. The thermal resistance may be a junction-to-case or junction-to-air resistance. The junction capacitance method is preferred if this is available. Figure IV. 5 in reference 6 gives a summary of the equations available in determining damage constants for various types of solid state devices.

From one of the data sheets available for the 1N4004, we have determined that the junction capacitance is 1.2 pF. The appropriate

formula from figure IV. 5 of reference 6 is

$$K = 1.1 \times 10^{-3} C_j V_{bd}^{0.81} \tag{8}$$

where $C_j$ is the junction capacitance. Solving this for K yields 0.169 watt-$(sec)^{\frac{1}{2}}$. Reference 6 also has a section called "Statistical Model Development" beginning on page 117 which presents a statistical relationship between empirical and estimated damage constants using a linear regression. This relationship is

$$\log \hat{K} = a + b \log K \tag{9}$$

where $\hat{K}$ is a corrected value and K is the value calculated from the capacitance or thermal resistance model. The constants a and b are found in table IV. 4 in reference 6 and depend on the method used to calculate K. Applying this linear regression to the old answer of 0.169 obtained above and using the correct a and b, a corrected value of K is obtained, and is 0.274 watt-$(sec)^{\frac{1}{2}}$.

The current through the broken down diode is then

$$I = 0.274t^{-\frac{1}{2}}/400 \text{ amperes}$$

$$= 0.000685t^{-\frac{1}{2}} = 0.00153f^{\frac{1}{2}} \tag{10}$$

and the circuit now looks like that of figure 28. It is now a relatively simple matter to solve the circuit for values of $V_{p1}$, $I_{p1}$, and $Z_{p1}$; the

subscript p1 designates port 1. The diode is now replaced by a resistor whose resistance equals the breakdown voltage divided by the damage current. Since the calculations are done for 10 frequencies, we do not present the threshold parameters. Another component of concern in our final circuit is the 0.1 $\mu$F capacitor at the port's terminals. The McGraw-Edison schematic parts list states that this capacitor is rated at 200 volts. In our damage analysis we do not model a broken down capacitor in detail but compare the coupled EMP voltage with the manufacturer's ratings.

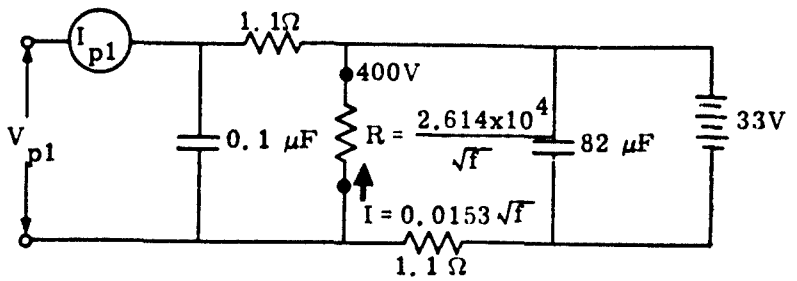



Figure 28. Final Simplified Battery Charging Port

b. The Ground Trip Port

Port 2 is the ground trip port and is shown in figure 29. Derivation of the schematic of figure 29 can be understood by referring to figure 24. The boxes labeled "$Z_{pt}$" refer to the impedance of that part of the phase trip circuitry applicable to the ground trip configuration and are discussed below.

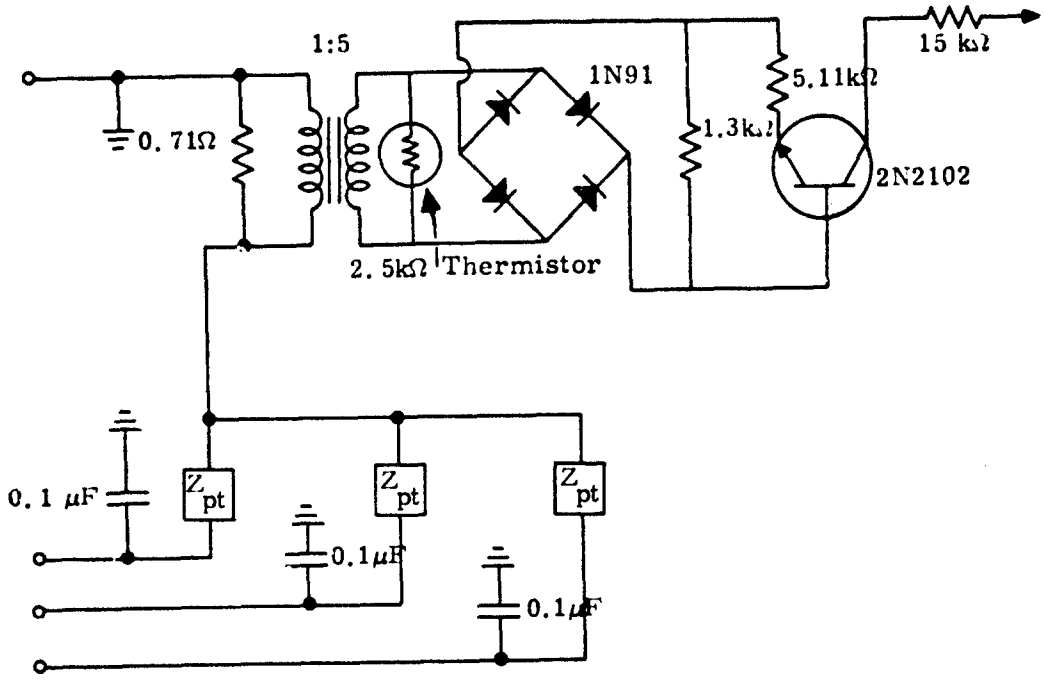



Figure 29. Ground Trip Port Schematic

The first observation which can be made is that the three wires representing the three phases coming from the cable to the phase trip circuitry must be driven in the sum mode in order to get any drive to the ground trip circuitry. If they are driven in the difference mode, there will be no net current flowing to the transformer primary of the ground trip fault sensing circuit. In the sum mode all three wires are driven the same, so in simplifying the circuit the three boxes labeled $Z_{pt}$ are placed in parallel and replaced with one box labeled $Z_{pt}/3$. The three 0.1 μF capacitors are likewise placed in parallel yielding a net capacitance of 0.3 μF directly across the terminals of the port.

In going to the transformer secondary circuit we again assume that since the bridge diodes are directly across the transformer terminals and the non-conducting ones are backed up with the full voltage, they are the first to burn out. The 2N2102 transistor is shunted by a 1300-ohm resistor and the emitter has a 5110-ohm resistor in series with it, placing the whole transistor in a high impedance path. From the manufacturer's data sheet on the 2N2102 transistor, we find that the base to emitter voltage is 1.1 volts with a test current of 15 mA flowing through the junction. We model the transistor as a 73.3-ohm resistor with this information.

Directly across the terminals of the transformer secondary is a thermistor. A thermistor is a non-linear resistance device whose resistance is dependent on the ambient temperature; however, we picked a value of 2500 ohms for this component because that is its listed nominal value. We assume that the EMP is of too short duration to affect the nominal resistance greatly.

At this point we have the thermistor, as a 2500-ohm resistor, in parallel with a 1300-ohm resistor. Paralleling this is the 73.3-ohm resistance from the transistor in series with a 5110-ohm resistor. As in port 1 we assume that two diodes in the rectifier bridge are conducting and that one of the two backed up diodes breaks down. The one which does not break down is assumed to have infinite impedance. The threshold damage characteristics of the 1N91 diode which does break down must be determined using the Wunsch model as before.

The 1N91 is a germanium rectifier whose peak inverse voltage rating is 100 volts. No junction capacitance or thermal resistance figures are available in manufacturer's data sheets for this rectifier. The replacement diode for the 1N91 is a silicon diode 1N4002. Since both diodes have the same peak inverse voltage we assume that their junction areas are the same (and therefore their junction capacitances). Once we have a capacitance we can apply the appropriate formula from figure IV. 5 in reference 6 for the germanium device. The capacitance we determine to be 2. 1 pF. The formula for the capacitance model of a germanium device is

$$K = 2.2 \times 10^{-3} C_j V_{bd}^{0.2} \qquad (11)$$

From this equation with our parameters we obtain a value of . 012 watt-$(sec)^{\frac{1}{2}}$ for the damage constant. The linear regression formula is not applied to this damage constant because approximate analysis is used to determine the junction capacitance. The schematic at this point looks like that of figure 30.

The threatened diode now, as in the previous port, looks like a resistor, whose resistance depends on the frequency. The impedance of 734 ohms and R, in parallel, may be transformed to the primary side of the ideal 1:5 transformer. This is accomplished by dividing the resultant resistance by the square of the transform ratio, or 25. This new resistance is then paralleled with the 0. 71 ohm resistor.

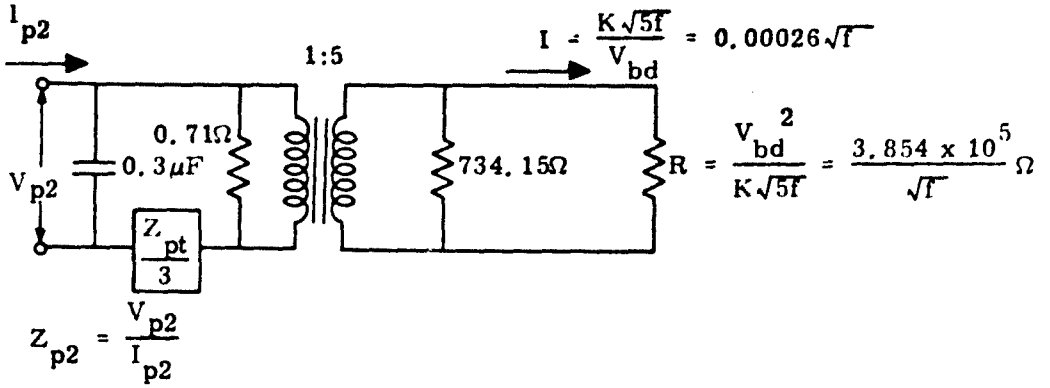



Figure 30. Intermediate Stage of Ground Trip Port Circuit Simplification

The circuit for the impedance $Z_{pt}$ is like that of figure 31. The impedances away from the arrows are again considered to be too high to have any effec' on the overall impedance of the circuit.

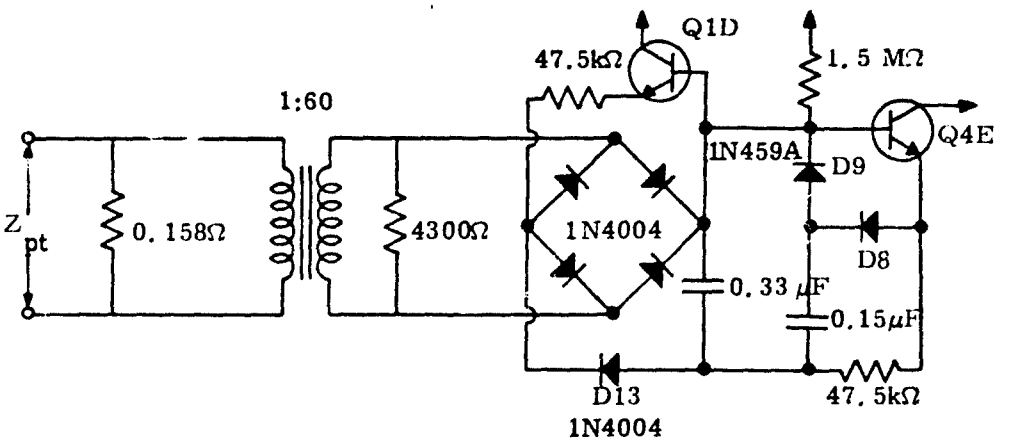



Figure 31. Portion of Phase Trip Circuit

All circuit components on the output side of the rectifier bridge are shared by three similar rectifier bridges, one for each phase.

So the equivalent impedance for the rectifier's load is multiplied by a factor of 3. When computing the final $Z_{pt}/3$ this factor of 3 is divided out giving the equivalent of three transformers with their primary and secondary shunts all in parallel but only one rectifier load circuit as is the actual case.

In simplifying the schematic of figure 31, we can immediately eliminate the transistor Q1D since the resistor in series with the emitter, as well as the resistor in series with the collector (not shown), are of such high values. The polarity of the diodes are such that current will flow from the bridge output through the base-emitter circuit of Q4E, then through D8, the 0.15 $\mu$F capacitor, and through D13 back to the bridge. The 4750-ohm resistor at the emitter of Q4E can be eliminated since it also is large compared to the rest of the circuitry. Since both D8 and Q4E are conducting, we assume that they do not fail and that all we need to do to model them is to find their resistance. D9 is backed up, but at a low potential, just the voltage drop across D8 and the Q4E base-emitter, so it should not fail if the voltage drop remains lower than its peak inverse voltage rating. D18 is a 1N4004 diode, the same as at the battery charging port. This diode has a conducting resistance of 1.1 ohms. From data sheets we estimate that the conducting or bulk forward resistance of the Q4E transistor base-emitter circuit is 73.3 ohms. Q4E is a 4JX11B1058 transistor. The bulk forward resistance of the 1N459A (D8) diode is 10 ohms.

The 1N4004 diodes in the bridge itself are assumed to be working normally with the backed up ones not failing. This is basically because the input cable is driven in the sum mode, and the potential across the terminals of $Z_{pt}$ is small.

The transformer is a step-up transformer with a ratio of 60:1. This means that the impedance as seen by the primary is the value calculated at the secondary divided by the ratio squared, or 3600. This impedance when paralleled with the 0.158 ohm resistor is $Z_{pt}$. Figure 32 is a step-by-step representation of the calculation of this impedance.

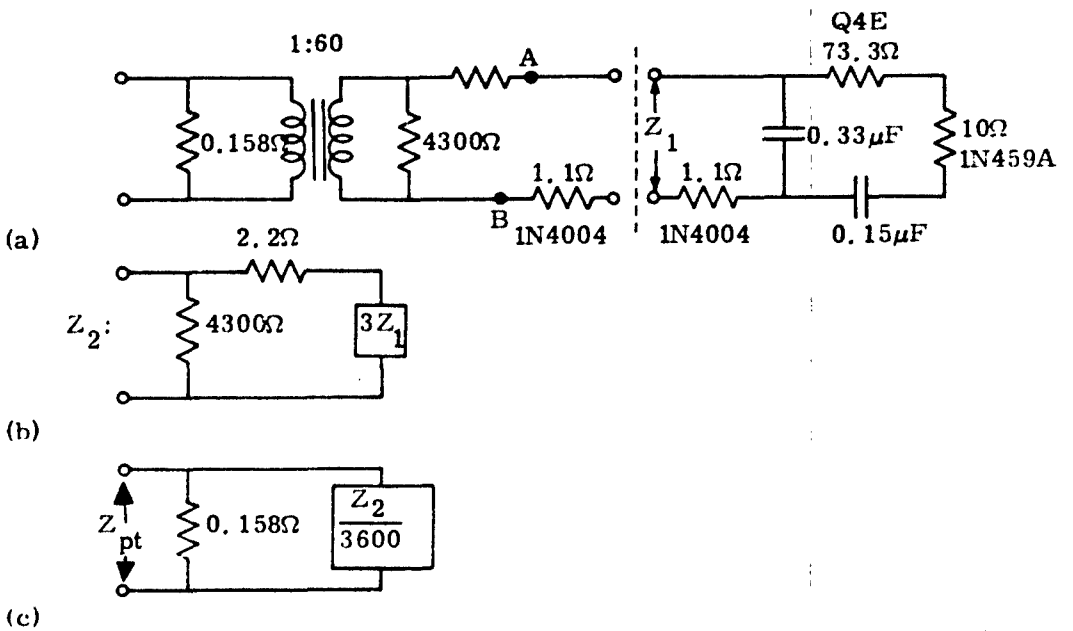



Figure 32. Breakdown of Phase Trip Impedance

Now $Z_{pt}$ is divided by 3 and placed in the circuit of figure 30. That schematic circuit is solved for the critical threshold values at the port's terminals since all circuit parameters in the model are now known.

c. The Phase Trip Port

In finding the impedance for the phase trip circuitry applicable to the ground trip port, we have already begun the analysis of port 3, the phase trip port. If the input lines to the terminals of this port are driven in the sum mode, there is no drive to the isolation transformer secondary since the primary is in effect shorted out.

In the difference mode consideration, the two outer phases are driven by a difference mode voltage and the center phase line is neutral. This places two of the primaries of the phase circuit in series and drive to their secondaries is possible.

Figure 31 is discussed above for the phase trip analysis and much of what is said there is still applicable; that is, the existence of the factor of 3 at the output of the rectifier bridge, and the finding that Q4E, D8, and D13 conduct and do not burn out. The only difference from our previous consideration is that we now assume that one of the backed up diodes at the bridge circuit fails, placing a shunt resistor between points A and B in the circuit of figure 32(a). This broken down diode is a 1N4004 and from the analysis of port 1 we know that the current through it is $0.0153\sqrt{f}$ amps, the resistance of the new shunt resistor is

2.614 x $10^4/\sqrt{t}$ ohms, and the voltage across it is 400 volts, the peak inverse voltage rating of the diode. With this information and following steps such as those of figure 32, we can solve for a new $Z_{pt}$, a $V_{pt}$, and an $I_{pt}$ at the terminal to break down the diode. Since the port terminals actually consist of two phase trip circuits in series, the impedance required is two times $Z_{pt}$, likewise the voltage required is two times $V_{pt}$. The current remains the same. The new values of these parameters are the critical threshold values and are subscripted by a 3 to denote port 3.

d. Sense Switch Port - Difference Mode

Figure 25 is referred to in the following discussion of the remaining three ports for both their sum and difference drives. The port we call port 4 is the sense switch port driven in the difference mode. The portion of the schematic of figure 25 applicable to the sense switch port is shown in figure 33.

The sense switch in the schematic of figure 25 is roughly in the center. It is surrounded by a dashed box with lettering immediately to the right of the box stating "closed when main contacts are closed" and "RE-WE reclosers." The two port terminals are labeled C and D.

In simplifying the circuit of figure 33 a polarity at the terminals must be assumed to see which diodes are conducting and which are backed up. If a positive polarity at D is assumed with respect to C practically all diodes are backed up; that is, to get back to C, a current

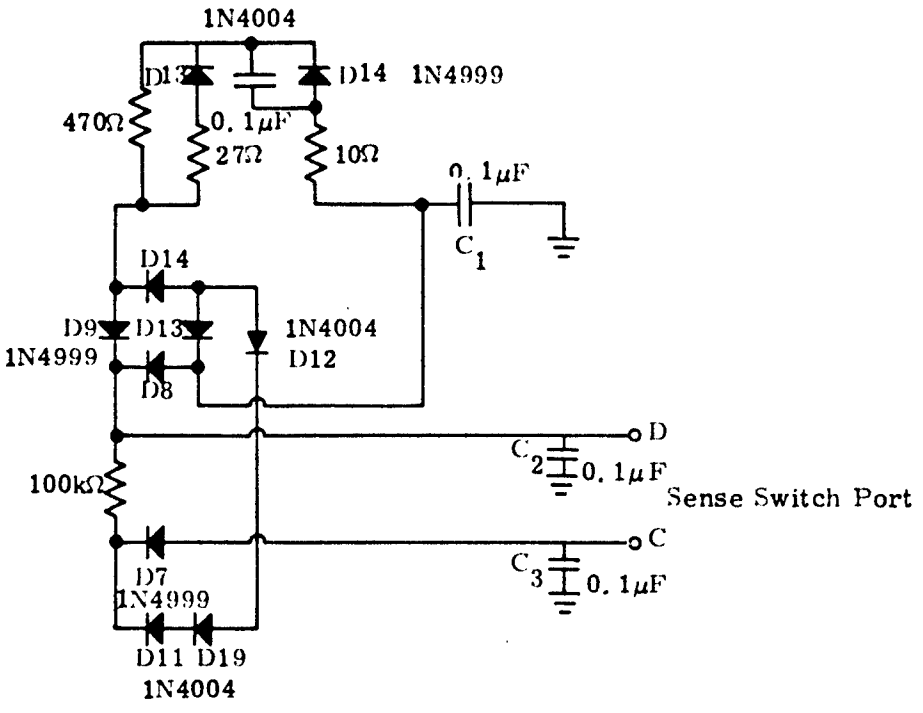



Figure 33. Portion of McGraw-Edison Recloser Schematic Applicable to the Sense Switch Port

must break down D8 in the bridge circuit, then proceed through the capacitor C1 through the ground and back to C via the capacitor C3. This is the easiest path, provided D8 breaks down. An alternate path is for current to break down D9 and go up through the 470-ohm and 27-ohm resistors through the conducting D13, break down D14 and back to C via the 10-ohm resistor, C1, and ground to C3. This is clearly a more difficult path. The next path is for current to break down D9 and D14 and then to go through the conducting D13 in the bridge and the C1, ground, C3 route. Or after breaking down D9 and D14 in the bridge, it could go through the conducting

D12, D19, and D11 diodes, break down D7, and on to C. All paths except the first one described involve the breaking down of more than one diode.

The next consideration is to make terminal C positive with respect to D. The shortest current path is through C3 to ground, and then since D8 conducts, C1 is placed in parallel with C2. There are no backed up diodes in this path. The next path is from terminal C to the conducting D7 and then a split between two more paths. One is through the 100 kΩ resistor, which is a very high impedance. The other is for current to break down D11, D19, and D12, then proceed through the conducting D13 and D8 in the bridge. The first choice involves a conducting diode only, and the second choice is the breakdown of three diodes; neither choice is very likely. The original path described is the most likely one to occur, and the one we select as the port representation. The resultant circuit is shown in figure 34. The 1N4999 diode is replaced by a resistor with a voltage drop across it equal to the diode's peak inverse voltage rating and with a current through it equal to the damage constant of this diode times the square root of five times the frequency all divided by the peak inverse voltage. Having this information we can determine threshold values as before. Following procedures outlined above we can compute a damage constant for this diode. The 1N4999 has a breakdown voltage of 200 volts. A junction capacitance for this device is not available, but the manufacturer's data sheet lists a junction to air thermal resistance of $30^{o}C/W$. The appropriate formula for the damage constant is

$$K = 972.2\ \theta_{jA}^{-1.24} \qquad (12)$$

where $\theta_{jA}$ is the thermal resistance. Applying our data and then the linear regression formula from the statistical analysis, we obtain a damage constant for this diode of 4.438 watt-$(sec)^{\frac{1}{2}}$.

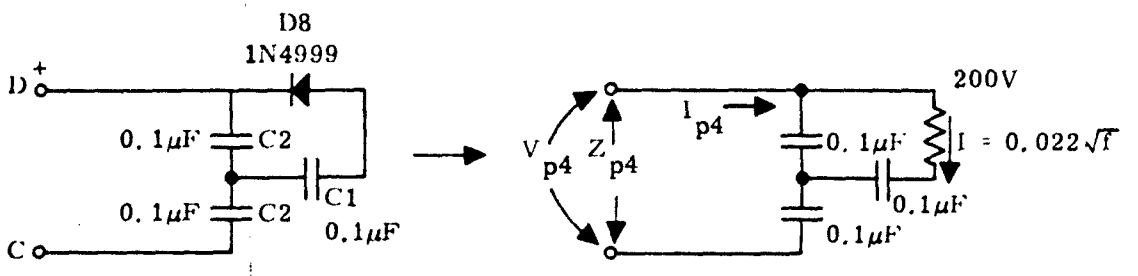



Figure 34. Sense Switch Difference Mode Port, Port 4

e. Sense Switch Port - Sum Mode

The sum mode drive to this port we designate as port 7. Figure 33 can be referred to also for the simplification of this port. First, in the sum mode terminal C and D are tied together and the return path we are looking for is to ground. This places the capacitors C2 and C3 in parallel shunting the terminals. A path must now be traced from the C,D point back to ground, and the only way this can occur is through the capacitor C1. Assume a positive polarity at the C,D terminal. The short path is to break down D8 again, as in the difference mode, and directly go to C1 and ground. The other path involves going through the conducting D7,

break down D11, D19, and D12, and go through the conducting D13 in the bridge and to C1.

Assume now a negative polarity at the C, D terminal. D8 now conducts, shorting the path to all other diodes in consideration, so that no diode is vulnerable. In the sum mode then the circuit is as shown in figure 35. The diode in question is the same as for the difference mode port, so we have all data available on it already.

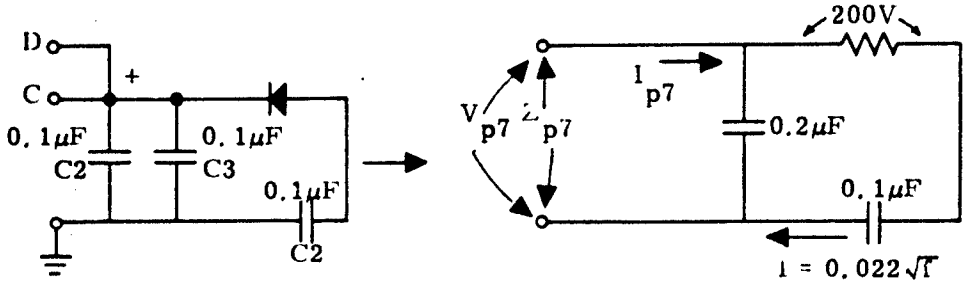



Figure 35. Sense Switch Sum Mode Port, Port 7

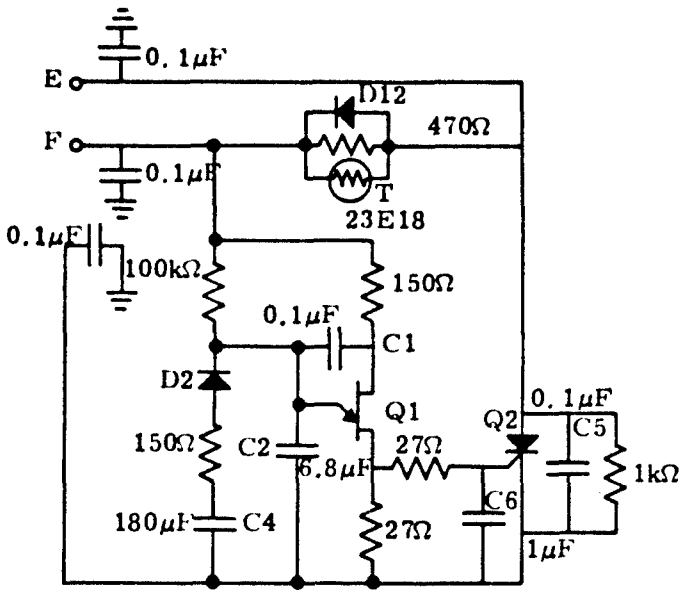
f. Rotary Solenoid Port - Difference Mode

The circuit for the rotary solenoid is found in the upper right-hand corner of figure 25. The part of the schematic applicable to our analysis is shown in figure 36(a). If a positive polarity is assumed at terminal E then D12 is conducting, presenting a short circuit to F. This is not a good representation of the port in a damage analysis. If F is positive with respect to E then D12 will be backed up and a possible

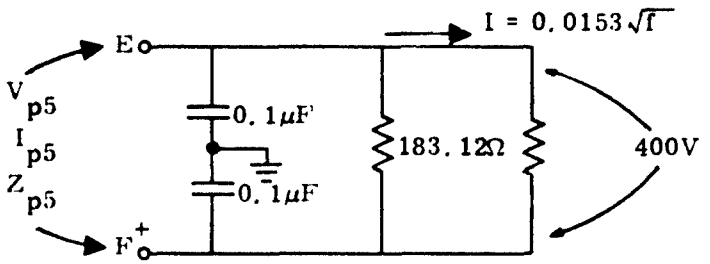
candidate for failure. The SCR (silicon controlled rectifier) Q2 and the diode D2 will also be backed up, but the paths involved represent high impedances as compared to the direct path to break down D12. D12 is again a 1N4004 for which we have a damage constant and a peak inverse voltage, so the voltage across it and the current through it are determined in obtaining the threshold values of $I_{p5}$, $E_{p5}$, and $Z_{p5}$. The thermistor is modeled as a resistor at its nominal value of 300 ohms. Figure 36(b) shows this port in this representation.

g. Rotary Solenoid Port - Sum Mode

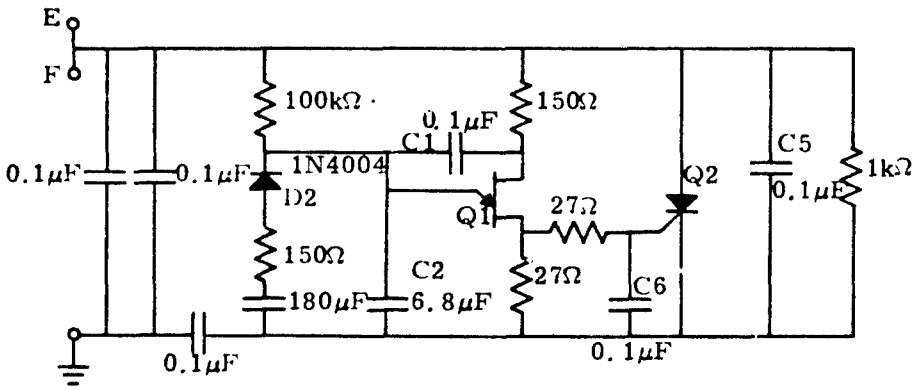
In the sum mode terminals E and F are tied together and a return path to ground must be found. Figure 36(c) is a diagram of this configuration. Tying the E and F terminals together eliminates the thermistor, D12, 470-ohm circuit by shorting it out. There are three solid state devices remaining in the circuit and the most vulnerable one is the SCR, Q2, since it is more nearly across the port terminals than the other two devices. The diode D2 in series with a 150-ohm resistor and a 180 $\mu$F capacitor is shunted by C2, a very low impedance at frequencies of concern. Also, the polarity required to break down D2 causes Q2 to conduct, protecting D2. The unijunction device, Q1, has its emitter terminal connected essentially to the return path to ground because of the low impedance C2. This causes the polarity of breakdown for Q1 to be the opposite of Q2 which conducts, protecting Q1. The remaining device is




(a) Rotary Solenoid Circuit




(b) Rotary Solenoid Difference Mode Port - Port 5




(c) Rotary Solenoid Circuit in Sum Mode Configuration

Figure 36. Rotary Solenoid Port of Entry

Q2 itself, which when conducting protects the other devices which are backed up, but is vulnerable in the other polarity. Assume the ground terminal to be positive with respect to the E, F terminal so that Q2 will be backed up. If Q2 is broken down and conducting its gate electrode shorts out C6 placing the two 27-ohm resistors in parallel, with one end tied to one base of the unijunction transistor, a 2N1671B transistor. According to the data sheet on this unijunction the interbase static resistance is from 4700 ohms to 9100 ohms. These value are very high compared to other impedances in the circuit, and although the unijunction device is considered to be conducting it may be eliminated from the circuit due to its high resistance. This also eliminates the two 27-ohm resistors in parallel since now they are not connected to anything. The 100 kΩ resistor at the cathode of D2 also may be eliminated. The 6.8 $\mu$F capacitor C2 has an impedance much lower than the branch it parallels - C4, D2, and the 150-ohm resistor in series. So this branch can be eliminated. The only components left are C2 in series with C1 and the 150-ohm resistor, this branch shunting Q2.

The silicon controlled rectifier, thyristor Q2, is a type C20B with a peak inverse voltage of 400 volts and a junction to case thermal resistance of $2^{\circ}C/W$. With this information we obtain a damage constant of 1.77 watt-$(sec)^{\frac{1}{2}}$ which we use in the calculations for figuring the port critical threshold values. This value includes the statistical linear regression factors mentioned earlier. The voltage across the thyristor must be

400 volts and the current through it $K/V_{bd}\sqrt{f}$ or $0.0044\sqrt{f}$ amperes for damage. The resultant equivalent circuit of the port is shown in figure 37.

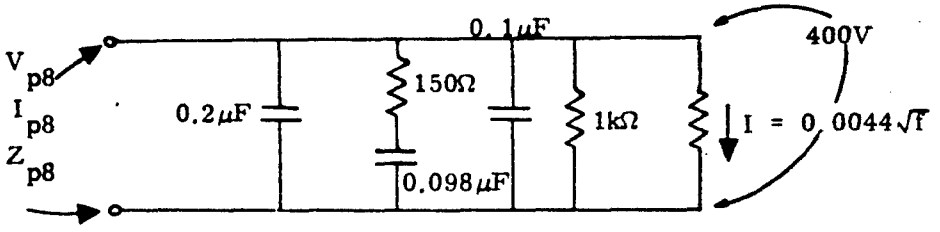



Figure 37. Rotary Solenoid Port Sum Mode - Port 8

h. Trip Coil Port - Difference Mode

The trip coil is found in figure 25 at the top center of the schematic. The port terminals are labeled A and B. The most direct path in the difference mode from one terminal to another is from A to the terminal labeled Y, in the adjacent dashed box to the left of the trip coil, through the 1N4999 diode D14 and C1 in parallel with it, to terminal X and on to B. The counter coil shunting the trip coil terminals is considered to have an inductive impedance which is too high at frequencies of interest to affect the circuit. The polarity for breakdown of D14 is with A positive with respect to B. D14 is a 1N4999 which appears above in the discussion of port 4 and for which we already have a damage constant. The equivalent circuit which is used in the analysis is given in figure 38.

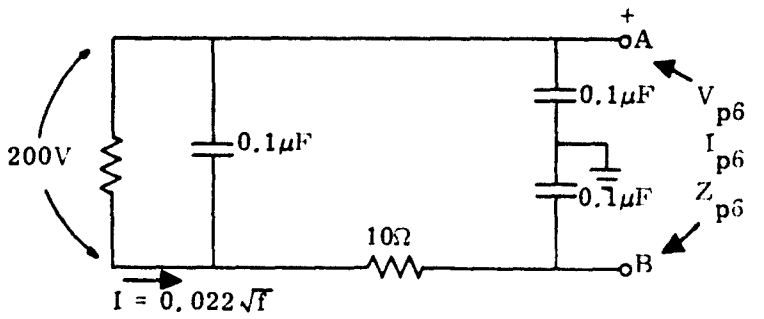



Figure 38. Trip Coil Difference Mode Port - Port 6

i. Trip Coil Port - Sum Mode

In the sum mode terminals A and B are connected, putting the capacitors to ground at each terminal in parallel. The path to ground is from the Y terminal through the D13, R2 and R3 combination to the W terminal in the dashed box adjacent to the counter coil in the schematic of figure 25. From W the path proceeds to the J terminal in the large dashed box below, and through D9 out to the D terminal at the sense switch. The path terminates at the ground to which the D terminal 0.1 μF capacitor is tied. The two vulnerable components in this path are D13 and D9, both 1N4999 diodes. They are positioned in such a way that one or the other conducts at all times. Since D13 in series with R2 is shunted by a 470-ohm resistor, we assume it is in a less vulnerable position than D9. If the ground terminal of the port is positive with respect to the A,B terminal, then D13 is conducting and D9 is backed up. The conducting D13 has a bulk forward resistance of about 1.6 ohms. This in series with the 27 ohms

paralleled with the 470 ohms gives an equivalent resistance of 27 ohms. The resultant equivalent circuit for port 9 is given in figure 39.

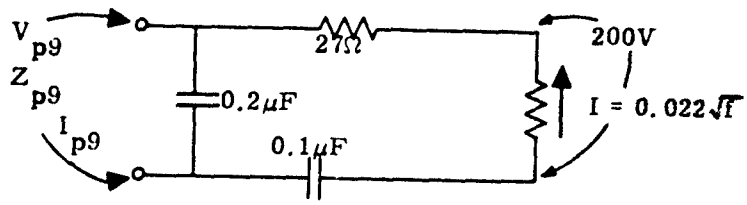



Figure 39. Trip Coil Sum Mode Port - Port 9

## 3. THE GENERAL ELECTRIC RECLOSER

The General Electric Recloser works in a similar manner to the McGraw-Edison unit. It has current transformers mounted on the bushings for its ground trip and phase trip circuitry. Signals from these are fed to the control unit where decisions are made whether to open a circuit or not. The main contacts for the General Electric recloser are enclosed in a vacuum chamber, whereas in the McGraw-Edison unit they are submerged in transformer oil. The big difference between the two units is that the recloser contacts, bushing transformers, and other hardware associated with the recloser unit are physically located within the same metal enclosure as the control circuitry in the General Electric unit. This makes for better shielding of the control unit since the only ports open to EMP are those associated with the bushing transformers. The unit operates from a customer's 115-volt supply (in this case the Kit

Carson Electrical Cooperative is the customer), so there is no battery associated with it. This supply drives a motor which opens the main contacts when activated.

Information on component types and values is in many cases unavailable, so the analysis of this recloser is not as complete as that of the McGraw-Edison type. Figure 40 is a portion of the recloser schematic diagram showing two ports - the ground and phase trip ports. The other port associated with the recloser is the 115-volt input, but it is not considered to be as vulnerable as the trip ports. Furthermore, of the two ports shown, the one considered to be more vulnerable is the ground trip port, because when the three incoming lines are driven in the sum mode the combined effect acts on the vulnerable circuitry. In the case of the phase trip port the sum mode yields smaller currents at the rectifier bridges by a factor of 3. The ground trip port, when the input is driven in the difference mode, has a net current which is zero or at least very small. The voltage required to burn out a rectifier diode in the phase trip port driven in the difference mode has to be twice as great as that required for a single rectifier circuit since the equivalent for this condition is two circuits in series. The most vulnerable port then is the ground trip port driven in the sum mode. This is the only one we analyze for the GE recloser.

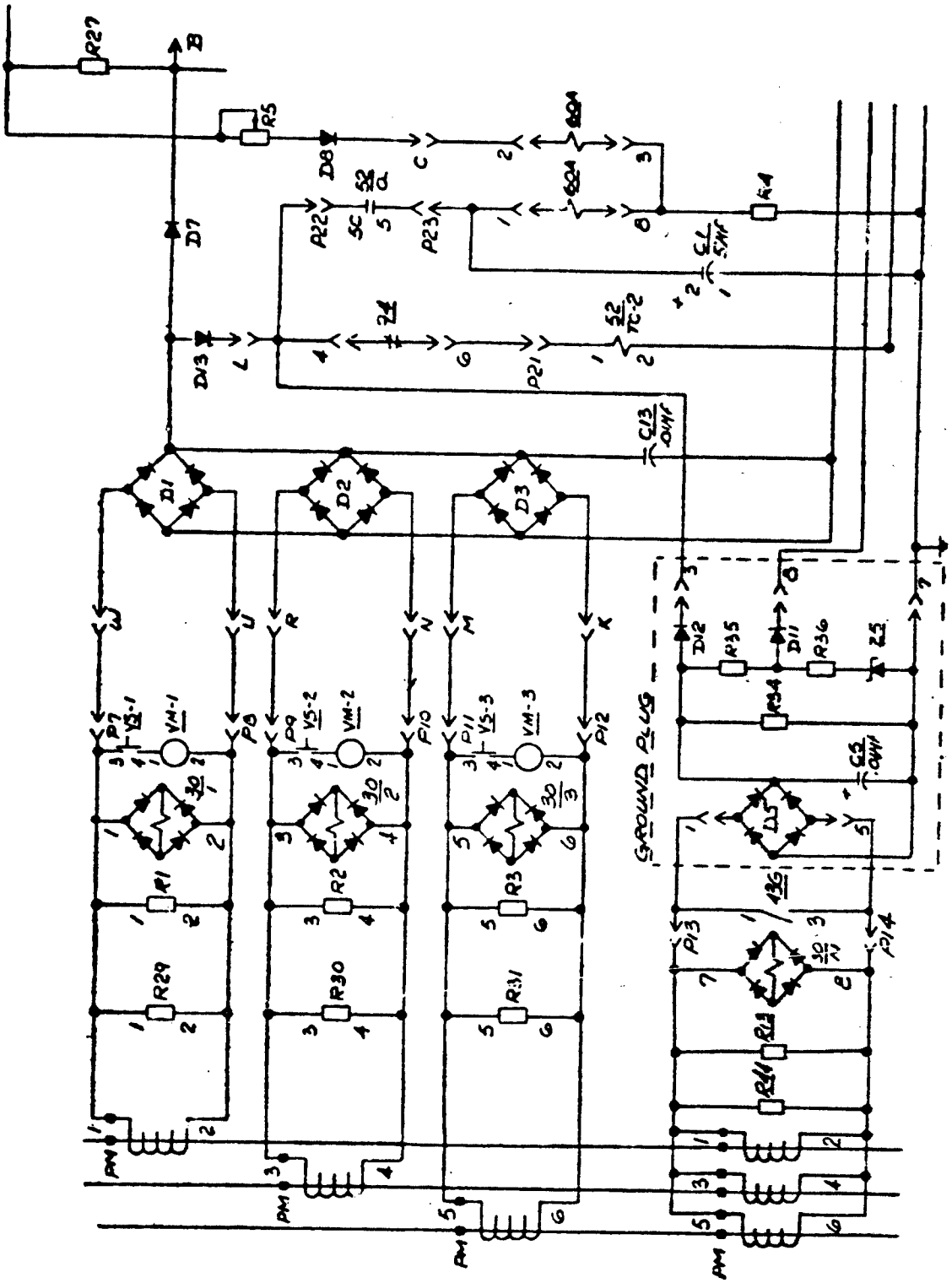



Figure 40. Portion of General Electric Schematic

Referring to figure 40, there is a resistor labeled R44 directly across the bushing transformer, which has 500 turns. This resistor is a 90-ohm, 10-watt resistor and is paralleled by R13. R13 is a plug-in resistor supplied by the user and is used to vary the sensitivity of the ground fault detection circuitry. The value of R13 which makes the circuit most vulnerable in the EMP analysis is infinity, so we consider R13 as not being there. The bridge diodes labeled 30/N are enclosed in a Motorola MOA 920-7 module. The type of diodes used are 1N4005 with a peak inverse voltage of 600 volts and a calculated damage constant of 0.31 watt-$(sec)^{\frac{1}{2}}$. The D5 rectifier bridge consists of 1N5061 diodes, also rated at 600-volt peak inverse voltage. The characteristics of this diode are identical to those of the 1N4005, so it also has a damage factor of 0.31 watt-$(sec)^{\frac{1}{2}}$. Across the output of the D5 bridge is a 0.01 $\mu$F capacitor and a resistor R34, which has an impedance of 10 k$\Omega$. This value is high enough to eliminate this branch. The rest of the circuitry is also considered to have a high impedance compared to the 0.01 $\mu$F capacitor, so we stop there.

The symbol across the 30/N bridge in figure 40 represents a relay coil. When enough current flows through the coil a relay is activated in another part of the control. At the frequencies we consider, the inductive impedance is too high to affect the circuit and we eliminate the coil. This also eliminates the 30/N bridge from consideration.

If one of the D5 diodes breaks down when backed up and it is represented as a frequency dependent resistor as before with the appropriate damage constant, the resultant circuit is as shown in figure 41. The bulk forward resistance of each of the two remaining conducting diodes is 1.1 ohms. These are shown by the single 2.2-ohm resistor in the figure.

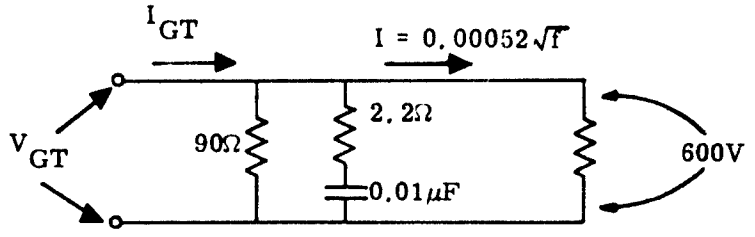



Figure 41. General Electric Ground Trip Port

# SECTION V

# INTERNAL COUPLING MODELS

## 1. GENERAL

In section III the external coupling problem is discussed and in section IV the recloser equipment failure models. In this section the interface between the two models is discussed. EMP energy reaches the recloser by means of the Beverage antenna and is influenced by the load on the system by such things as the frame, voltage regulators, etc. The resultant voltage at the recloser and the current flowing through it are now known by the solution of circuits presented in section III. The current flowing through the recloser is the same as that flowing through the inductance between the two recloser bushing capacitances (figs. 16 and 22).

In the case of the McGraw-Edison recloser, coupling to the recloser control box from the recloser takes place due to electric and magnetic field coupling inside the recloser from the wire carrying the main reclosure current to various components mentioned in the previous section; these are the bushing current transformers, sense switch, trip coil, and rotary solenoid. In addition, current flowing through the recloser support stand, due to the bushing capacitance from the internal conductor to ground, couples to the external cable leading from the recloser to the control.

In the General Electric system there is no external cable to consider, since both the recloser and the control are within the same metal box. The recloser portion is shielded from the control portion by a metal divider and all wires leading from one section to another pass through grommets. These wires, like in the McGraw-Edison recloser, are from the bushing current transformers. The motor which actually drives the vacuum recloser is located in the control section. All other communication to the recloser is mechanical. Thus, the problem of coupling to things like sense switches and rotary solenoids does not exist.

In this section results from the external coupling analysis as well as knowledge of coupling mechanisms are applied to calculate voltages and currents which reach the ports described in the previous section.

## 2. MAGNETIC TRANSFORMER COUPLING

The most apparent means of coupling is through the bushing current transformers. Ports 1, 2, and 3 are tied directly to the transformers through the cable and form what we call the directly coupled ports. There is no data available on these transformers which describe how the transformers behave at the frequencies of concern. In section 3 of reference 5 some tests are reported on a current transformer but of a different design from the ones in both types of reclosers considered here.

The current transformer in this study consists of a toroidal winding on an iron doughnut-shaped core placed around the bushing. Knowledge of the exact characteristics of this transformer is needed and estimates can be made on the basis of the reference 5 study, but in trying to keep within the scope of the study we have considered it as an ideal transformer. That is, the current at the transformer's output is assumed to be the current flowing through the recloser divided by the turns ratio. In the case of the McGraw-Edison recloser this ratio is 1000, and in the case of the General Electric recloser the ratio is 500.

The recloser has three wires passing through it and in our model we have considered them as one source, since the Beverage antenna consists of three wires but is only one EMP source. Port 1, the battery charging port, has only one bushing current transformer instead of three, so only one-third of the total current reaches the port. Port 2, the ground trip port, has as its input three transformers in parallel so that all the energy reaches it. Port 3, the phase trip port driven in the difference mode, is equivalent to having the two outer bushing transformers connected in series, the middle one not being driven. This gives a factor of 2 for a total of 2000 turns by which to divide the source current. In addition, there is only one current source for the three circuits because of the difference mode drive, so the current needs to be divided by another factor of 3.

The General Electric ground trip port has three bushing transformers in parallel, so the only division of current that needs to be done is by the 500 for the turns ratio. The phase trip port is not considered in the study, but it also has three bushing current transformers.

## 3. ELECTRIC TRANSFORMER COUPLING

The bushing current transformer consists of a ferromagnetic doughnut placed over a ceramic cylinder whose center is also made of a ferromagnetic metal. The electric field can couple to the terminals at the transformer by means of the capacitance formed through the ceramic between the two metal surfaces. Page 118 in reference 7 gives the following formula for estimating the capacity of a concentric cable:

$$C = \frac{7.354\epsilon}{\log_{10}(D/d)} \text{ pF per foot} \qquad (13)$$

where $\epsilon$ is the dielectric constant of the material between the conductors, D is the inside diameter of the outer cylinder, and d is the outside diameter of the inner conductor.

Figure 20 in this report gives the radii for the inner and outer conductors. The thickness of the transformer is 1.3 inches (0.108 feet) and the dielectric constant of the insulator is 6. Substituting the figures in the above formula, a capacity of 5.58 pF is obtained. The current which will couple will be the voltage at the center conductor divided by the

capacitive reactance due to this capacitance. This is true for each bushing transformer, but as in the magnetic coupling case, the current then has to be divided by 3 for port 1 since only one of the three wires in the input line is involved. The port 3 difference mode current due to the capacitance needs to be divided by a factor of 6 as before.

The General Electric ground trip port, as is the case in the McGraw-Edison port 2, has a bushing current transformer for each of the three input wires. There were no dimensions available for the bushing sizes, but since the voltage class that they have to handle is the same (15 kV), it is assumed that they have the same dimensions and that the bushing current transformers are also of the same size. The current which couples due to the capacitive coupling is the voltage at the recloser divided by the capacitive reactance of 5.58 pF. In both the GE and in the McGraw-Edison port 2 cases there are three bushing-transformer capacitances. Since they are in parallel their total capacitance is three times that of one transformer. However, each wire in the sum mode has one-third the voltage that the whole line (as a three wire line) has, giving one-third the current. These two factors cancel each other.

4. ELECTRIC INTERNAL CABLE COUPLING

The cable inside the recloser housing lies perpendicular to the wires which carry the current due to the EMP. In this position the magnetic coupling is small enough to be ignored. The electric coupling due

to the stray capacitance is significant, since the unshielded cable in the recloser is surrounded only by transformer oil and a plastic wrap. Figure 42 gives dimensions of the recloser box with locations of the EMP-carrying wires going in and out of the box. This figure is useful in determining various geometric orientations for the internal coupling analysis.

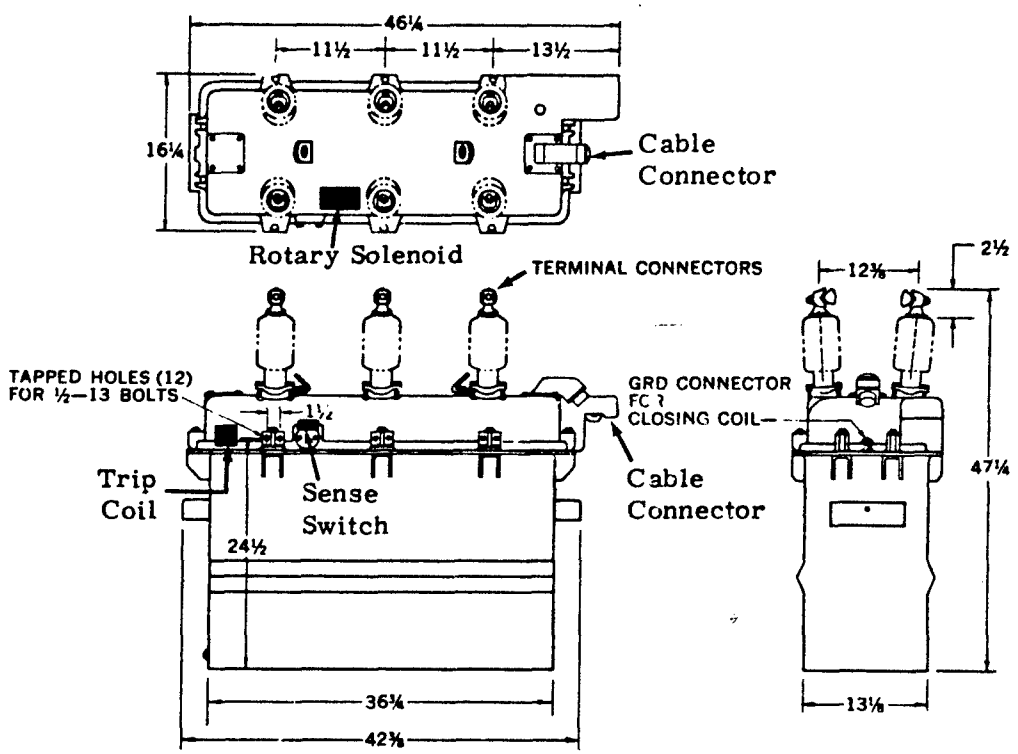



Figure 42. Dimensions of the McGraw-Edison Recloser, Three Views

The interior cable runs the length of the recloser "head" from the trip coil to the cable connector at a distance of about 5-1/4 inches from the plane formed by the input set of three wires and 3-1/4 inches from the plane formed by the output set. The distance from the cable to the plane formed by the top of the recloser is 1-7/8 inches. The value of electric field intensity at the cable location is needed so that an induced current in any of the cable wires can be determined. First, let us assume that the top plate forms a ground plane. Secondly, assume that the set of three wires, driven in the sum mode, which enter the recloser from the Beverage antenna side do form a plane with a voltage determined from the external coupling problem. The output set of three wires also form a plane with the same potential, but the current flows in the opposite direction so that the electric field lines from the two planes add in phase and general direction. The configuration is like that of figure 43.

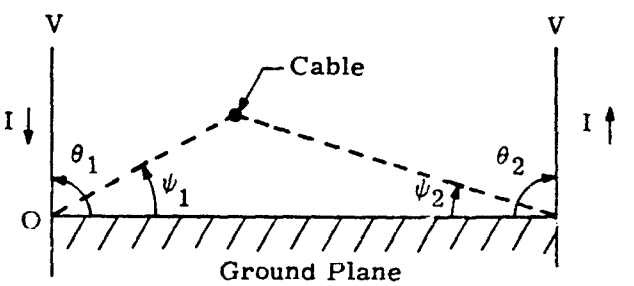



Figure 43. Configuration for Electric Field Coupling to Cable

V in figure 43 is the voltage at the recloser as calculated by the external coupling problem. The angles $\theta_1$ and $\theta_2$ are the angles of the voltage planes with respect to the ground plane. In this approximation one will assume these are 90°; therefore $\theta_1$ is arctan (1.875/3.25) and $\theta_2$ arctan (1.875/5.25), based on the dimensions given earlier for the cable location. A simple solution to the voltage at the cable due to one of the source planes is

$$V_{c_1} = V \frac{\psi_1}{\theta_1} = V \frac{30°}{90°} = V/3 \tag{14}$$

This solution is simply the ratio of the two angles formed by the cable location and the source plane location with respect to the ground plane. This solution assumes a uniform decrease of voltage between V and O at the ground plane and ignores other geometries in the recloser box. The contribution from the second voltage source plane is likewise

$$V_{c_2} = V \frac{\psi_2}{\theta_2} = V \frac{19.65°}{90°} = V(0.2184) \tag{15}$$

so that the total potential difference at the cable is

$$V_c = V_{c_1} + V_{c_2} = 0.5517V \tag{16}$$

The current source for each wire in the cable will be this voltage divided by the capacitive reactance of the wire with respect to the ground plane. The formula for the capacitance of a wire of diameter d a distance h from a ground plane in a medium with dielectric constant $\epsilon$ is

$$C = \frac{7.354\epsilon}{\log_{10}\left(\frac{4h}{d}\right)} \text{ pF/foot} \qquad (17)$$

according to reference 7. This formula includes the effect of the image in the ground plane. The cable is 32 inches long, each wire is 1/16 inch in diameter, and the distance above the ground plane is 1-7/8 inches. The dielectric constant for transformer oil is 2.24. Inserting these values in the above equation yields a capacitance of 21.1 pF per wire in the cable. The current flowing in each wire is then $V_c/X_c$ where $X_c$ is the impedance due to this capacitance as a function of frequency.

This current is then multiplied by 3 for the ground trip port since there are three wires in the cable associated with it. There is only one battery charging port wire in the cable, so no extra factor applies. There are two wires each for the remaining three sum mode ports (sense switch, rotary solenoid, trip coil) and so a factor of 2 is applied to this particular drive to those ports.

## 5. ELECTRIC COUPLING TO THE SENSE SWITCH, ROTARY SOLENOID, AND TRIP COIL TERMINALS WITH A SUM MODE DRIVE

The individual components in the recloser from which the ports get their name can also couple to the electric field by virtue of their stray capacitances. The procedure is similar to the analysis of the cable; that is, a potential difference due to the field at a particular location inside the box is calculated and then the induced current is obtained by dividing this potential difference by the capacitive reactance of the component. In each case the ground plane selected is the inner surface of the box closest to the component under analysis. Image considerations due to the ground plane are included. Unlike the cable analysis the source is not considered to be a plane but rather a line source (or sources, depending on the location of the component) with a voltage value equal to that calculated from the external coupling problem as before. A detailed explanation of the capacitance and field potential calculations is not presented here, but a table of results is given below. Table 1 presents the field potential $V_\rho$ as a fraction of the source voltage V. The subscript $\rho$ denotes the geometric dependence of the voltage.

Table 1

SUM MODE PORTS FIELD POTENTIAL AND CAPACITANCE VALUES

| | C (pF) | $V_\rho$ |
|---|---|---|
| Port 7 | 2.78 | 0.344V |
| Port 8 | 4.32 | 0.079V |
| Port 9 | 3.36 | 0.059V |

## 6. DIFFERENCE MODE PORTS MAGNETIC COUPLING

The area formed by the individual components in the recloser are subject to the magnetic field lines caused by current flowing in the input wires. The magnetic flux density at the location of a specific component may be calculated from Biot and Savart's law

$$B = \frac{\mu_o I}{2\pi r} \tag{18}$$

where $\mu_o$ is the permeability of free space, I is the current flowing in the source wire, and r is the equivalent distance of the object from the source. Once the flux density is known, the total flux is computed from

$$\Phi = BA \tag{19}$$

where A is the area under analysis. From Faraday's law the induced emf at the component is

$$V = \frac{d\Phi}{dt} \tag{20}$$

The induced emf is the voltage across the difference mode terminals and is the voltage source at the ports due to the magnetic coupling effect. Assuming the flux to have a harmonic time dependence $e^{j\omega t}$, we have

$$\frac{d\Phi}{dt} = j\omega\Phi = V \tag{21}$$

as the solution to the voltage in the frequency domain. Combining the above formulas we get

$$V = j\omega \frac{\mu_o}{2\pi} \frac{A}{r} I \tag{22}$$

In the case of the sense switch the loop area which is under consideration is that formed by the wire pair leading from the switch contacts to a terminal strip in the recloser. The geometric situation is such that the magnetic field lines are perpendicular to this area. The areas for both the rotary solenoid and the trip coil are those of the components themselves. These last two components are coils of wire wound around the area of interest, so the numerical solution to the above equation is multiplied by the number of turns for each coil. The rotary solenoid is composed of 1148 turns and the trip coil of 708 turns.

The geometric considerations in obtaining the loop area A and the source to loop distance r for each component are not presented here, but table 2 gives A/r for the sense switch and An/r, where n is the number of turns, for the other two ports so that the relative importance of this coupling between the three ports may be seen. The remaining parts of the expression for voltage are the same for all the ports.

Table 2

RATIO OF AREA TIMES NUMBER OF TURNS TO THE RADIUS FOR MAGNETIC COUPLING CALCULATIONS OF THE DIFFERENCE MODE PORTS

| | An/r |
|---|---|
| Port 4 | 0.00969 (n = 1) |
| Port 5 | 4.09005 (n = 1148) |
| Port 6 | 6.65190 (n = 708) |

## 7. THE CABLE BETWEEN THE RECLOSER AND THE CONTROL

The recloser and control unit are connected to each other by means of an eleven-conductor cable. Three conductors come from the current transformers, one for each phase for the phase trip sensing circuitry. One wire comes from the battery charging current transformer; there is a pair for each of the components (sense switch, rotary solenoid, trip coil), and the remaining wire is a ground wire. The cables used at Los Cordovas are not shielded, but the newer units do come with shielded cables. The total length of this exterior cable is 6 feet.

The problems involved in modeling the cable include calculating the mutual inductance between wires, the capacitance between wires, capacitance to ground for each wire, and the self inductance of each wire. The ground in this case is the recloser control box since almost the total length of the cable is in its proximity.

The first task performed in the analysis is to consider the three lines to port 2 driven in the sum mode as a three wire transmission line

above a ground plane. Formulas A-8 and A-9 from appendix A in reference 2 are applied for this purpose as an approximation. The solution to these formulas produces a figure for the inductance of this three wire system. The formulas are not repeated here, but the inductance obtained is 0.789 $\mu$H. The symbol for this inductance is $L_{(3)}$. This answer ignores any proximity effects from adjacent conductors which also carry currents. The basis for this assumption is that the three port 2 wires driven in parallel in the sum mode will carry the largest current as compared to the rest of the wires in the cable. Ports 1, 2, and 3 all receive direct drive from the current transformers but the physical and mode drive considerations point toward this assumption. The rest of the ports get their drive from electric or magnetic field coupling, and the assumption is made that these currents are smaller.

The next step in calculating the inductances of the other wires in the cable is to calculate a coupling coefficient. First, one can say that the field at a point in the cable is inversely proportional to the distance r from the source such that

$$B = K_a/r \tag{23}$$

where $K_a$ is a coefficient which depends upon such factors as the permeability of the surrounding media and the current flowing through the source. The inductance per unit length may be obtained by integrating the above with respect to r

$$L = \int_{r_1}^{r_2} B\,dr = \int_{r_1}^{r_2} \frac{K_a\,dr}{r} = K_a \ell n \frac{r_2}{r_1} \tag{24}$$

In the case of a single wire $r_1$ is the radius of the wire, and $r_2$ is twice the distance to the ground plane to account for the image. In our consideration the cable is about 1 inch thick and lying 1/2 inch from the surface of the control box. We consider that the average distance of an individual wire from the ground plane was 1 inch. The diameter of each wire is 0.08 inch. This gives an inductance of

$$L = K_a \ell n(50) \tag{25}$$

The mutual inductance M may be computed from the same formula but now $r_1$ is the distance between wires in the cable. We chose an average value of 1/2 inch for $r_1$. The mutual inductance is then

$$M = K_a \ell n(4) \tag{26}$$

The coupling coefficient is the ratio of mutual inductance to the self inductance, or M/L. We call this value $K_c$ which is equal to $\ell n(4)/\ell n(50)$ or 0.354. The coefficient $K_a$ is canceled by the M/L division and does not need to be computed.

Port 1 just has a single wire leading from the current transformer through the cable to the control box. Its inductance is calculated from

the coupling coefficient and the three wire inductance which we obtained before. The inductance of a single wire in the three-wire system is

$$3L_{(3)} = L_s + 2K_c L_s \tag{27}$$

where $L_s$ is the single wire inductance and the $2K_c L_s$ is the effect of mutual coupling from the other two wires. Solving this for $L_s$ we get

$$L_s = \frac{3L_{(3)}}{1 + 2K_c}$$

$$= 3(0.789\ \mu H)/(1 + 2(0.354)) = 1.386\ \mu H \tag{28}$$

as the inductance of the port 1 single wire.

The difference mode ports 3, 4, 5, and 6 each have a pair of wires leading from the recloser to control. Port 3 actually has three but one is considered neutral. The pair of wires carry currents in opposing directions, so the expression for their equivalent inductance is

$$L_- = 2L_s(1 - K_c) \tag{29}$$

The (-) subscript denotes the difference mode drive. The negative sign before the coupling coefficient indicates that the inductances subtract due to the opposite currents. The inductance obtained with the above expression is 1.791 $\mu$H. This is the inductance used for the cable for the difference mode ports.

Ports 7, 8, and 9 are sum mode ports with a pair of wires each in the cable. The currents are in the same direction so the expression for their inductance is

$$L_{+} = \frac{1}{2} L_s(1 + K_c) = 0.94\ \mu H \tag{30}$$

This expression is similar to the difference mode inductance above but now the coefficient is 1/2 instead of 2, since the two wires may be thought of as being parallel. The sign is positive before the coupling coefficient indicating the currents flow in the same direction.

The current which will couple to these sum mode ports from currents in the port 1 and port 2 wires will do so throughout the length of the cable, but in this approximation we will consider the cable as consisting of lumped elements and having all the coupling occur at the cable's midway point. This leaves 0.47 $\mu$H as the inductance left between the coupling point and the port terminals at the control box. In the sum mode the coupling from ports 1 and 2 to 7, 8, and 9 is electric and we therefore need a value of the capacitance between wires.

The inductance calculated above for the three-wire system in the cable is 0.789 $\mu$H ($L_{(3)}$). This is over the length $\ell$ of the cable, 6 feet or 1.829 meters. The relationship between inductance and capacitance is

$$C = \frac{\mu_o \epsilon_o \ell}{\left(\frac{L_{(3)}}{\ell}\right)} = \frac{(4\pi \times 10^{-7}) \times (8.85 \times 10^{-12}) \times 1.829}{\left(\frac{0.789 \times 10^{-6}}{1.829}\right)} \text{ F} \qquad (31)$$

From equation (31) the capacitance to ground for the three-wire system is 47.15 pF, and so the capacitance for a single wire is 15.72 pF. Assuming a dielectric constant of 2 as an average between the insulating material and air, the final capacitance to ground is 31.44 pF for each wire. Assuming an average separation of wires and distance above the ground plane as in the inductance calculation and a dielectric constant of 3 for the insulating material, we have calculated a capacitance between wires of 61.05 pF.

The total capacitance between the current-carrying port 1 wire and the two wires for any one of the sum mode ports is 122.1 pF. Likewise there are three wires for the port 2 coupling for a total of 366.3 pF. There will be a total of 488.4 pF through which current can couple to each sum mode port. The voltage which is applied to this capacitance to complete the coupling is the current carried by the port 1 or port 2 wire times the impedance of this wire. The impedance of the wire is one-half the inductive reactance of the wire plus the impedance due to the port circuitry at the control box. We assume coupling takes place at the middle point of the wire length. The port 1 wire has an inductance of 1.386 $\mu$H. The impedance due to half this inductance is added to $Z_{p1}$.

the port impedance, and then this sum is multiplied by the current the wire is carrying. There are three port 2 wires and so the current which multiplies the impedances is multiplied by 3. The port 2 wire system has an inductance of 0.789 $\mu$H. One-half of this reactance is added to $Z_{p2}$ and then the sum, when multiplied by three times the port 2 current, yields the voltage due to the three-wire system coupling. The voltage due to the port 1 wire is then added to the voltage due to the three port 2 wires. These voltages are coupled from four sources to the same wire at the same point, so they may be considered to be in parallel with an average value of one-fourth the above sum. The resulting expression for the coupling voltage due to the four current carrying wires, taking the comments immediately above into consideration, is

$$V_c = \frac{I_{p1}\left(Z_{p1} + j\omega \frac{1.386}{2} \times 10^{-6}\right) + 3I_{p2}\left(Z_{p2} + j\omega \frac{0.789}{2} \times 10^{-6}\right)}{4} \qquad (32)$$

The coupled current due to this source for each of the sum mode ports is this voltage divided by the capacitive reactance to ground, 488.4 pF. This current is applied through the 0.47 $\mu$H inductance of the wire pair. The values of the variables in equation (32) depend on frequency and are calculated from the circuit parameters of figures 28 and 30.

The current which is being carried by the port 1 and port 2 wires may also couple to the three difference mode ports, ports 4, 5, and 6,

through magnetic coupling. The voltage appearing at the port wires is of the form

$$V = j\omega MI \tag{33}$$

where M is the mutual inductance between the wires which carry the current and the pair of wires which has the induced currents in opposite directions for the ports. The mutual inductance can be expressed as

$$M = K_g L \tag{34}$$

where L is the inductance of a single wire, calculated earlier as 1.386 $\mu$H, where $K_g$ is a coupling coefficient of the form

$$K_g = K_1 - K_2 \tag{35}$$

which takes into account the opposing currents in the port's wire pairs. This coupling coefficient is calculated from the following:

$$K_g = K_1 - K_2 = \frac{1}{\ell n \frac{2h}{a}} \left[ \ell n \frac{2h}{D_1} - \ell n \frac{2h}{D_2} \right] = \frac{\ell n \frac{D_2}{D_1}}{\ell n \frac{2h}{a}} \tag{36}$$

the 2h is, as before, twice the distance from a wire to the ground plane, a is the radius of the wire, $D_1$ is one distance between wires and $D_2$

another. These formulas are based on the calculation of the coupling coefficient in equations (23) through (26). The difference here is that we have one wire considered the source and two wires which have current induced on them in a difference mode manner. That is why we have a $D_1$ and $D_2$ as distances to the source wire from the receiving wires. The argument of the log in the denominator, 2h/a, is, as before, 50. The $D_2/D_1$ ratio must be decided based on some sort of "average" separations of wire within the cable. Before we had an "average" separation of 1/2 inch; obviously, we cannot use this value for both $D_1$ and $D_2$ because if both wires are the same distance from the source, the induced currents are equal but opposite and yield a net resulting current of zero. The cable is 1 inch thick, so the wires cannot be separated by a distance larger than this. After some statistical calculations we have chosen a $D_2/D_1$ ratio of 1.275. This gives a coupling coefficient value of $K_g = 0.0626$. Substituting this into equation (34) gives a value for M of 0.0868 $\mu$H. The current I in equation (33) is the sum of the port 1 and port 2 currents. The magnetic coupling into each of the difference mode ports is expressed as

$$V = j\omega(I_{p1} + I_{p2})0.0868 \times 10^{-6} \qquad (37)$$

Another means of coupling to the cable is from currents flowing in the recloser support stand from bushing capacitances (or current flowing

through broken-down bushings) which allow currents from the source wires to flow to the stand. The inductance through which the control box is coupled to the stand allows a voltage difference between boxes. This voltage difference appears directly across port 1 in series with the cable inductance and a discrete capacitor inside the recloser which is discussed below. The voltage also appears across port 2 in series with the cable inductance and a resistor, also to be discussed below. Figure 14 in section III illustrates this coupling by means of a circuit diagram. There is a ground wire inside the cable which is connected to both the recloser and the control boxes which also have this voltage difference, $V_s$ as labeled in figure 14, directly across it. If we consider electric coupling to other wires in the cable as before, that is at mid-cable, and assume each set of wires leading to the sum ports to be of half length and in parallel, then the voltage appearing at the coupling point is $0.125\ V_s$ due to the ground wires.

Another form of coupling due to the current flowing in the ground wire is magnetic coupling to the difference mode ports. The voltage is the coupling coefficient, $K_g = 0.0626$, the solution to equation (36), times $V_s$.

In addition to $V_s$ affecting the drive to ports 1 and 2 directly and to all ports through the ground wire inside the cable with magnetic and electric coupling, the support stand current couples to the cable throughout

the length of cable lying alongside the stand. Although both electric and magnetic coupling take place, only electric is considered because we estimate that on the average the difference mode pair of wires for each port is the same distance from the source thereby yielding a net induced current of zero. The voltage at the sum mode port wire pair is $V_s$ times the interwire capacitance divided by the ground capacitance times the fraction of the cable length which will couple to the stand current. The result is 0.088 $V_s$; this is smaller than the coupling through the internal ground wire.

## 8. EQUIVALENT CIRCUITS FOR INTERNAL AND BETWEEN-BOX COUPLING

In addition to the electric and magnetic coupling devices, and before the equivalent circuits can be drawn, mention must be made of discrete components inside the recloser box which are part of the circuits. The battery charging current transformer has a 1000-ohm, 24-watt resistor in series with it. The current flowing through the transformer also flows through this resistance. In addition, there is a 0.2 $\mu$F capacitor rated at 2500 volts directly across the transformer terminals. Each of the bushing current transformers which feed the phase and ground trip ports has a 100-ohm, 25-watt resistor across its terminals. The port 2 equivalent is three 100-ohm resistors in parallel, or 100/3 (33.333...). The port 3 equivalent is two resistors in series, or 200 ohms.

Port 4 has no discrete component other than the sense switch itself, but it already has been represented, through its terminals, as an area for magnetic coupling. It is represented above as a stray capacitance for electric coupling. The port 5 component is a rotary solenoid composed of 1148 turns. The equivalent inductance of this coil from page 58 in reference 7 is

$$L = 0.0117\, n^2 h \log_{10} \frac{d_2}{d_1}\ \mu H \tag{38}$$

where n is the number of turns, h is the thickness of the toroid, $d_1$ the inner diameter, and $d_2$ the outer diameter. The solution to this equation with the rotary solenoid's parameters is $4.643 \times 10^3\ \mu H$. This inductance is added to the 1.791 $\mu H$ due to the cable wire and rounded off to produce an inductance of 4645 $\mu H$. In the sum mode the terminals of the coil are driven together, effectively placing the coil out of the circuit.

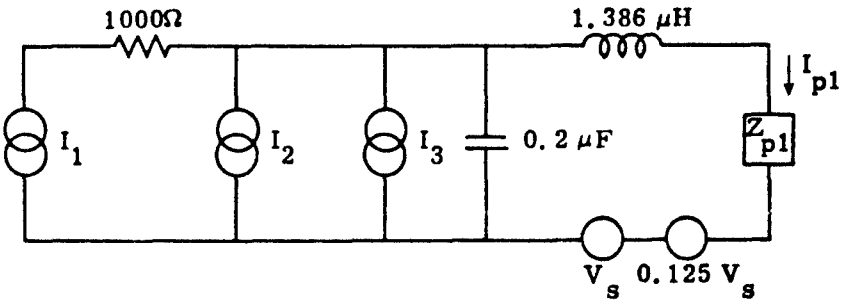
The remaining component is the trip coil which, like the rotary solenoid, is out of the picture in the sum mode, but in the port 6 consideration, the inductance must be computed. The inductance from page 62 in reference 7 is

$$L = \frac{0.8\, a^2 n^2}{6a + 9b + 10c}\ \mu H \tag{39}$$

where n is the number of turns, which is 708, and a, b, and c are the dimensions of the coil as indicated in reference 7. The solution to this equation is $1.388 \times 10^4$ $\mu$H. The 1.7 $\mu$H from the cable is insignificant compared to the coil inductance.

Figure 44 is a summary of the coupling discussion given in this section presented in circuit diagram form. Values of V and I are those obtained from the external coupling calculations of section III and are assumed to be the values at the recloser and flowing through the recloser due to the EMP excitation.

(a) Port 1 Coupling

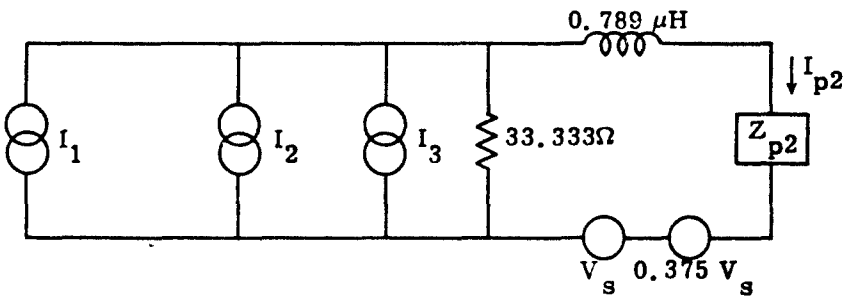



Magnetic Transformer Coupling $I_1 = (I/1000)/3$

Electric Transformer Coupling $I_2 = 5.58 \times 10^{-12} j\omega V/3$

Electric Coupling to Internal Cable $I_3 = 0.5517V(21.1275 \times 10^{-12} j\omega)$

(b) Port 2 Coupling



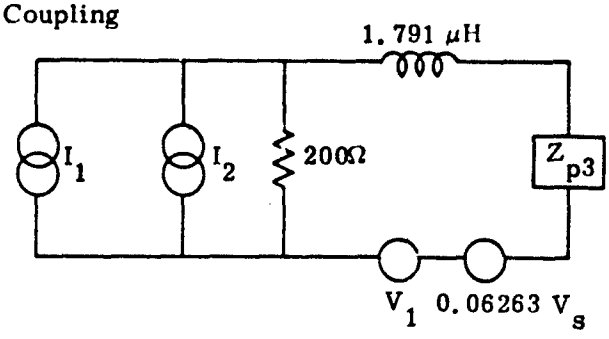

Magnetic Transformer Coupling $I_1 = I/1000$

Electric Transformer Coupling $I_2 = 5.58 \times 10^{-12} j\omega V$

Electric Coupling to Internal Cable $I_3 = 3 \times 0.5517V(21.1275 \times 10^{-12} j\omega)$

Figure 44. Internal Coupling Circuits

(c) Port 3 Coupling

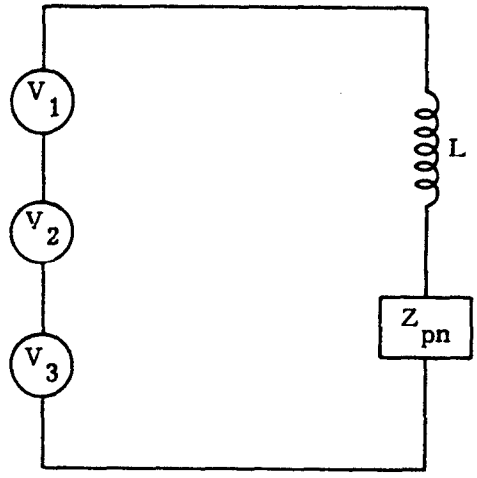



Magnetic Transformer Coupling $I_1 = (I/1000)/6$

Electric Transformer Coupling $I_2 = 5.58 \times 10^{-12} j\omega V/6$

Cable Magnetic Coupling $V_1 = 0.0868 \times 10^{-6} j\omega(I_{p1} + I_{p2})$

(d) Coupling to Difference Mode Ports (4, 5, 6)




Cable Magnetic Coupling $V_1 = 0.0868 \times 10^{-6} j\omega(I_{p1} + I_{p2})$

Cable Magnetic Coupling from Ground Wire Current $V_2 = 0.06263\ V_s$

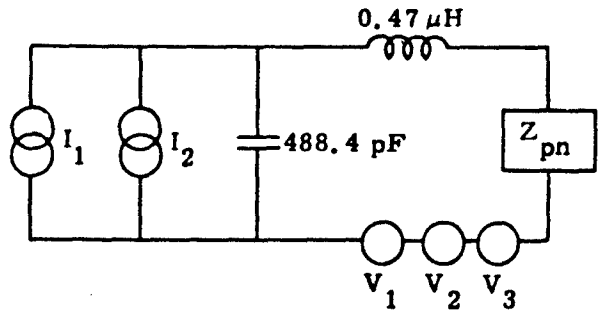
Magnetic Coupling to Individual Components in the Recloser $V_3 = j\omega \frac{\mu_o}{2\pi} A/r\ I$

Inductance of Individual Component Plus the Cable Wire Inductance (for: Port 4 = 1.791 μH, Port 5 = 4645 μH, Port 6 = 13882 μH) L

Impedance of Individual Port $Z_{pn}$

Figure 44. (Continued)

(e) Coupling to Sum Mode Ports (7, 8, 9)




Electric Coupling to Internal Cable $I_1 = 2 \times 0.5517V(21.1275 \times 10^{-12}j\omega)$

Electric Coupling Within Exterior Cable

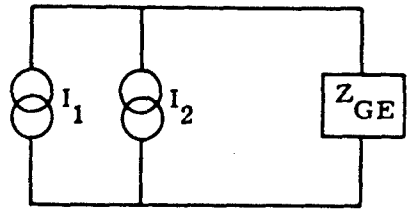
$$V_1 = \frac{1}{4}\left\{I_{p1}\left(Z_{p1} + j\omega \frac{1.386 \times 10^{-6}}{2}\right) + 3I_{p2}\left(Z_{p2} + j\omega \frac{0.789 \times 10^{-6}}{2}\right)\right\}$$

In-Cable Electric Coupling from Ground Wire Cable $V_2 = 0.125\ V_s$

Electric Coupling from Stand Current $V_3 = 0.088033\ V_s$

Electric Coupling to Individual Component Inside Recloser $I_2 = V_{pn}j\omega C_n$

(f) General Electric Recloser Ground Trip Port




Magnetic Transformer Coupling $I_1 = I/500$

Electric Transformer Coupling $I_2 = 5.58 \times 10^{-12}j\omega V$

Figure 41. (Continued)

# SECTION VI

# RESULTS AND CONCLUSIONS

## 1. BUSHING BREAKDOWN ANALYSIS

Section III-5 discusses the possibility of bushing breakdown; this is accomplished if the voltage (due to lightning or EMP) exceeds a threshold value. The calculations performed in that section indicate that if the potential exceeds 147.7 kV the dielectric strength of the 15 kV class bushings is exceeded and breakdown will occur. The exact nature of the breakdown is not clearly understood, although the general opinion is that if it does occur, through the body of the porcelain, considering the 60 Hz follow current, the damage is irreversible due to catastrophic changes in the crystal lattice structure of the ceramic. The subject of dielectric breakdown is discussed in references 13, 14, and 15, but the development of a model, perhaps analogous to the Wunsch model for semiconductor breakdown, is desirable in order to better understand this particular phenomenon. The model used in our analysis is simple in keeping within the scope of study and it is felt that a better model must be made for better approximation to the final results.


13. O'Dwyer, J. J., The Theory of Dielectric Breakdown of Solids, Oxford University Press, New York, 1964.

14. Whitehead, S., Dielectric Breakdown of Solids, Oxford University Press, New York, 1951.

15. Creedon, J., Volume Dependent Electrical Breakdown in Solids, PIIR-20-70, Physics International Company, San Leandro, CA, June 1970.

The results of this study, which assume that EMP comes through the distribution lines (Beverage antennas), indicate that the 147.7 kV potential necessary to damage a bushing in our model does occur. The bushings on the customer distribution side of the recloser fail throughout the range between 400 kHz and 5.5 MHz. In the old configuration, with the autotransformer bushings on line LI-500, we obtain voltages at the autotransformer bushings which exceed the breakdown value. The customer distribution side bushings fail through a somewhat larger range than that of the LI-200 bushings at the recloser, as might be expected. In addition, the substation side bushings at the autotransformer fail around 5 MHz. Other bushings involved in the analysis, for example those at the General Electric recloser, are relatively isolated from the Beverage antenna and do not fail. Figure 45, a plot of the magnitude of the voltage at the McGraw-Edison recloser and at the LI-500 autotransformer versus frequency assuming no failure, shows the range through which failure is indicated. In the coupling model the voltage assumed at the bushing in case of failure is the breakdown voltage, with the appropriate phase, as mentioned in section III-5.

As a damage mechanism, bushing failure may cause the high voltage line to be shorted to the case of the piece of equipment, resulting in a short circuit which may cause other reclosers to trip, fuses to burn out, possible equipment failure (regulators, transformers, meter boxes,

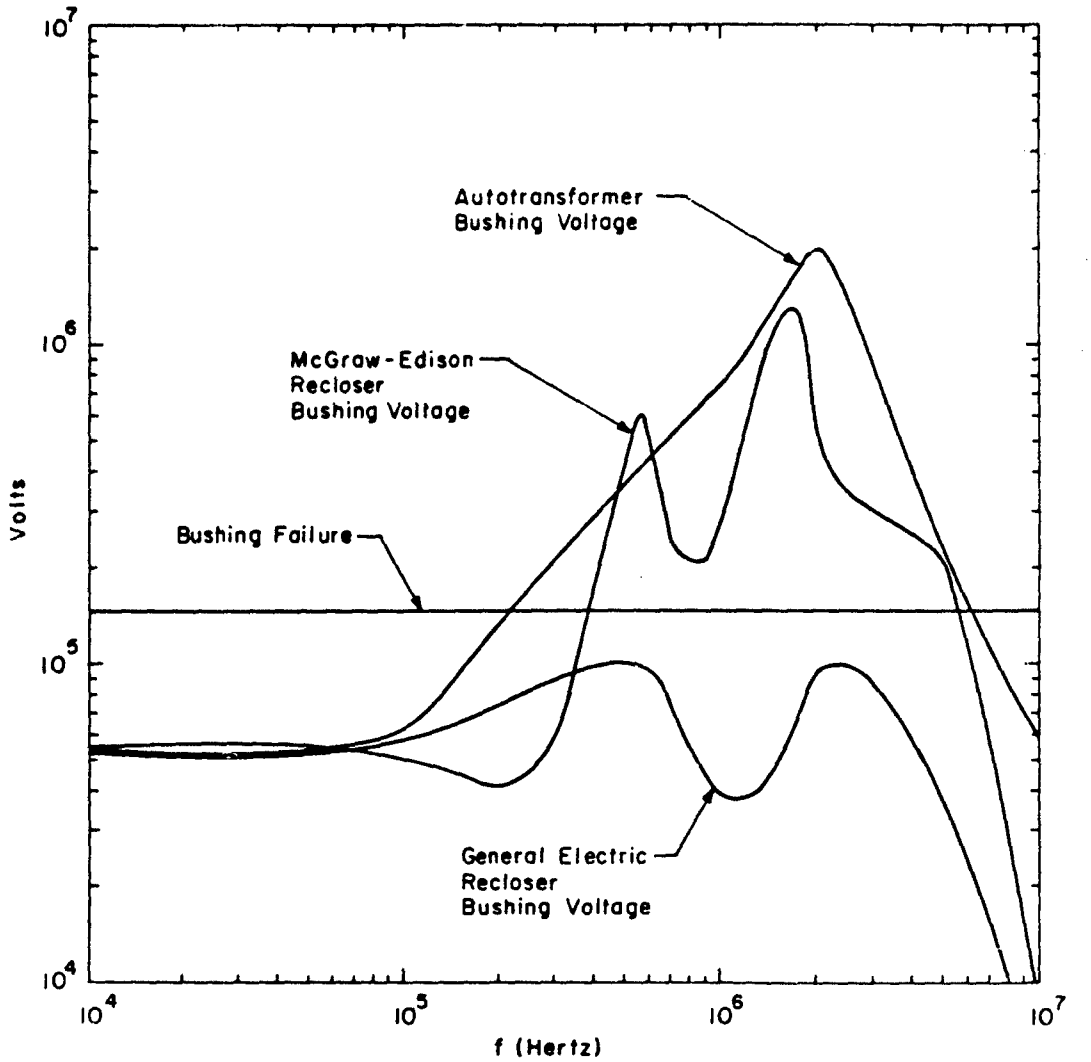



Figure 45. Bushing Voltage Ignoring Failure

etc.) due to resulting high currents. The minimum damaging effect is probably leakage of current and thus loss of efficiency. A damaged bushing must be replaced as promptly as possible after the damage in order to continue efficient operation.

One method for preventing bushing failure is to install lightning arrestors closer to the bushings. The lightning arrestors at the frame, or pole in the autotransformer situation, do fire at these potentials, but the inductance due to the relatively long wire lengths between the arrestors and a common ground prevents much of the current from flowing through the arrestor, causing the potential at the top of the arrestor to remain much the same as it is without the arrestor firing. If the arrestor were mounted directly across the bushing between the conductor and the equipment case, then upon firing it would present a nearly perfect short for the duration of the pulse, protecting the bushing (and the equipment in the case).

During our final visit to the Los Cordovas substation we noticed that several of the bushings on the LI-500 McGraw-Edison recloser had been damaged. Parts of the bushing insulation had spalled off and there were body cracks. The cause was apparently due to lightning striking the 144-foot section. We were unable to inspect the bushings at the autotransformer during this visit to see if that end of the 144-foot section had bushing damage. The set of damaged bushings had not been repaired,

apparently because this particular recloser is no longer in use since the activation of the new part of the substation. This damage was a concrete example that indeed bushings can be damaged by short pulses of high voltage. The mechanism is apparently shock propagation in a brittle material.

## 2. POLYETHYLENE BREAKDOWN ANALYSIS

The other dielectric subject to high voltages is the polyethylene surrounding each of the three high power lines which comprise the underground cable between the new LI-500 configuration and the substation. In section III-7 this subject is discussed and the calculations indicate that the breakdown voltage is 84.9 kV.

The model used is the same as for the bushing (a voltage source with the proper phase) and is placed at the locations where the cable is likely to break down. In our model we approximated the possibility of breakdown over the length by assuming breakdown occurred at either end. Figure 46 illustrates the voltages at both ends of the cable. The voltages at the substation end of the cable are calculated under the assumption that if breakdown voltages are exceeded at the antenna end, the equivalent dielectric capacitance is replaced by an 84.9 kV source.

In both figures 45 and 46, note that the magnitude of all the voltages shown approach a value of approximately 54 kV at low frequencies. This is the value of the firing potential of the lightning arrestors

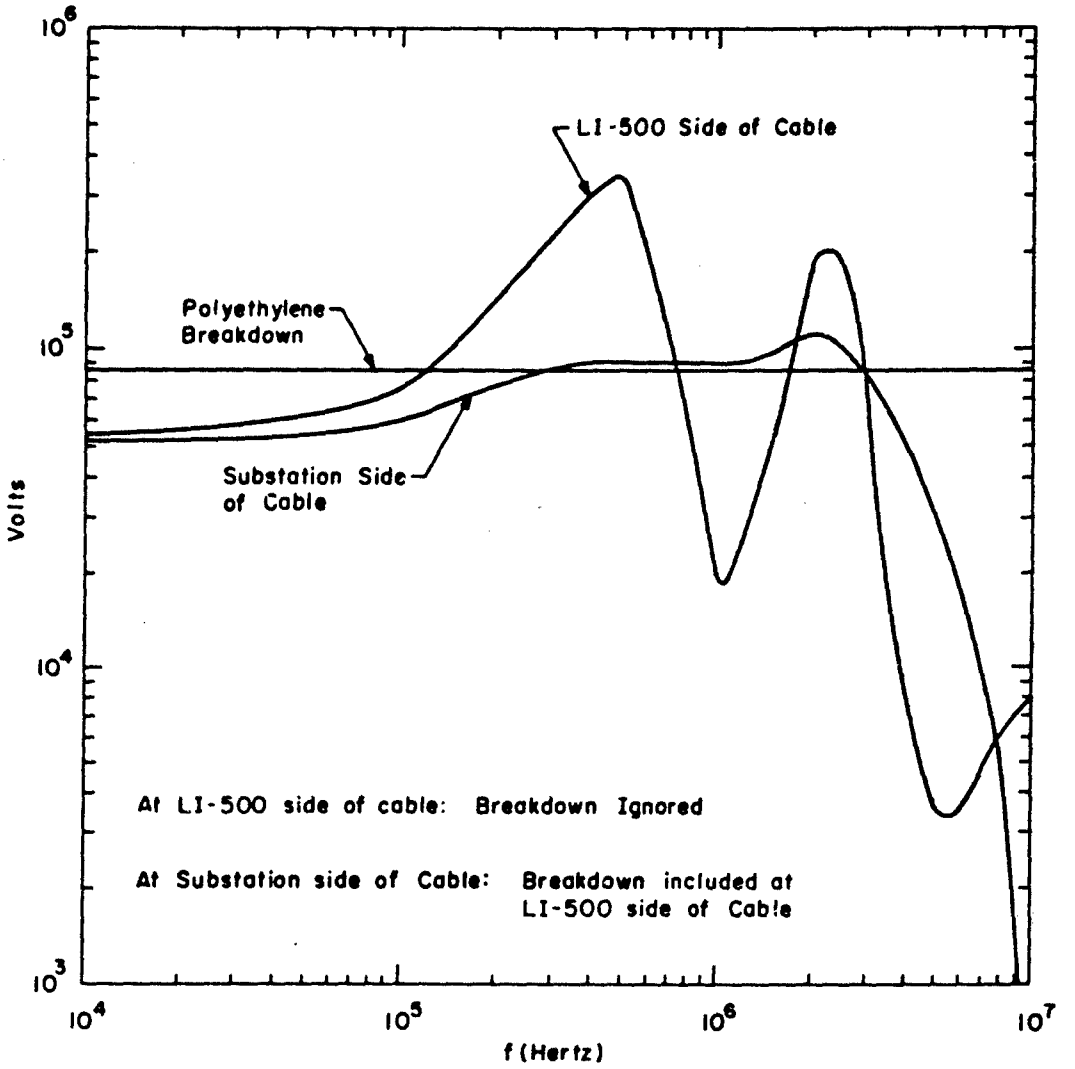



Figure 46. Voltage at Insulation of Cable

involved. At low frequencies the arrestors are effective because the arrestor to ground impedance due to the inductance of the path is low, allowing the arrestor circuitry to keep the voltage at the connection at the firing voltage. The arrestors would be effective even at high frequencies if their return path impedance were kept small enough.

From figure 46 we can see that breakdown voltages are exceeded at both ends of the cable throughout a wide frequency range. The breakdown at the antenna end attempts to keep the voltage at the substation end at the breakdown voltage roughly between 200 kHz and 2 MHz, but other parameters in the calculations raise the substation end voltage to values above breakdown.

As in the bushing ceramic situation, the exact nature of this breakdown is not clear and an analogous Wunsch breakdown model would be desirable. Since polyethylene is a flexible dielectric, the possible damage effects in case the breakdown voltages are exceeded include burning holes in the insulation or melting it. If holes are burned through during the breakdown period, the mechanical strength of the remaining insulation would still be enough to keep the center conductor from shorting out against the outer sheath when voltages return to normal. Also, it is likely that the holes are self-healing, as in a liquid dielectric, or small enough to cause negligible leakage current so that no permanent disabling damage occurs. It is possible that permanent damage will

exist, and replacement of portions of the cable will be necessary before normal operation can resume.

## 3. VOLTAGES ACROSS CAPACITORS AT THE PORTS

Every one of the nine ports associated with the McGraw-Edison unit under consideration has one or more capacitors connected directly across its terminals. Port 1 has one 0.1 $\mu$F capacitor; port 2 has three 0.1 $\mu$F capacitors in parallel across its terminals; ports 3, 4, 5, and 6 have two 0.1 $\mu$F capacitors in series; and ports 7, 8, and 9 have two 0.1 $\mu$F capacitors in parallel. The parts list for this recloser states that all these capacitors are rated at 200V. In checking the voltage at the terminals one will have to see if the 200V are exceeded in the case of the capacitors being in parallel, or 400V in the case of two capacitors in series.

The numerical results of the analysis indicate that the port 1 capacitor rating voltage is exceeded throughout the range between 300 kHz and 3 MHz. Port 4 has two capacitors in series, one shunted by some other components which for this check we assume have a relatively high impedance, so that 400V exceeds their rating. This figure is exceeded at only one frequency, namely 500 kHz. The voltage ratings are not exceeded at any other port. Although the port 1 capacitor rating is exceeded, we do not model any failure into the analysis.

Since port 1 has voltages at its terminal which exceed the capacitor rating, figure 47 is presented to show the voltage curve as a function of frequency. The port 4 voltage exceeds the rating at one one frequency, and voltages at either side frequency on which calculations were made are down two orders of magnitude. This indicates a sharp resonance at that frequency, and damage to the capacitor is unlikely since the amplitude at this frequency should be corrected downward by a bandwidth factor.

The General Electric recloser ground trip port has a capacitor in its circuit, but it is not in a particularly vulnerable position and its voltage rating is not exceeded.

4. SEMICONDUCTOR FAILURE

With the completion of the exterior, interior, and between-box coupling models and the individual port representation, we are in a position to combine everything and see just how much current flows into the port, and compare that with the current necessary to damage a solid state device. A simple ratio of the coupled current to the threshold current gives us an answer. Table 3 gives the results of the model combination. These results are for the McGraw-Edison recloser.

If the ratio is above 1 then the device failure probability is at least 50 percent. We have boxed values above 0.1 in table 3 to indicate at least a remote chance of failure. Statistical analysis of port failure such

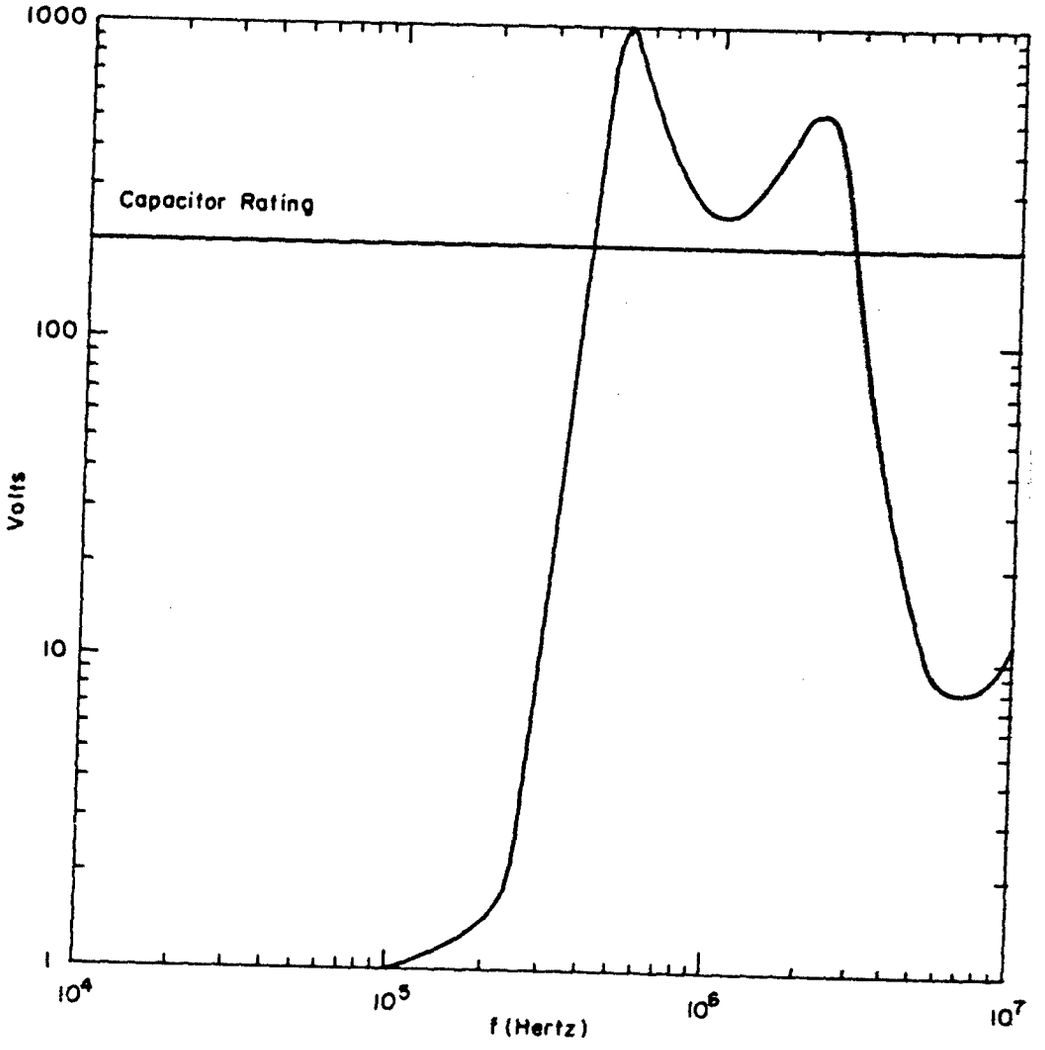



Figure 47. Magnitude of Voltage at the Port 1 Terminals

Table 3

FAILURE RATIOS FOR THE NINE MC GRAW-EDISON RECLOSER PORTS

| Freq. (Hz) | Port 1 | Port 2 | Port 3 | Port 4 | Port 5 | Port 6 | Port 7 | Port 8 | Port 9 |
|---|---|---|---|---|---|---|---|---|---|
| 1.0E+04 | 1.41E-04 | 5.22E-03 | 1.35E-04 | 3.81E-06 | 4.60E-03 | 1.12E-03 | 8.36E-03 | 4.00E-03 | 5.24E-03 |
| 2.0E+04 | 2.67E-04 | 1.06E-02 | 1.55E-04 | 1.54E-05 | 3.63E-03 | 7.46E-04 | 1.19E-02 | 4.12E-03 | 7.10E-03 |
| 5.0E+04 | 3.79E-04 | 2.63E-02 | 1.54E-04 | 1.24E-04 | 1.67E-03 | 3.94E-04 | 1.83E-02 | 4.12E-03 | 8.95E-03 |
| 1.0E+05 | 1.24E-03 | 4.80E-02 | 1.30E-04 | 5.68E-04 | 7.74E-04 | 2.02E-04 | 2.26E-02 | 3.73E-03 | 8.10E-03 |
| 2.0E+05 | 1.79E-02 | 8.57E-02 | 1.11E-04 | 2.37E-03 | 3.17E-04 | 8.40E-05 | 2.45E-02 | 3.05E-03 | 5.73E-03 |
| 5.0E+05 | 1.26E+00 | 1.49E+00 | 2.88E-04 | 2.82E+00 | 6.19E-04 | 1.16E-04 | 1.27E-01 | 1.18E-02 | 1.60E-02 |
| 1.0E+06 | 3.17E-01 | 1.27E+00 | 2.13E-04 | 1.28E-01 | 2.46E-04 | 3.35E-05 | 1.49E-01 | 1.17E-02 | 1.19E-02 |
| 2.0E+06 | 6.61E-01 | 5.39E+00 | 1.43E-03 | 2.57E-01 | 2.01E-04 | 1.32E-05 | 2.34E-01 | 1.66E-02 | 1.25E-02 |
| 5.0E+06 | 1.54E-02 | 9.55E-01 | 3.86E-04 | 1.37E-02 | 5.12E-05 | 1.66E-06 | 2.04E-01 | 1.33E-02 | 6.55E-03 |
| 1.0E+07 | 1.41E-02 | 3.43E-01 | 1.06E-03 | 9.64E-03 | 3.92E-06 | 4.41E-08 | 7.82E-01 | 5.22E-02 | 1.86E-02 |

as found in reference 6 would perhaps be useful in determining likelihood of failure. In addition to boxing the figures for each port above 0.1, the ratios which exceed 1 are underlined to indicate where they occur.

From the table one can see that ports 3, 5, 6, 8, and 9 are not particularly vulnerable. The most vulnerable appears to be port 2, the ground trip port, but failure values are indicated in ports 1 and 4 for 500 kHz. The largest ratio is for port 2 at 2 MHz. The largest ratios for ports 7, 8, and 9 occur at 10 MHz. These are due primarily to the resonance at 10.5 MHz which is caused by the 488.4 pF capacitance and 0.47 $\mu$H inductance in the internal coupling circuit for these ports. Similar calculations (being aware of the model frequency limitations) at 20 MHz of the slope of the ratio curve for these ports indicate that the ratios were down by a factor of five.

Figure 48 is a graph of the vulnerability ratios for ports 2, 4, and 7, with the maximum ratio at each frequency taken as a vulnerability level for the whole recloser. The largest vulnerability ratio obtained for the General Electric Ground Trip Port is 0.3. The ratio curve for this port is also included in figure 48.

Since the McGraw-Edison port 2 is the most vulnerable for that recloser and the General Electric ground trip port is the most vulnerable (and the only one taken into consideration) for that recloser slots of the coupling current to these ports and the threshold currents are

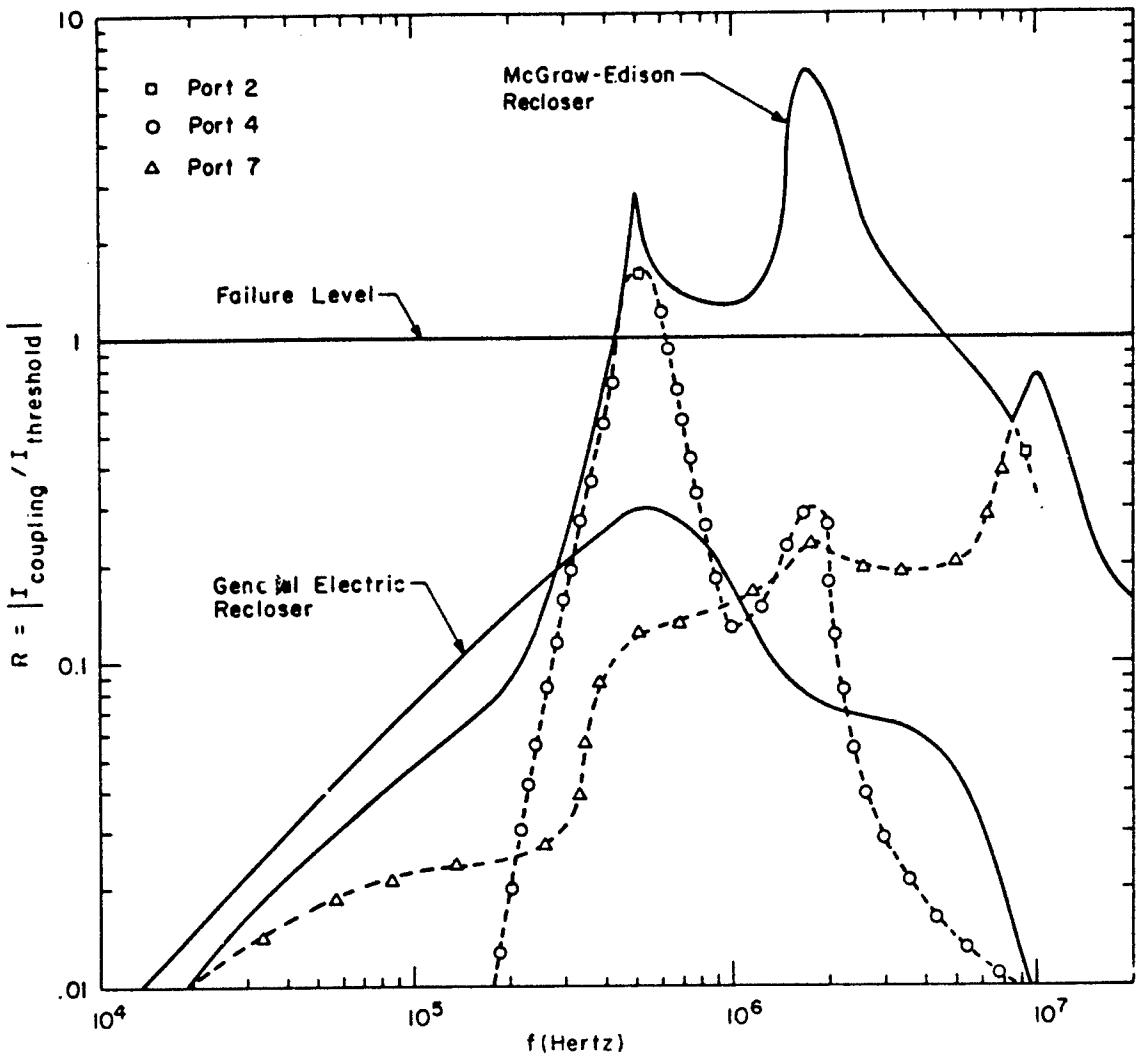



Figure 48. Vulnerability Ratio versus Frequency for the McGraw-Edison and General Electric Reclosers

presented in figure 49. This graph gives the coupling currents in amperes and what it takes to fail the ports, to get a general idea as to the magnitudes involved.

The consequences of a port failing may be deduced from the circuit diagrams. For example if port 2 does fail (we use this as an example since it is the most vulnerable), then it is likely that the 5:1 isolation transformer will burn out; the failing diode is in the rectifier bridge. This particular failure may be circumvented by taking port 2 completely out of the circuit by having the "ground trip blocking switch" in the number 1 position (refer to figure 24). Having port 2 out of the circuit will not hamper normal phase trip operation of the recloser and it will then not be sensitive to ground faults. Since it is the most vulnerable perhaps it would be a good idea to take it out of the circuit in cases of national emergency.

Once a port fails it is likely that the damaged recloser components will have to be replaced and tripping will have to take place manually by means of knifeswitches until their replacement. The knifeswitches on at least one side of each recloser are fused, so if large currents do go through a recloser the fuse may burn out, providing protection to other equipment. Replacement of fuses is manual, causing a delay in return to normal operation.

Failure of a recloser does imply that manual intervention is necessary, either to replace the damaged components or throw knifeswitches.

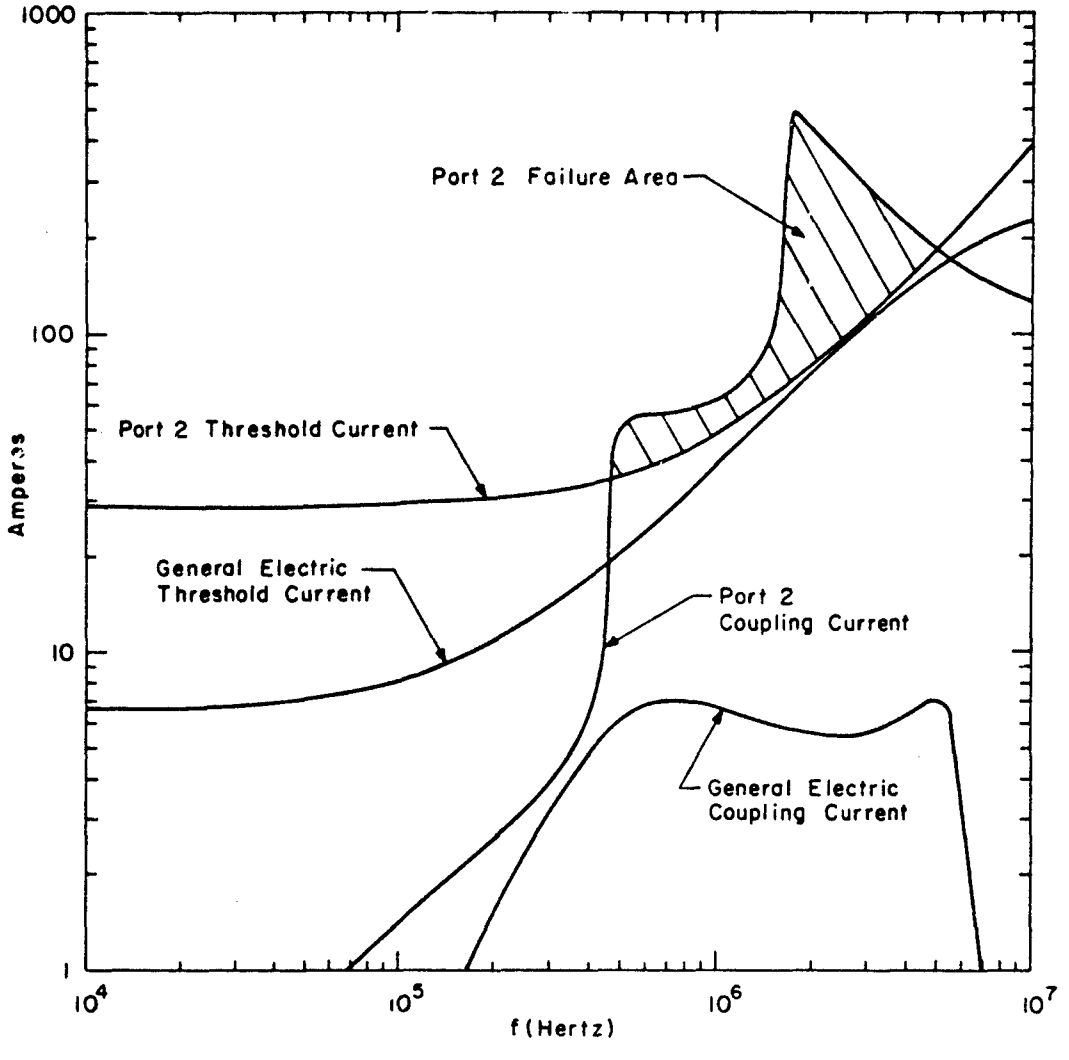



Figure 49. Threshold and Coupling Currents for Port 2 of the McGraw-Edison Recloser and the General Electric Recloser Ground Trip Port

The consequences of manual intervention imply time delays. The analysis does show that the McGraw-Edison recloser fails at three of the nine ports throughout various frequencies. On the other hand the General Electric recloser does not fail. The buried cable, the lack of a control cable, and the relatively small inductance in the lightning arrestor circuits are the major factors in the relatively small amount of coupling to the GE recloser. One is led to the conclusions that distribution lines should be buried whenever possible, and leads to various connections should be kept as short as possible.

In the McGraw-Edison recloser one major coupling factor is the unshielded cable. Coupling to it is affected by fields internal to the recloser and the current flowing through the support stand causing coupling to the unshielded external cable. The fact that the recloser and the recloser control unit are separated by the stand inductance causes a voltage difference between the two boxes which makes current flow in the cable ground wire. This type of coupling consideration is best handled in the design stage by shielding the cable. All McGraw-Edison ports do have capacitors across the terminals; since a capacitor shows low impedance at high frequencies this is a good means of preventing failure by sound engineering practices.

By referring to the graphs of the results, one can see that the two most important areas of frequency are around 500 kHz and 2 MHz. The

resonances around these frequencies are doe to the reactive and inductive parameters which result from wire lengths, bushing capacitances, transformers modeled as capacitors, etc. Resonances like these cannot be eliminated but being aware of their existence is important in understanding the overall response of a system to EMP. Resonance effects could perhaps be minimized in the station design stage.

## 5. SUMMARY

The objective of this study is to determine the vulnerability of the Kit Carson Electrical Cooperative as a typical rural power distribution system. The substation we analyse is the one at Los Cordovas because it is the largest in the system and its failure would cause the most impact on the Taos community. In addition Los Cordovas is the only one in the system that has electronically controlled reclosers with solid state components which one assumes are the most vulnerable parts of the system.

With the overhead customer distribution lines performing as antennas and the substation (old or new part) as a load, the calculational results indicate that failure is indeed highly likely. The old part of the substation has reclosers with several ports which indicate that more than the threshold currents could couple to and fail solid state devices. In addition there probably is damage to the porcelain bushings on the input side of the recloser. The recloser at the new part of the substation does

not fail and its bushings do not fail, but the ends of the underground cable do receive voltages which are higher than the calculated breakdown value of the polyethylene insulation.

The consequences of these failures as applied to Kit Carson are not very good since other (perhaps more expensive) damage could result. Power to the consumers would likely terminate until repairs could be done. In the presumed post attack situation, emergency repairs could be slow in coming. Prevention of failure could be accomplished by shunting the bushings and the cable with lightning arrestors at points which would minimize ground return paths. The best preventive measures are those taken in the design stages and this should be done by engineers who design the substation equipment and the power engineers who plan the substation. The new part of the Los Cordovas station was better designed from a lightning protection viewpoint than the old part and this may be a good indication that better engineering practices are in effect in more modern substations.

The accuracy of this study could be investigated further by laboratory and field testing and development of failure models for equipment other than the solid state devices. The coupling model could be made more sophisticated to include higher frequencies and by the more accurate modeling of components such as the voltage regulators and transformer. Testing of these devices to determine high frequency characteristics, such as a transfer function, could be done in this effort.

A detailed analysis is not done on other substations in Kit Carson; however if the customer distribution lines of the other substations are similar in characteristics to the Los Cordovas Beverage antenna, then the bushings at the power transformer secondaries are likely to break down. Since the pulse is too short to burn out the fuses at the knife-switches then damage to the transformer is likely.

The overall result is that this particular electrical cooperative is vulnerable to possible damage. An analysis similar to this of cooperatives in other parts of the country is desirable in order to statistically analyze the vulnerability of rural power systems throughout the United States. Further thoughts on EMP effects on the power system are given in appendix D. Possible effects of EMP on a customer are discussed in appendix E.

## APPENDIX A

## THE BEVERAGE ANTENNA AND 80 FOOT SECTION

### 1. GROUND CONDUCTIVITY, DIELECTRIC CONSTANT, AND PROPAGATION CONSTANT

Mentioned in section III-3 of this report is the fact that ground resistivity measurements were taken at the Los Cordovas substation and thus information concerning ground characteristics was gathered. The measurements mentioned in that section were concerned with the ground resistance in the vicinity of the substation and include the resistance of the ground mat within the station. In determining antenna characteristics, values for conductivity and a dielectric constant of the earth and soil which form the ground plane are needed. In addition to the ground mat resistance measurements, one other measurement was taken in the substation and two outside the substation with the three electrode meter mentioned in that section.

Such measurements can be used to get ground conductivity by using the techniques outlined in appendix B-2 in reference 6. The formula from that report is

$$\rho = 2\pi R_m \left[ \frac{\log \frac{4\ell}{a} - 1}{\ell} - \frac{1}{r_{1x}} + \frac{1}{r_{12}} \right]^{-1} \qquad \text{(A-1)}$$

where $R_m$ is the measured mutual resistance, $\ell$ is the length of the x (common) electrode in the earth, a is the diameter of the x electrode,

and r is the spacing between electrodes with the subscripts indicating which distance is considered. In this particular set of measurements, $\ell$ is 0.154 meter, a is 7/32 inches, and the interelectrode spacing $r_{1x}$ and $r_{12}$ is approximately 2 meters. The difference between the reciprocals of the interelectrode spacing is considered small as compared to the other term and is therefore ignored. Solving equation (A-1) for $\rho$ with the three values of $R_m$ and averaging the results, we obtain a value of 72.83 ohm-meters or $\sigma = 1/72.83 = 0.0137$ mhos/m as the ground conductivity at 100 Hz, the measuring frequency. This figure may be extrapolated to higher frequencies by using figures 7 and 9 of reference 16 which are also reproduced as figures B.1 and B.2 in reference 6. These two figures are graphs of the conductivity $\sigma$, and the dielectric constant $\epsilon/\epsilon_o$ as functions of known conductivity at 100 Hz. Table A-1 gives these two parameters for the ten values of frequency used in the analysis.

Once we have values of the conductivity and the dielectric constant, we are in a position to evaluate the propagation constant of the earth from the formula

$$\gamma = \sqrt{j\omega\mu_o(\sigma + j\omega\epsilon)} \qquad \text{(A-2)}$$

16. Scott, J. H., "Electrical and Magnetic Properties of Rock and Soil," EMP Theoretical Notes, Volume 1, Note 18, Air Force Weapons Laboratory, Kirtland AFB, NM, May 1967.

Table A-1

GROUND CONDUCTIVITY AND DIELECTRIC CONSTANT AT THE LOS CORDOVAS SUBSTATION, TAOS, NEW MEXICO

| f (MHz) | $\sigma$ (mhos/m) | $\epsilon/\epsilon_o$ |
|---|---|---|
| 0.01 | 0.014 | 670 |
| 0.02 | 0.014 | 400 |
| 0.05 | 0.014 | 240 |
| 0.10 | 0.014 | 150 |
| 0.20 | 0.015 | 110 |
| 0.50 | 0.016 | 70 |
| 1.00 | 0.017 | 50 |
| 2.00 | 0.018 | 40 |
| 5.00 | 0.019 | 30 |
| 10.00 | 0.020 | 26 |

which is in urits of meters$^{-1}$. In equation (A-2), $\mu_o$ is taken to be the magnetic permeability of free space, $4\pi \times 10^{-7}$ henries/meter, $\sigma$ is the frequency dependent conductivity of table A-1, and $\epsilon$ the dielectric constant $\epsilon/\epsilon_o$ of table A-1 multiplied by the electric permittivity of free space, $8.854 \times 10^{-12}$ farads/meter.

2. THE THREE WIRE ANTENNA SYSTEM

The approach to be used is first to consider the three lines as connected in parallel and then to find the impedance per unit length and

admittance per unit length of the resulting line. The impedance per unit length, $Z_t$, is made up of three parts,

$$Z_t = Z_1 + Z_2 + Z_3 \tag{A-3}$$

where the subscript 1 indicates the series self-impedance of the wire, the subscript 2 indicates the gap impedance between the ground and the wire, and the subscript 3 indicates the series ground impedance.

Since in the previous section of this appendix, the ground characteristics are determined, we look at $Z_3$ first. From equation 8.34 of reference 3, an inductance factor involving ground effects is

$$W = \ell n \frac{1 + \gamma h}{\gamma h} \tag{A-4}$$

where h is the height of the wire above the ground. The height of our particular set of wires is 17 feet (5.18 meters). The inductance due to the ground effects is

$$L_g = \frac{\mu_o}{2\pi} W \tag{A-5}$$

and so

$$Z_3 = j\omega \frac{\mu_o}{2\pi} W \tag{A-6}$$

The gap inductance of the three wire system is given in equation A-10 of reference 2 as

$$L \sim \frac{\mu_o}{2\pi} \ell n \left[ \frac{4h^3}{aD^2} \left( 1 + \frac{5D^2}{8h^2} \right) \right] = 0.785 \ \mu H/m \qquad (A-7)$$

where D is the separation of the wires, 34 inches in this case, a is the radius of the wire, 0.23 inch, and the other parameters are as before. So that

$$Z_g = j\omega L \qquad (A-8)$$

From equation A-13 in reference 2 the wire self impedance is

$$Z_w = \frac{(1 + j)}{2\pi a} \left( \frac{1}{\sigma_a \delta_a} \right) \qquad (A-9)$$

Since we have a combination of three wires the impedance is divided by 3 and we have

$$Z_1 = \frac{Z_w}{3} \qquad (A-10)$$

The material from which the wire conductor is made is aluminum. The $\sigma_a$ and $\delta_a$ of equation (A-9) are the conductivity and skin depth, respectively, of the aluminum. The conductivity of aluminum is $3.54 \times 10^7$ mho/meter and the skin depth may be approximated by $0.085/\sqrt{f}$ meters.

The admittance of the wire is

$$Y = j\omega C \qquad (A-11)$$

where

$$C = \frac{\mu_o \epsilon_o}{L} = 14.15 \text{ pF/m} \qquad (A-12)$$

The propagation constant of the wire and the characteristic impedance may be calculated from

$$\gamma_w = \sqrt{Z_T Y}$$

$$Z_o = \sqrt{\frac{Z_T}{Y}} \qquad \text{(A-13)}$$

This is the characteristic impedance used in the solutions of the circuit diagrams of figures 16, 18, and 22. The propagation constant gives us further insight into the wire characteristics as a transmission line. The phase shift of a signal traversing a length of the line is given as

$$\theta = \ell\left(\mathrm{Im}(\gamma_w)\right) \qquad \text{(A-14)}$$

and the attenuation of the signal is given as

$$F = e^{\mathrm{Re}(\gamma_w)\ell} \qquad \text{(A-15)}$$

where $\ell$ is any length along the line. The effective length of the wire as an antenna may be calculated from the absolute value of

$$\ell_{eff} = \frac{1}{\gamma_w - \frac{j\omega}{c}\cos(\psi)} \qquad \text{(A-16)}$$

where $\psi$ is the angle of incidence of the pulse above the horizon, and c is the speed of light.

## 3. THE OPEN-CIRCUIT VOLTAGE AT THE TERMINALS OF THE ANTENNA

From equations 64 and 65 of reference 2 we have the open circuit voltage for the transmission-line mode

$$V_{oc}^{T} = \frac{E_o \sin(\psi)\left[1 - R_v \ell^{-j\frac{\omega}{c}2h\sin(\psi)}\right]}{\gamma_w - j\frac{\omega}{c}\cos(\psi)}$$

$$R_v = \frac{\epsilon_r\left(1 + \frac{\sigma}{j\omega\epsilon}\right)\sin\psi - \sqrt{\epsilon_r\left(1 + \frac{\sigma}{j\omega\epsilon}\right) - \cos^2\psi}}{\epsilon_r\left(1 + \frac{\sigma}{j\omega\epsilon}\right)\sin\psi + \sqrt{\epsilon_r\left(1 + \frac{\sigma}{j\omega\epsilon}\right) - \cos^2\psi}} \qquad \text{(A-17)}$$

where $E_o$ is the incident pulse, to be discussed later, and $\epsilon_r$ is the $\epsilon/\epsilon_o$ of table A-1.

From equation 66 of reference 2 we have the antenna response open circuit voltage as

$$V_{oc}^{a} = -\cos(\psi)\, E_o\left[h + R_v \frac{1 - \ell^{-j\frac{\omega}{c}2h\sin(\psi)}}{j\frac{\omega}{c}2\sin(\psi)}\right] \qquad \text{(A-18)}$$

Adding the transmission line and antenna modes, we have an open circuit voltage as

$$V = V_{oc}^{t} + V_{oc}^{a} \qquad \text{(A-19)}$$

The only undefined parameter in the above expression is the incident pulse, $E_o$. From page 13 in reference 4 an EMP pulse may be approximately represented as a sum of two exponential terms of the form

$$E_o(t) = E(\ell^{-\alpha t} - \ell^{-\beta t}) \qquad \text{(A-20)}$$

where, for the analysis in reference 4 they use

$$E = 5 \times 10^4 / 0.9646 \text{ volts/meter}$$

$$\alpha = 1.5 \times 10^6 \text{ sec}^{-1}$$

$$\beta = 2.6 \times 10^8 \text{ sec}^{-1}$$

These are the values used in this study.

This is a time domain representation, but this analysis is in the frequency domain. An approximation to the Fourier transform of equation (A-20) is

$$E_o(\omega) = E\left(\frac{1}{\alpha + j\omega} - \frac{1}{\beta + j\omega}\right)\Delta\omega \qquad \text{(A-21)}$$

where $\Delta\omega$ is the bandwidth of the incident pulse. Its units are $\text{sec}^{-1}$, which places the units of $E_o$ as volts/meter. For this analysis the bandwidth is taken to be the difference between logarithmic midway points of the radian frequencies being studied. The calculational results of equation (A-19) are presented in table A-2.

Table A-2

MAGNITUDE OF OPEN CIRCUIT VOLTAGE IN MEGAVOLTS
AT TERMINALS OF BEVERAGE ANTENNA

| f(kHz) / ψ(degrees) | 10 | 20 | 50 | 100 | 200 |
|---|---|---|---|---|---|
| 5 | 0.3568 | 0.6958 | 1.133 | 1.552 | 2.551 |
| 10 | 0.3506 | 0.6873 | 1.132 | 1.572 | 2.622 |
| 15 | 0.3304 | 0.6450 | 1.056 | 1.457 | 2.409 |
| 20 | 0.3042 | 0.5892 | 0.9526 | 1.301 | 2.117 |
| 30 | 0.2480 | 0.4718 | 0.7432 | 0.9925 | 1.571 |
| f(MHz) / ψ(degrees) | 0.5 | 1 | 2 | 5 | 10 |
| 5 | 2.419 | 1.905 | 1.923 | 1.258 | 0.8839 |
| 10 | 2.551 | 2.050 | 2.103 | 1.381 | 0.9311 |
| 15 | 2.308 | 1.823 | 1.832 | 1.157 | 0.7437 |
| 20 | 1.980 | 1.530 | 1.503 | 0.9296 | 0.5956 |
| 30 | 1.417 | 1.072 | 1.045 | 0.6640 | 0.4520 |

## 4. THE 80-FOOT SECTION

As mentioned in the main text, the 80-foot section between the terminals of the antenna and the old Los Cordovas main frame is considered as an antenna in its own right to pick up the EMP incident pulse. The 80 feet are divided into six sections in keeping with the maximum length requirements for the 1 MHz model; so, $\ell$ is 13.3 feet (4.07 meters) in the following discussion.

Figure A-1 is a circuit diagram equivalent of the 80-foot section. The $Z_o$ and V are the antenna parameters whose solutions are given earlier in this appendix. The inductance L is the three parallel wire inductance and C is the capacitance for this length ($\ell$) of section. The capacitance for one end section is divided in two and the other half is lumped at the other end for better distribution. $V_\ell$ is the induced voltage from the pulse due to magnetic coupling and $V_c$ is that voltage due to electric coupling.

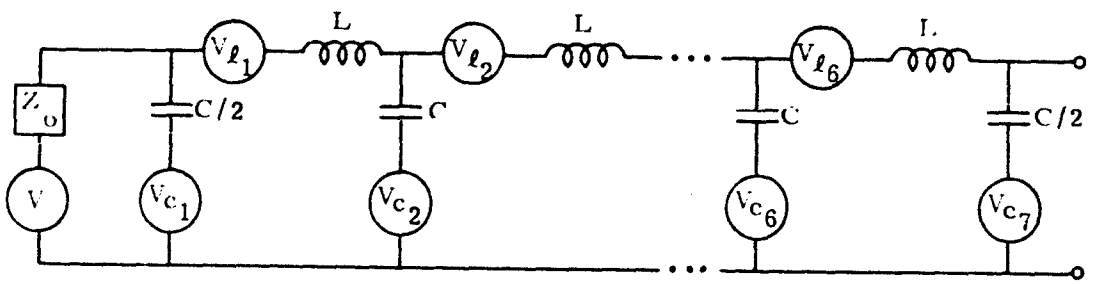



Figure A-1. Circuit Diagram of 80-Foot Section

In solving for the parameters of figure A-1 we refer to equations (A-7) and (A-12) in this appendix. The individual values in those equations are now a bit different. The wire separation is 4 feet, the height above the ground is 20.5 feet, and the wire diameter is 5/16 inch. Inserting these values into equation (A-7) we get an inductance of 0.756 $\mu$H/meter or 3.07 $\mu$H for the length $\ell$. Inserting this value into equation (A-12), we get 59.73 pF for the capacitance.

The voltage due to the electric field may be expressed as

$$V_c = h\cos(\psi)E_o \tag{A-22}$$

where $E_o$ is the solution to equation (A-21). This is the voltage due to direct incidence; however, the 80-foot section lies at an angle of $8.25^o$ with respect to the perpendicular of the Beverage antenna. So there is a phase shift per section expressed as

$$\Delta\theta = \frac{\ell\omega}{v_p} \tag{A-23}$$

where $v_p$ is the propagation velocity and is given by

$$v_p = \frac{c}{\cos(\psi)\sin(8.25^o)} \tag{A-24}$$

The results of equation (A-22) are then multiplied by the phase shift to give

$$V_{c_1} = V_c$$

$$V_{c_2} = V_c \ell^{-j\Delta\theta}$$

$$V_{c_3} = V_c \ell^{-j2\Delta\theta}$$

$$\vdots$$

$$V_{c_7} = V_c \ell^{-j6\Delta\theta} \qquad \text{(A-25)}$$

as the voltages to place in the circuit of figure A-1.

The voltage due to magnetic coupling may be expressed as

$$V_\ell = -j\omega \ell h B_\ell \qquad \text{(A-26)}$$

where $B_\ell$ is in webers/$m^2$ and is given by

$$B_\ell = j \sin(8.25^o) \frac{E_o}{c} \qquad \text{(A-27)}$$

The phase shift factor also applies here, but if we consider the inductance to be lumped in the middle of each section we get half values of the shift for each section and the voltage at each section is

$$V_{\ell_1} = V_\ell \ell^{-\Delta\theta/2j}$$

$$V_{\ell_2} = V_\ell \ell^{-3/2\Delta\theta j}$$

$$\vdots$$

$$V_{\ell_6} = V_\ell \ell^{-11/2\Delta\theta j} \qquad \text{(A-28)}$$

Now the voltage from the Beverage antenna is transferred to the substation through the 80-foot section with the 80-foot section acting as an antenna. The results are shown in table A-3.

From table A-3 we see that a worst-case condition occurs for an angle of incidence of $10^{o}$. This is the value that is used in further calculations. Table A-4 shows the impedance which appears at the substation main frame. Comparing table A-3 with table A-2, one sees that the 80-foot section has a rather minor effect.

Table A-3

MAGNITUDE OF OPEN CIRCUIT VOLTAGE IN MEGAVOLTS
AT END OF 80-FOOT SECTION

| f(kHz) / ψ(degrees) | 10 | 20 | 50 | 100 | 200 |
|---|---|---|---|---|---|
| 5 | 0.3566 | 0.6952 | 1.130 | 1.544 | 2.526 |
| 10 | 0.3504 | 0.6867 | 1.129 | 1.564 | 2.597 |
| 15 | 0.3303 | 0.6524 | 1.053 | 1.450 | 2.385 |
| 20 | 0.3041 | 0.5886 | 0.9502 | 1.294 | 2.094 |
| 30 | 0.2476 | 0.4713 | 0.7413 | 0.9870 | 1.552 |
| **f(MHz) / ψ(degrees)** | **.5** | **1** | **2** | **5** | **10** |
| 5 | 2.351 | 1.782 | 1.633 | 1.7448 | 0.8454 |
| 10 | 2.483 | 1.923 | 1.799 | 0.8752 | 0.9846 |
| 15 | 2.243 | 1.702 | 1.534 | 0.6738 | 0.8583 |
| 20 | 1.919 | 1.416 | 1.223 | 0.4736 | 0.7357 |
| 30 | 1.366 | 0.9769 | 0.8077 | 0.2539 | 0.6004 |

Table A-4

MAGNITUDE OF THE CHARACTERISTIC IMPEDANCE AT THE END OF THE 80-FOOT SECTION FOR $\psi = 10°$

| f (kHz) | Z (ohms) | f (MHz) | Z (ohms) |
|---|---|---|---|
| 10 | 287.681 | 0.5 | 241.898 |
| 20 | 279.872 | 1 | 229.824 |
| 50 | 269.698 | 2 | 216.052 |
| 100 | 262.096 | 5 | 239.433 |
| 200 | 253.814 | 10 | 260.025 |

## APPENDIX B

## PARAMETER VALUES AT THE OLD PART OF THE LOS CORDOVAS SUBSTATION

### 1. THE MAIN FRAME

In the event that voltages at the end of the eighty-foot section exceed the lightning arrestor discharge voltage, the entire frame is connected to the circuit. Figures 11 and 12 of this report are presented as the results of the modeling. The technique followed in obtaining parameter values for the frame is to consider the components of the stick model of figure 11 individually as wires and obtain inductance and capacitance values for them. For example, the lower cross girder of the west side face of the frame is considered to be a wire whose equivalent diameter, d, is 44 inches; the length, $\ell$, is 207 inches; and h, the height above a ground plane is 166.75 inches. From equation 22 on page 50 of reference 7 the appropriate formula for the inductance is

$$L = 0.00580\ell\left[2.303 \log_{10}(4\ell/d) - Q\right]\mu H \qquad \text{(B-1)}$$

In this formula Q is a function of $\ell/2h$ and is given in tabular form as table 9 in reference 7. The inductance of the lower cross girder as obtained from this equation is 1.71 $\mu$H. Similarly, the capacitance is calculated from the expression

$$C = \frac{7.354\ell}{\log_{10}(4h/d) - S}\ pF \qquad \text{(B-2)}$$

found on page 114 of reference 7. Here S, like Q in the previous equation, is a function of $\ell/2h$ and is presented in tabular form in reference 7. The capacitance of the lower cross girder computed from this equation is 179 pF.

After proceeding in the same manner with appropriate formulas for all the wire segments of the stick model, we combine the parameters in series and parallel, as appropriate, to end up with one value of inductance and one value of capacitance for the west wall. Since the east wall is identical, its parameter values are the same, and the results for the west wall are used.

The point on the frame to which the LI-200 lightning arrestor for the middle phase wire is connected will be considered to be in the exact center of the 407-inch segment on the north wall. This divides the frame into two halves, placing them in parallel. So the next parameters to be calculated are those for half the 407-inch segment. These results are combined with those of the west wall and the resulting circuit inductances are divided by 2, and the capacitances multiplied by 2, to account for the parallel combination.

The distance between the LI-200 arrestor connecting point and the equivalent adjacent connecting point for LI-100 (or LI-300) is 133.5 inches. If we assume that current from the LI-200 arrestor only flows through this distance but that current from all five lines flow through the

rest of the frame, the inductances for the side wall and the remaining part of the 203.5-inch girder need to be multiplied by the factor of 2.9 introduced in section III-3 of this report. Similarly the capacitances are divided by the 2.9 for that part of the frame.

The frame portion which is common to all five lines has a total length of $2 \times (207 + 70)$ or 544 inches. In keeping with our 160-inch maximum length for wires we divide the length into four parts and represent that portion of the frame as a lumped element artificial transmission line.

There is a wire leading from point "A" (actually three of them) through the lightning arrestor and to the connecting point on the main frame. An inductance and a capacitance may be calculated from similar formulas to those of equations (B-1) and (B-2) and connected to the girder and frame parameters in the circuit. The values for this wire have to be operated on by a factor of 3 (inductance divided and capacitance multiplied) to account for the fact that there are three wires considered to be in parallel.

The results of the modeling and calculations are shown in circuit diagram form in figure 12 of this report. The factors of 2.9 and 3 are applied when appropriate.

## 2. THE RECLOSER SUPPORT STAND

The current flowing through the recloser case and support stand is important in its contribution to the coupling to the various ports. An

equivalent circuit diagram is presented in figure 14 of this report. The various parameters to the right of the symbol $V_s$ are discussed earlier in this report, and a discussion of the parameters to the left of this symbol are discussed in this appendix.

The recloser control box is connected to the support stand by being bolted to a cross element on the stand. See the photograph of figure 13 to better visualize this part of the system. The inductance labeled 0.155 $\mu$H in figure 14 is the inductance due to the portion of the control box and the cross member which contain the appropriate current path. The inductance value is obtained by modeling the cross member as a wire with the appropriate dimensions and applying formulas found in reference 7. The part of the control box which contributes to the inductance is modeled as a rectangular bar, and equation 26 from page 51 of reference 7 is applied.

The recloser and support stand are modeled as a plate sitting on four cylinders. The mutual inductance effects of the four legs are included in the calculations. The total inductance for the recloser and stand is 1.12 $\mu$H. This figure is multiplied by 2 since we consider the inductance as being composed of two equal values in parallel. The portion of the inductance across which the control box is bolted to the stand is 0.722 $\mu$H. The values of 0.097 $\mu$H and 1.41 $\mu$H shown in figure 14 are due to fractions of the actual distances across which the box is bolted as compared to the overall height of the stand and recloser.

Having all these parameter values for the circuit of figure 14 we can calculate an equivalent impedance and thus determine the amount of current flowing. The voltage $V_s$ can then be calculated in the usual manner as a voltage drop across a specific impedance.

3. THE OLD PART OF THE LOS CORDOVAS SUBSTATION

The resultant circuit diagram of the model is shown in figure 16. The general method used in obtaining the parameter values is to take into consideration the geometrical parameters of the lengths of wires in question and calculate inductance and capacitor values from equations out of reference 7 as illustrated earlier in this appendix.

The various lengths are too numerous to allow the repetition of formulas and solutions for each one, but table B-1 is a summary of the results. Individual values due to these lengths are then redistributed to take into account the 160-inch maximum for our frequency considerations as explained above in section III-3. The values given in figure 16 do not correspond directly with those of table B-1, but the sum of all inductance values is the same for both sets, as is the sum of the capacitances. In both cases the appropriate 2, 9 and 3 factors are applied where required.

Table B-1

PARAMETERS PERTINENT TO THE OLD
LOS CORDOVAS SUBSTATION

| Section | (Inches) | C (pF) | L ($\mu$H) |
|---|---|---|---|
| Point "A" to recloser | 138.0 | 107.04 | 1.38 |
| Internal to recloser | 29.8 | 1200.00 | 0.20 |
| Recloser to knifeswitch | 44.0 | 36.54 | 0.38 |
| Knifeswitch to insulator | 70.7 | 91.20 | 0.39 |
| Insulator to jumper and jumper | 131.8 | 166.74 | 0.67 |
| Jumper to insulator | 70.8 | 18.50 | 1.94 |
| Insulator to regulator | 220.3 | 62.17 | 5.49 |
| Internal to regulator | 59.6 | 413.79 | 1.16 |
| Regulator to knifeswitch | 85.5 | 21.62 | 2.42 |
| Knifeswitch to insulator | 67.0 | 19.09 | 1.51 |
| Insulator to stub | 286.2 | 63.62 | 9.09 |
| Stub | 286.2 | 63.62 | 4.54 |
| Stub to transformer | 102.0 | 24.83 | 3.00 |
| Transformer | - | 2467.24 | - |
| TOTAL | | 4856.00 | 32.17 |

# APPENDIX C

## THE NEW PART OF THE LOS CORDOVAS SUBSTATION

### 1. EXTERNAL COUPLING

The circuit diagram which represents the external coupling model for the new part of the Los Cordovas Substation is presented in figure 22 of this report. The methods by which parameter values are obtained are the same as those used in appendix B, namely that the inductances are found for specific lengths of wire from formulas out of reference 7. Figure 22 gives a pictorial representation of the facility with the pertinent lengths of wire labeled so that the equivalent circuit diagram below the pictorial diagram may be easily followed. Actual lengths and formulas out of reference 7 are not given here, but the resultant values are given in figure 22.

The boxes labeled "$Z_o$" and "buried cable" in figure 22 pertain to the buried power cable which carries the 60 Hz current from the new part of the substation to the old LI-500 site. The treatment of these parameters are discussed in the next section.

### 2. THE BURIED CABLE

$Z_o$ in figure 22 is the characteristic impedance of the outer sheath of the buried cable to infinite ground. For the purposes of determining $Z_o$ the cable is considered to be a buried wire with a diameter equal

to the diameter of the outer sheath. The propagation constant for a half-buried bare conductor, from equation 8.02 in reference 3 (Sunde) is

$$\Gamma^2 = \frac{\gamma^2}{2} \tag{C-1}$$

where $\gamma$ is the same as defined by equation (A-2) in appendix A of this report, the propagation constant of the earth. By half-buried, Sunde means that the axis of the wire lies in the plane of the earth's surface. For a conductor with radius, a, buried at a depth, d, the propagation constant becomes, from equation 8.04 in reference 3,

$$\Gamma' = \Gamma\left[\frac{\ell n\left(\frac{1.12}{\Gamma a}\right)}{\ell n\left(\frac{1.12}{\Gamma a'}\right)}\right]^{1/2} \tag{C-2}$$

where,

$$a' = (2ad)^{1/2} \tag{C-3}$$

The characteristic impedance can now be calculated from equation 8.16 of reference 3 as,

$$Z_o = \frac{j\omega\mu_o}{4\pi\Gamma'} \ell n\left(\frac{1.12}{\Gamma' a'}\right) \tag{C-4}$$

Between the autotransformer site and the substation, the depth of burial is 42 inches (1.067m). We do not have one buried conductor, but three;

Sunde states that the total characteristic impedance of a bundle of conductors may be obtained by considering them as one conductor with some equivalent radius if the bundle of wires is driven together, in the sum mode, as is the case here. Each one of our cables has a diameter of 1 inch, so we approximated the equivalent diameter of the three conductor bundle as 2 inches. The radius, a, which is used in equations C-2 and C-3 is then 1 inch, or 0.0254 meter. Figure C-1 is a portion of the data sheet which describes the cable.

**"Rome-XLP" Cross-Linked Polyethylene Primary UD Cable—25 kv, 100% Insulation Level (Grounded Neutral) Concentric Wire Neutral-Full Size**



**Description:** Copper or aluminum conductor, extruded conductor shield, 260 mils "Rome-XLP" cross-linked polyethylene insulation, "Rome Poly-Shield" extruded insulation shield, No. 14, No. 12, or No. 10 solid coated copper wires uniformly spaced around the cable as a concentric serve with a conductivity equal to the power conductor.

Figure C-1. Portion of Buried Cable Data Sheet

The characteristic impedance may also be described in terms of impedance per unit length and admittance per unit length by

$$Z_o = \sqrt{\frac{Z_\ell}{Y_\ell}} \tag{C-5}$$

$$\text{but,} \quad \Gamma' = \sqrt{Z_\ell Y_\ell} = Y_\ell Z_o = \frac{Z_\ell}{Z_o} \tag{C-6}$$

$$\text{so,} \quad Z_\ell = Z_o \Gamma' \tag{C-7}$$

$$\text{and} \quad Y_\ell = \frac{\Gamma'}{Z_o} \tag{C-8}$$

The next step, after the electrical description of the outer sheath, is to describe the center conductor. From equation 27 on page 52 of reference 7 the inductance of a concentric cable is

$$L = 0.14 \log_{10}(r_2/r_1) + 0.015 \ \mu H/\text{foot} \tag{C-9}$$

where $r_1$ is the radius of the outside of the inner conductor and $r_2$ is the radius of the inner side of the outer conductor. In our cable $r_2$ is 0.5 inch and $r_1$ is 0.1625 inch. Solving for the inductance from equation (C-9) and converting to meters, we obtain an inductance of 0.273 $\mu$H/m. Similarly the capacitance of a concentric cable, from equation 145 of reference 7 is

$$C = \frac{7.354K}{\log_{10}(r_2/r_1)} \text{ pF/foot} \qquad \text{(C-10)}$$

where K is the dielectric constant of the material, 2.275 for polyethylene. The solution to this equation with our parameters is 112.45 pF/m after converting tc meters. These values of inductance and capacitance are for a single wire, but we have three considered to be in parallel, so the above inductance will be divided by 3 to get 0.091 $\mu$H/m and the capacitance will be multiplied by 3 to get 337.35 pF/m. Since the cable is 150 feet long (45.72m) the total inductance due to the center conductor is $L_c = 4.16$ $\mu$H, and the total capacitance is $C_c = 0.0154$ $\mu$F.

The circuit diagram for the cable representation is as shown in figure C-2. In this figure the total inductances, capacitances, impedances, and admittances for the center conductor and sheath are divided into n sections to represent the cable as a lumped element transmission line with three terminals at each end. The center conductor capacitance from one section is divided by two and placed on one end, with the remaining half placed on the other end. The same is done with the admittance from the sheath. The symbol $\ell$ represents the cable length.

Although the diagram of figure C-2 is a reasonable model for the buried cable, its solution is difficult due to the many loops involved, so it is simplified by considering one section and performing T and $\pi$ transformations on it as illustrated in figure C-3.

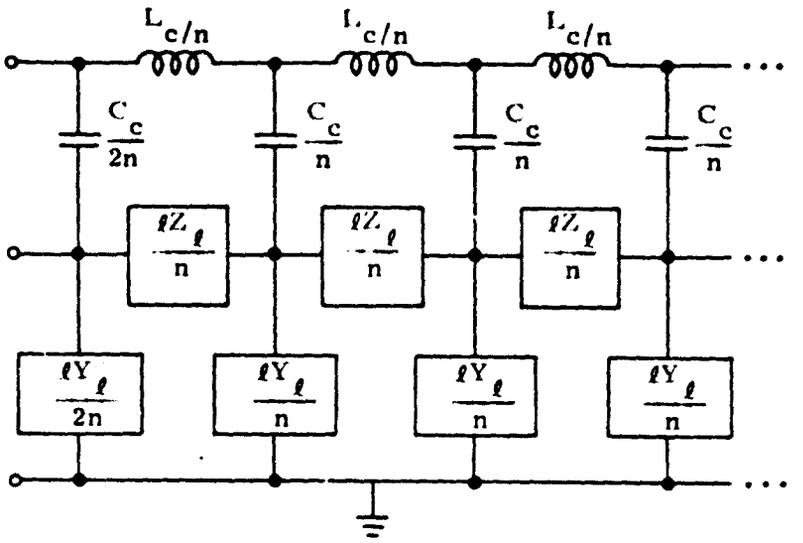



Figure C-2. Circuit Diagram Representation of Buried Cable

Figure C-3a is one section of the cable as shown in figure C-2 where the capacitance and admittance at each end are divided in half for each section. In figure C-3b the sheath part of the cable is transformed from a $\pi$ to a T by dividing the impedance of the sheath section in half and combining the admittance from the ends. Figure C-3c depicts the transformation from a $\pi$ to a T of the center conductor and impedance parts of the section. In this step the inductance is divided in two and placed at each end. The capacitances from the center conductor add in parallel, as do the impedances from the sheath. From the numerical work we determine that the sheath impedance $\ell Z_\ell/4n$ is small as compared to the series impedance due to $\ell Y_\ell/n$ and $C_c/n$ and so it is eliminated. Figure C-3d goes from a T to a $\pi$ by adding the inductances and

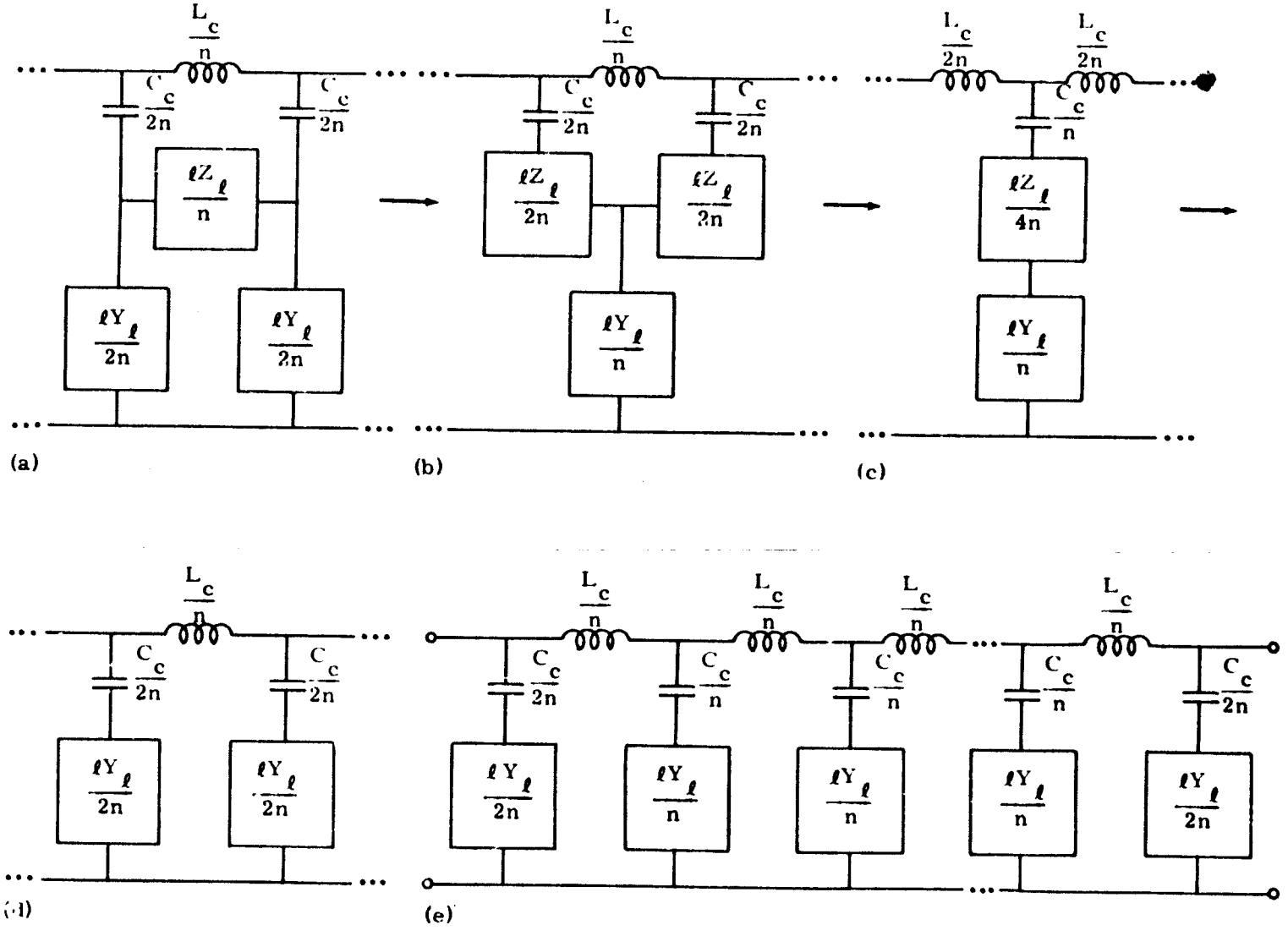



Figure C-3. Sequence of T and π Transformations on a Line Section Performed for Simplification

splitting the capacitances. Figure C-3e combines all the sections to form the whole cable as we represent it with n sections.

In solving the circuit of figure 22 in this report, an open circuit voltage and an impedance, taking into account lightning arrestor discharge voltage and polyethylene breakdown, are obtained at the entrance terminals to the box labeled "buried cable." These values are then propagated down the n sections of figure C-3e to obtain a voltage and an impedance at the end of the cable; these are then used as input values in solving the circuit to the right of the buried cable. The voltage appearing at the recloser is the input voltage to the port failure problem. Voltages are checked for lightning arrestor discharge, polyethylene breakdown at the substation end, and bushing breakdown.

The total length of the cable is 150 feet of 45.72 meters. In this particular analysis we want our model to be accurate to about 5 MHz, so the number of sections that the cable is divided into needs to be determined. We have a propagation constant for the outer sheath, but we actually need one for the entire cable in order to calculate the ratio of the propagation velocity to the free space speed of light so as to calculate a wavelength for 5 MHz and thus keep the section lengths less than one radian long. An admittance to ground for the outer sheath is calculated in equation (C-8). The admittance from the center conductor may be expressed as

$$Y_c = j\omega C \tag{C-11}$$

where C is the capacitance of the center conductors to ground calculated earlier as 337.3 pF/m. The total admittance of the cable to ground may be expressed as

$$Y_g = \frac{Y_\ell Y_c}{Y_\ell + Y_c} \tag{C-12}$$

which is the series admittance of the two conductors. The impedance of the cable is the inductive reactance, $X_L$, due to the center conductor. The propagation constant of the whole cable may be expressed as,

$$\Gamma_c = \sqrt{X_L Y_g} \tag{C-13}$$

The ratio of the propagation velocity to the speed of light is given by

$$r_v = \frac{\omega}{\mathrm{Im}(\Gamma_c)c} \tag{C-14}$$

At 5 MHz the imaginary part of $\Gamma_c$ is $0.162\mathrm{m}^{-1}$, giving an $r_v$ of 0.648. This means a wavelength at 5 MHz is

$$\lambda = \frac{0.648c}{f} = \frac{(3 \times 10^8)0.648}{5 \times 10^6} = 38.88\mathrm{m} \tag{C-15}$$

and a radian wavelength is 6.2 meters, our section length. This implies that the underground cable must be divided into seven sections to keep the accuracy of the model to this frequency. So, the n of figure C-3 is equal to 7.

## APPENDIX D

## GUIDELINES

### 1. PREVENTION

In the particular case of the Kit Carson Electrical Cooperative power system, failure occurs because:

a. Grounding paths are too long, rendering lightning arrestor protection relatively ineffective.

b. Internal coupling in the McGraw-Edison recloser is enhanced by an unshielded control cable.

c. Current flowing in the recloser case and support stand due to bushing capacitance and/or bushing breakdown couples to unshielded control cable between recloser and recloser control. (McGraw-Edison)

d. Separate recloser and control, causing need for cable in the first place (McGraw-Edison), contributes to coupling.

e. Ceramic bushings have breakdown voltages lower than EMP voltages which appear there.

f. Buried cable insulators (polyethylene) have breakdown voltages lower than EMP voltages which appear there.

g. Semiconductors which fail have lower failure threshold values than those which couple to them.

h. There are insufficient low impedances to high frequencies shunting the semiconductors which fail.

i. System resonances are present, causing some frequencies to be more vulnerable to coupling.

j. Overhead customer distribution lines act as antennas to pick up the EMP.

Obviously, the prevention of failure due to the above reasons for failure could be accomplished by eliminating the reasons. The following list contains solutions to the problems listed as a through j above.

a. Install lightning arrestors close to the equipment they are to protect.

b. Shield all cables to which coupling can occur.

c. Same as b.

d. Keep reclosers and their control units within the same enclosure, as in the General Electric recloser.

e. Lightning arrestors closer to the bushings would fire at voltages lower than the bushing breakdown voltage, protecting them. Also higher rated bushings would need higher voltages before breakdown occurs.

f. Again lightning arrestors closer to the equipment would help; or use an insulating material with a higher dielectric strength; or surround the center conductor of the cable with more insulator.

g. Use semiconductors with higher Wunsch model breakdown constants.

h. Shunt the vulnerable components with larger capacitors or use a resistance material with a high negative coefficient of resistance like "Thyrite" as a shunt.

i. Resonances due to the system cannot be eliminated, but perhaps the Q of the resonance can be lowered to damp the resonance effects. Or perhaps the system resonance can be lowered to frequency values which are less important, for example to frequencies where the lightning arrestors are more effective.

j. Bury all customer distribution lines.

Most of the reasons for failure given could be eliminated during the design stages for both the recloser design and the substation design. The improvement of design is obvious in the comparison of the old part of the Los Cordovas substation to the new part. The only failure in the new part was due to insulation breakdown of the buried cable between the overhead distribution lines of the old LI-500 and the new substation. The second recloser in the new portion has buried line all the way to the customer. Part of the reason for the cable insulation failure is the fact that the overhead lines (an old design) were tied to a buried cable (a new design) so that it was the integrating of an old system with a new system that did not quite work from a vulnerability point of view.

2. COUNTERMEASURES

In recovering from failure due to a nationwide attack, the rural power system personnel should be familiar with which parts of their

system are vulnerable and be able to repair or bypass the damaged components as soon as possible, still allowing power to serve their customers while repairs are being made. For example, in the McGraw-Edison recloser the most vulnerable port was Port 2, the ground fault sensing and tripping port. If this has been determined as having failed, a quick fix would be to place the "ground trip blocking switch" in the position that throws the ground trip circuit out of the entire circuit. In anticipation of battery charging port failure, charged batteries should be available to power the unit and still permit tripping.

At the other substations in Kit Carson there are no reclosers, so failure will probably occur because of bushing damage to the power transformer. There may be damage to the transformer also. The maintenance personnel should know how to change bushings rapidly, and in anticipation of transformer failure, have a portable transformer which could be put into use rapidly.

A publication which could prove useful to a power and systems engineer, who should be concerned with the effects of EMP on such a system, is listed here as reference 17. Chapter seven of this publication concerns power-system practices for EMP protection; the information presented there agrees with the findings of this report.

---

17. Vance, E. F., Electromagnetic-Pulse Handbook for Electric Power Systems, DNA 3466F, Defense Nuclear Agency, Washington, D. C., February 1975.

## APPENDIX E

## EMP EFFECTS ON THE POWER SYSTEM CUSTOMER

Customers of the power system include private residences, radio broadcast stations, Civil Defense Emergency Operating Center (EOCs), factories, etc. Several studies have been done on EMP effects on customers. The study of reference 6 concerns a military microwave repeater station. The main antennas here are the power lines coming into the station. Both that study and this one are done on one particular facility, but both show that a power system, from the substation end to the customer end, is subject to damage from EMP.

The extent of damage at the customer end depends on the equipment to which the 60 Hz lines are connected. For example, damage occurs in both studies in the diodes of rectifier bridges. The primary equipment of concern at an EOC is communications gear. The circuits in communication gear which are most exposed to EMP coupling to a power line are the power supply circuitry; the rectifier diodes are the first solid-state components in the EMP path. Protection techniques for EOCs are outlined in reference 18* Reference 19* outlines protection techniques as applied to an AM broadcast station.

* See the following page for references.

The particular coupling to such customers as the EOCs and broadcast stations would have to be determined from the physical layout of the particular customer's incoming power lines. Obviously, if the line came into the center from an underground cable system the facility is less vulnerable than if it comes in from overhead wires. The vulnerability has to be determined by factors such as this and other factors; for example, the extent to which protective devices such as lightning arrestors are effective. In general, before vulnerability can be determined for a particular power system customer from an EMP viewpoint a coupling model should be developed, however crude.

If power fails due to the substation failure but not to EMP failure at the customer then the customer's mission could fail unless countermeasures are put into effect. Countermeasures here include things like having emergency power generators or battery banks on which to draw power. In national emergencies customers like the EOCs should be prepared with spare communications equipment and emergency generators in order to recover quickly from failure due to EMP effects on power systems.

---

18. Johnston, ed., EMP Protection for Emergency Operating Centers, Defense Civil Preparedness Agency TR-61A, July 1972. Also reprinted as Nuclear EMP Protection Engineering and Management Note 8 by Lawrence Livermore Laboratory, Livermore, California.

19. Clark, D. B., Low Cost EMP Protection for AM Broadcast Station Transmitters, U.S. Naval Civil Engineering Laboratories, Port Hueneme, California, April 1975. (Under DCPA Work Order DAHC-20-73-C-0057)

## REFERENCES


1. Beverage, Harold H., Chester W. Rice, and Edward W. Kellogg, "The Wave Antenna - A New Type of Highly Directive Antenna," Trans. A.I.E.E., Vol. 42, p. 215, 1923.

2. Vance, E. F., and S. Dairiki, Analysis of Coupling to the Commercial Power System, AFWL TR-72-21, Air Force Weapons Laboratory, Kirtland AFB, NM, August 1972.

3. Sunde, Erling D., Earth Conduction Effects in Transmission Systems, Dover Publication, New York, 1968.

4. Marable, J. H., J. K. Baird, and D. B. Nelson, Effects of Electromagnetic Pulse (EMP) on a Power System, ORNL-4836, Oak Ridge, Tennessee, December 1972.

5. Baird, J. K., and N. J. Frigo, Effects of Electromagnetic Pulse (EMP) on the Supervisory Control Equipment of a Power System, ORNL-4899, Oak Ridge, Tennessee, October 1973.

6. Babb, D. D., R. M. Brown, and H. Frank, Analysis of Communications Systems, AFWL TR-74-149, Air Force Weapons Laboratory, Kirtland AFB, NM, November 1974.

7. Terman, F. E., Radio Engineer's Handbook, McGraw-Hill Book Company, New York, 1943.

8. Greenwood, Allan, Electrical Transients in Power Systems, John Wiley & Sons, Inc., New York, 1971, Chapter 15.

9. Hodgman, M. S., R. C. Weast, and S. M. Selby, editors, Handbook of Chemistry and Physics, 39th edition, Chemical Rubber Publishing Company, Cleveland, Ohio, p. 2345, 1958.

10. Wunsch, D. C., and R. R. Bell, "Determination of Threshold Failure Levels of Semiconductor Diodes and Transistors Due to Pulse Voltages," IEEE Trans. Nucl. Sci., Vol. NS-15, pp. 244-259, December 1968.

11. Boeing Company, The, and Braddock, Dunn and McDonald, Inc., EMP Electronic Analysis Handbook, Boeing Document D224-10022-1, under AFWL Contract F29601-74-C-0028, Appendix B, Air Force Weapons Laboratory, Kirtland AFB, NM, May 1973.

12. Wunsch, D. C., R. L. Cline, and G. R. Case, Theoretical Estimates of Failure Levels of Selected Semiconductor Diodes and Transistors, Braddock, Dunn and McDonald, Inc. Rep BDM/A-42-69-R, reissued August 14, 1970, under Contracts F29601-69-C-0132 and F29601-70-C-0019, AD 878-091, Air Force Weapons Laboratory, Kirtland AFB, NM.

13. O'Dwyer, J. J., The Theory of Dielectric Breakdown of Solids, Oxford University Press, New York, 1964.

14. Whitehead, S., Dielectric Breakdown of Solids, Oxford University Press, New York, 1951.

15. Creedon, J., Volume Dependent Electrical Breakdown in Solids, PIIR-20-70, Physics International Company, San Leandro, CA, June 1970.

16. Scott, J. H., "Electrical and Magnetic Properties of Rock and Soil," EMP Theoretical Notes, Volume 1, Note 18, Air Force Weapons Laboratory, Kirtland AFB, NM, May 1967.

17. Vance, E. F., Electromagnetic-Pulse Handbook for Electric Power Systems, DNA 3466F, Defense Nuclear Agency, Washington, D. C., February 1975.

18. Johnston, ed., EMP Protection for Emergency Operating Centers, Defense Civil Preparedness Agency TR-61A, July 1972. Also reprinted as Nuclear EMP Protection Engineering and Management Note 8 by Lawrence Livermore Laboratory, Livermore, California.

19. Clark, D. B., Low Cost EMP Protection for AM Broadcast Station Transmitters, U.S. Naval Civil Engineering Laboratories, Port Hueneme, California, April 1975. (Under DCPA Work Order DAHC-20-73-C-0057)

12. Wunsch, D. C., R. L. Cline, and G. R. Case, Theoretical Estimates of Failure Levels of Selected Semiconductor Diodes and Transistors, Braddock, Dunn and McDonald, Inc. Rep BDM/A-42-69-R, reissued August 14, 1970, under Contracts F29601-69-C-0132 and F29601-70-C-0019, AD 878-091, Air Force Weapons Laboratory, Kirtland AFB, NM.

13. O'Dwyer, J. J., The Theory of Dielectric Breakdown of Solids, Oxford University Press, New York, 1964.

14. Whitehead, S., Dielectric Breakdown of Solids, Oxford University Press, New York, 1951.

15. Creedon, J., Volume Dependent Electrical Breakdown in Solids, PIIR-20-70, Physics International Company, San Leandro, CA, June 1970.

16. Scott, J. H., "Electrical and Magnetic Properties of Rock and Soil," EMP Theoretical Notes, Volume 1, Note 18, Air Force Weapons Laboratory, Kirtland AFB, NM, May 1967.

17. Vance, E. F., Electromagnetic-Pulse Handbook for Electric Power Systems, DNA 3466F, Defense Nuclear Agency, Washington, D. C., February 1975.

18. Johnston, ed., EMP Protection for Emergency Operating Centers, Defense Civil Preparedness Agency TR-61A, July 1972. Also reprinted as Nuclear EMP Protection Engineering and Management Note 8 by Lawrence Livermore Laboratory, Livermore, California.

19. Clark, D. B., Low Cost EMP Protection for AM Broadcast Station Transmitters, U.S. Naval Civil Engineering Laboratories, Port Hueneme, California, April 1975. (Under DCPA Work Order DAHC-20-73-C-0057)